Connectomics-Based Network Analyses and Structure-Symptom Relationships in Obsessive-Compulsive Disorder

Tim Jonas Reess

Graduate School of Systemic Neurosciences

LMU Munich

Dissertation at the
Graduate School of Systemic Neurosciences
Ludwig-Maximilians-Universität München

April 26th, 2018

Supervisor
Prof. Dr. Kathrin Koch
Institut für Diagnostische und Interventionelle Neuroradiologie
Klinikum rechts der Isar, Technische Universität München

First Reviewer: Prof. Dr. Kathrin Koch
Second Reviewer: Dr. Afra Wohlschläger

Date of Submission: April 26th, 2018
Date of Defense: July 25th, 2018

ABSTRACT

Obsessive-compulsive disorder (OCD) is a highly debilitating psychiatric disorder. While current accounts of pathophysiological models emphazise the role of cortico-striato-thalamo-cortical (CSTC) circuitry, there is accumulating evidence indicating other brain regions to be critically involved in disease mechanisms. Furthermore, first evidence points towards potential alterations in neurodevelopment to be of importance in OCD. However, the majority of studies examining structural alterations in OCD have focused on assessing locally confined measures, effectively disregarding potential network-like relationships between various brain regions. Though recent evidence indicated hippocampus volume alterations to be of importance in OCD, a relationship between structure and symptoms was lacking when assessing symptoms in isolation. In this regard, it appears to be unclear, whether patients with specific symptom profiles may also present with differential changes in hippocampus morphology.

With the translation of graph theoretical concepts used in modern network science to brain research, it is now feasible to model the brain in terms of structural and functional networks, to assess topological features, and to identify differences between healthy subjects and psychiatric populations. Against this background, the first two Projects of the current thesis aimed at assessing differences in structural brain networks between OCD patients and healthy controls employing network modeling techniques and graph theoretical analyses methods. More specifically, Project 1 focused on the assessment of networks derived on the basis of white matter tractography. It was shown that regions outside the typically described CSTC circuitry appear to be of importance. In this regard, the left uncinate fasciculus connecting temporo-limbic to frontal areas may be critically involved. Additionally, various network measures indicated a potentially important role for amygdala and the temporal pole. Project 2 focused on the examination of networks based on gyrification covariance patterns, where gyrification was used as a proxy for neurodevelopment. It was shown that differences in gyrification-based covariance patterns may potentially be linked to time-locked periods of neurodevelopment, underlining the proposition of neurodevelopmental changes in OCD. Project 3 applied clustering methods to group patients according to their entire symptom profiles and subsequently related cluster status to hippocampus volumes. Results indicated that different symptom profiles indeed go along with volumetric differences in hippocampus, generally implying the

potential usefulness of taking into consideration the interrelation between various symptoms.

Taken together, the projects underline the necessity to further clarify the role of brain regions not typically associated with OCD pathophysiology and to incorporate these into current models. Additionally, the likely involvement of neurodevelopmental factors for the disease will hopefully spark new research while the consideration of symptom interrelations may be of use to reveal structure-symptom relationships that were previously not assessable.

ABBREVIATIONS

ACC - anterior cingulated cortex

BG - basal ganglia

BOLD - blood-oxygen-level dependent

CBT - cognitive behavioral therapy

CSTC - cortico-striato-thalamo-cortical

CT - computed tomography

DLPFC - dorsolateral prefrontal cortex

DSI - diffusion spectrum imaging

DWI - diffusion weighted imaging

DTI - diffusion tensor imaging

GPe - globus pallidus externa

GPi - globus pallidus interna

GLM - general linear model

lGI - local gyrification index

lOFC - lateral orbitofrontal cortex

mOFC - medial orbitofrontal cortex

MRI - magnetic resonance imaging

NBS - network-based statistic

NOS - number of streamlines

OCD - obsessive-compulsive disorder

OFC - orbitofrontal cortex

PCC - posterior cingulate

PET - positron emission tomography

SSNRI - selective serotonin-norepinehrine reuptake inhibitor

SSRI - selective serotonin reuptake inhibitor

SMA - supplementary motor area

SNr - substantia niagra

SPECT - single-photon emission computed tomography

TBI - traumatic brain injury

TBSS - tract-based spatial statistics

UF - uncinate fasciculus

VBM - voxel-based morphometry

VBR - ventricle to brain matter ratio

LIST OF FIGURES

TABLE OF CONTENTS

Chapter 1

General Introduction

1.1 Phenomenology of Obsessive-Compulsive Disorder

Consider the following episode:

After drowning the last zip of freshly brewed hot coffee you are getting ready to leave the apartment. What's on the agenda for today? 8 o'clock, meeting with your boss; 9 o'clock, meeting with a client to discuss business strategies for a new start-up; in the afternoon, team meeting to implement new SOPs etc. As you are pulling out of your driveway it suddenly hits you. Did I turn of the stove after making coffee? What if I left it on? Maybe even the moka is still sitting on the stove. Should I go back and check? I'd be running late though. But if I don't check and it is still on, god knows what might happen? The whole place might burn down! The doubt prevails and you go back to check. The stove is turned off and the moka is safely sitting in the sink. You are sensing a feeling of relief and finally drive off to work.

The above example or some variant thereof is most likely familiar to many of us. A quick thought suddenly appearing, causing doubt and anxiety or distress leads us to perform a certain behavior to reduce the distress. After performing the behavioral act, the distress disappears and we move on. Something quite similar happens in case of obsessive-compulsive disorder (OCD), though with a major and important difference. While a healthy person will most likely be relieved after performing a specific act and be reassured that the cause of discomfort has been resolved, patients suffering from OCD experience a short temporary relief, only to find themselves in the same situation over and over again for extended periods of time. They enter a circle of intrusive thoughts leading to distress and anxiety which leads to ritualized behavior and temporary relief. The following section will define the disorder more formally and report basic facts about symptoms, epidemiology, course, and treatment options.

1.1.1 Symptoms

OCD is a severely debilitating psychiatric disorder formally characterized by obsessions, i.e. intrusive and unwanted recurrent thoughts, images, or urges, and compulsions, i.e. acts that are performed in a repetitive manner. The performed acts can be mental and/or behavioral in nature and normally aim at reducing feelings of anxiety and distress often induced by obsessions. Furthermore the obsessions are recognized as products of the own mind (American Psychiatric Association, 2013). While a small percentage of patients may suffer either from obsessions or compulsions, the majority (>95%) report both symptoms to co-occur (Shavitt et al., 2014). The disease presents with a broad variety of symptoms from different symptom dimensions and is thus often considered to be rather heterogeneous (Leckman et al., 1997; Pauls et al., 2014). Clinically, the most prevalent symptom dimensions appear to be related to: contamination and cleaning; doubt about harm and checking; unacceptable thoughts and mental rituals; symmetry and ordering; cleanliness and washing as well as hoarding (Leckman et al., 1997; Williams et al., 2013). Importantly, up to 80% of all patients present with more than just one symptom (Ruscio et al., 2010) and cases of pure subtypes are extraordinarily rare, further highlighting the disease's heterogeneity (Mataix-Cols, Rosario-Campos, & Leckman, 2005). Despite the fact that diagnostics of OCD is typically based solely on the presence of obsessions, compulsions, and some form of distress or anxiety, a recent study points towards impairments in various neuropsychological domains that partially predict differential effects in response to cognitive behavioral therapy (CBT) or pharmacological treatment (D'Alcante et al., 2012). Meta-analytic aggregation of neuropsychological impairments in OCD however, revealed only small to medium effect sizes for various domains (Abramovitch, Abramowitz, & Mittelman, 2013) and the authors generally question the usefulness of neuropsychological alterations as potential endophenotypes.

1.1.2 Epidemiology, Disease Burden, and Comorbidity

With a one year prevalence of 1.2% among adults and a lifetime prevalence of 2.3% (Ruscio et al., 2010), OCD is ranked as the fourth most common psychiatric disorder (Veale & Roberts, 2014), with estimated annual costs in excess of 10 billion dollars in the US alone (Eaton et al., 2008). Additionally, OCD has a profound impact on patient's quality of life which is comparable to the impact reported in schizophrenia and depressive disorders and larger than for example in heroin dependence and hemodialysis patients (Macy et al.,

2013). First evidence also indicates a differential effect of obsessions and compulsions on quality of life (Stengler-Wenzke et al., 2007). A recent study highlighted the significantly increased risk of completed suicide (odds ratio=9.83) as well as attempted suicide (odds ratio=5.45) in OCD patients compared to healthy controls (Fernandez de la Cruz et al., 2017). The risk was reduced when adjusting for other psychiatric comorbidities, nevertheless remained at a substantially high level, pointing to important interaction effects of comorbidities for the disease. It is estimated that at least 50% of all patients additionally suffer from one or more psychiatric disorders (Abramowitz, Taylor, & McKay, 2009). The most common comorbid psychiatric disorders among OCD patients are major depressive disorder (MDD) with over 25%, obsessive-compulsive personality disorder and various forms of anxiety disorders (Brakoulias et al., 2017). However, accounts of other comorbid disorders are frequent. For example, reported co-occurrence rates of OCD and attention deficit/hyperactivity disorder (ADHD) have been rather inconsistent with estimates ranging between 0-60%, with variations likely due to methodological, theoretical, and phenomenological differences (Abramovitch et al., 2015). Additionally, Pallanti et al. (2011) reported a relationship between treatment non-responders and comorbid disorders while Hasler et al. (2005) provide evidence for a relationship between comorbid disorder and different symptom dimensions that patient's are suffering from. Finally, Hofer et al. (2018) reported that for adolescent and young adults prior OCD is a risk factor for developing bipolar disorder, bulimia nervosa, and anxiety disorders. Taken together, OCD can be described as a common psychiatric disorder with high impact on well-being and functioning that is commonly associated with other comorbid disorders.

1.1.3. Course

Disease onset is typically gradual (Abramowitz et al., 2009), however accounts of patients developing OCD like symptoms within weeks after traumatic brain injury (TBI) have been published (Childers et al., 1998). For a general overview of brain injuries associated with the development of OCD see Rydon-Grange and Coetzer (2015). In the US, the average age of onset is 19.5 years with more than 25% of all patients reporting an onset as early as 14 years or younger (Ruscio et al., 2010). Results from a large international collaboration study reported the average onset to be about 18 years (Brakoulias et al., 2017). The distribution of age of onset typically reveals a bimodal distribution with an early peak in adolescence and a second peak in early adulthood (Rasmussen & Tsuang, 1986) and there

is an ongoing debate regarding a sensible cut-off to define early and late onset OCD (Anholt et al., 2014). Interestingly, late onset OCD (age at onset > 35 years) was found to be rather uncommon with fewer than 15% of all cases (Rasmussen & Eisen, 1992). Additionally, Grant et al. (2007) provided first evidence of potentially better response to CBT in late onset OCD. If untreated, OCD has in most cases a chronic course (Abramowitz et al., 2009). In adults, remission rates without treatment are comparably low, i.e. about 20%, as reported by Skoog and Skoog (1999) in a forty year follow-up study. Similarly, a further study comprising over 200 patients found a partial recovery in only 22.1% of all patients over a five-year course without treatment (Eisen et al., 2013).

1.1.4 Treatment Options

The two most common treatment options for OCD are pharmacotherapy and various forms of psychological treatment. Meta-analytic results of randomized controlled trials provide evidence for efficacy of selective serotonin reuptake inhibitors (SSRIs) with a mean effect size of 0.91 (Eddy et al., 2004) and thus SSRIs are recommended as the first line of pharmacological treatment, though other pharmacological treatment options are available, e.g. clomipramine and venlafaxin. On the other side of the spectrum, CBT was identified to be effective (Abramowitz, 2006) with effect sizes of 1.31 for comparisons between patients treated with CBT and waiting-list patients (Ost et al., 2015). Nevertheless, Eisen et al. (2013) report relapse rates of 59% for pharmacologically treated, remitted patients, while rates for patients treated with CBT are found to be lower but still undesirably high (O'Neill & Feusner, 2015). For an extensive review of both treatment approaches see Abramowitz et al. (2009). Apart from CBT and pharmacological treatment, there has been an increased interest in alternative options such as deep-brain stimulation and surgical intervention for treatment resistant cases as well as prescription of neuroleptics (Hirschtritt, Bloch, & Mathews, 2017). Furthermore, preliminary evidence points towards the potential benefit of transcranial direct current stimulation for treatment resistant patient (Brunelin et al., 2018).

1.2. Pathogenesis and Neurobiology of OCD

One of the very first accounts of pharmacological intervention for OCD, using the mono-amine oxidase inhibitor phenelzine, dates back to the late 1960's. In a case study, Annesley (1969) mentions: "The discovery that certain neurotic illnesses will respond specifically to drugs implies a biochemical basis for some of these disorders". It took some 20 years until an article called: "Neurobiology of obsessive compulsive disorder: a possible role for serotonin" appeared in the Journal of Clinical Psychiatry (Winslow & Insel, 1990), explicitly using the word "neurobiology" in combination with OCD. More than 25 years later and mainly driven by the advent of *in-vivo* neuroimaging methods but also results from other fields such as pharmacological studies, genetics as well as animal model research etc., hundreds of articles have been published, aiming at further illucidating the neurobiological foundations of OCD by constantly refining disease models. Current accounts of pathogenesis identify genetic and environmental factors as well as neurobiological alterations as key factors. The following section will briefly describe aspects of genetics and environmental factors before providing a more extensive description of the prevailing neurobiological model, taking into account historical evidence on functional as well as structural brain alterations. Due to the scope of this manuscript, the descriptions will be selective and tend towards results based on human neuroimaging studies. Nevertheless, various lines of evidence derived from multiple methods have certainly influenced the current conceptualization of circuitry thought to be involved in OCD pathophysiology.

1.2.1 Genetic and Environmental Factors

Due to the fact that SSRIs are considered the first-line pharmacological treatment in OCD with proven efficacy, there has been a substantial interest in examining serotonin transporter polymorphisms. A recent meta-analysis of genetic association studies indeed reported an association of such polymorphisms with OCD as well as a gender specific polymorphism involving catecholamine modulation with trend significant results for dopamine- and glutamate-related polymorphisms (Taylor, 2013). However, association of genes was overall modest. Furthermore, it appears likely that there are substantial interactions between effects of multiple genes and phenotypic heterogeneity typically observed in OCD (Sinopoli et al., 2017). Meta-analysis of twin studies indicated that the largest proportion of variance in OCD symptoms is accounted for by additive genetic

effects as well as non-shared environmental factors (Taylor, 2011) pointing towards a complex interplay of biopsychosocial factors. For an attempt to integrate genetic, environmental, and neurobiological findings into a comprehensive model, see Pauls et al. (2014).

1.2.2 A Neurobiological Model of OCD

Several lines of evidence from multiple fields of study were aggregated over the years to form what is now often referred to as the cortic-striato-thalamo-cortical (CSTC) model of OCD. As can already be derived from the name, the model implicates several key regions such as basal ganglia (BG), various cortical regions, and thalamus. Furthermore it emphasizes the circuit character due to anatomical connections forming a loop. Historically, the BG were considered to be merely responsible for the "automatic execution of learned motor plans" (Marsden, 1982) and thus simply labeled a motor control organ. In line with this interpretation, the idea of a BG involvement in cognitive or even emotional processing was typically rejected. With a substantial increase in research efforts and the integration of various anatomical and physiological findings, this traditional view started to change. A seminal review by Alexander, DeLong, and Strick (1986) eventually shifted the concept of BG being a system only subserving motor functions towards being a system of segregated circuits with potentially different functional properties. This change in concept brought about strong implications also for clinical research. Namely, that damage to circuits may lead to alterations not only in motor behavior but possibly even cognition. Furthermore, it was suddenly conceivable that damage within a segregated circuit may result in a different outcome, i.e. symptom, than damage located within another circuit. Thus, symptoms were not necessarily limited to the motor domain. Soon after this conceptual shift, these ideas were absorbed by clinical researchers interested in OCD as well as other disorders and it was hypothesized that a pathogenetic mechanism of OCD may be a dysfunction in BG / striatal and thalamocortical circuits, though various authors favored slightly different structures and functional relationships in their accounts to describe neurobiological models of OCD (Insel, 1988; Modell et al., 1989; Rapoport & Wise, 1988). Fueling this new focus of research were studies conducted in OCD using various newly established neuroimgaing methods such as computed tomography (CT) and magnetic resonance imaging (MRI). While the first CT study conducted in OCD (Insel et al., 1983) reported no differences in ventricle to brain matter ratio (VBR), soon thereafter

multiple studies reported not only alterations in VBR (Behar et al., 1984) but also alterations in caudate volume (Luxenberg et al., 1988) and ventricular volume (Stein et al., 1993). Similarly, MRI-based studies revealed volume alterations mainly in caudate (Robinson et al., 1995; Scarone et al., 1992) and ACC (Garber et al., 1989). However, some studies also reported no differences between patients and controls (Aylward et al., 1996; Kellner et al., 1991). Altogether, MRI and CT studies appeared to confirm alterations in BG to be present in OCD. In parallel, new imaging methods provided results strongly impacting the conceptualization of neurobiological models of OCD. While CT as well as MRI only provided information about structural measures, PET and brain perfusion single-photon emission computed tomography (SPECT) had the advantage of deriving information about metabolism, a marker essentially related to brain function. Now it was possible to not only study structural abnormalities between patient and control groups, but also derive information about functional differences as well as observe functional changes in response to therapy or symptom provocation. A seminal study conducted using positron emission tomography (PET) reported increased metabolic rates in orbital gyrus and caudate (Baxter et al., 1987). The finding of increased ortbital gyrus metabolisms has since been replicated multiple times (Baxter et al., 1988; Nordahl et al., 1989; Sawle et al., 1991) with some studies also indicating alterations in various other regions such as the anterior cingulated cortex (ACC) (Perani et al., 1995; Swedo et al., 1989). Furthermore pre-/post-treatment PET studies found activity in orbitofrontal cortex (OFC) to decrease with pharmacological intervention. For a comprehensive review of PET and SPECT studies as well as early structural MRI studies, see Saxena et al. (1998). Several studies additionally found decreased metabolism in caudate (Benkelfat et al., 1990; Mindus & Nyman, 1991; Saxena et al., 1999) and loss of pathological correlations between key regions, i.e. OFC, thalamus and caudate (Baxter et al., 1992; Schwartz et al., 1996). Taken together, multiple independent studies found increased orbitofrontal metabolism in comparison to healthy subjects while there was evidence for increased caudate metabolism as well as involvement of thalamus.

As a general framework, fronto-striatal-thalamic circuits are considered to possess a direct and an indirect pathway (Saxena & Rauch, 2000). Originating within the frontal cortex, extensive projections excite striatal regions. Subsequently, a direct, inhibiting pathway projects to the globus pallidus interna (GPi) and substantia niagra (SNr) that in turn has an inhibiting effect on medial dorsal thalamus. Thus striatal inhibition of the inhibitory GPi and SNr leads to an increased excitation of thalamus and feedback to cortex. The indirect

pathway is based on inhibiting striatal projections to globus pallidus externa (GPe) and subthalamic nucleus that in turn send inhibiting projections directly to GPi and SNr and thus enhance the inhibiting effect on medial dorsal thalamus, effectively inhibiting feedback to cortex. Additionally, Saxena and Rauch (2000) propose that different sub-regions of frontal cortex project to separate striatal target regions, with projections from supplementary motor area (SMA) targeting putamen, dorsolateral prefrontal cortex (DLPFC) targeting the dorsolateral head of caudate nucleus, OFC targeting the ventromedial head of caudate, and ACC, posterior cingulate (PCC), and parahippocampal gyrus projecting to nucleus accumbens. Translating these basic features of fronto-striatal-thalamic circuitry to OCD pathophysiology, Saxena and Rauch (2000) proposed a response bias towards various stimuli in OCD that is mediated by frontal-subcortical circuits. In healthy condition the processing of stimuli is assumed to be mediated via the direct pathway with a counter balancing influence of the inhibiting, indirect pathway. In OCD patients, the authors suggest the existence of an imbalance between direct and indirect pathways in favor of the direct excitatory pathway. As a result, stimuli draw attention to themselves resulting in the inability to switch to other forms of behavior while also resulting in performing behaviors in a ritualistic manner. This mechanism is supposed to be responsible for the production of findings of hyperactive circuitry typically reported in neuroimaging studies. About a decade later, the framework of CSTC circuitry involvement is still considered the main foundation of neurobiological models of OCD. In a seminal paper, Milad and Rauch (2012) summarized the state of the art regarding the subsystems assumed to be involved in the pathophysiology of OCD. Additionally, they discuss the role of various regions outside the classical CSTC circuits regarding disease mechanisms and argue for a much needed extension of the classical framework (for a graphical representation of their model, see Figure 1). In this conceptualization, there are three explicitly separated circuits, each related to specific functions: the affective circuit linked to affect and reward processing; the dorsal cognitive circuit linked to working memory and executive functions; the ventral cognitive circuit linked to motor and response inhibition. However, Milad and Rauch (2012) claim the CSTC model to be insufficient and suggest other regions to be of importance. One critique involves the assumption of segregated fronto-striatal circuits. Especially in case of the reward circuitry, this assumption was shown to be flawed and connections are indeed more integrated than previously assumed (Haber & Knutson 2010).

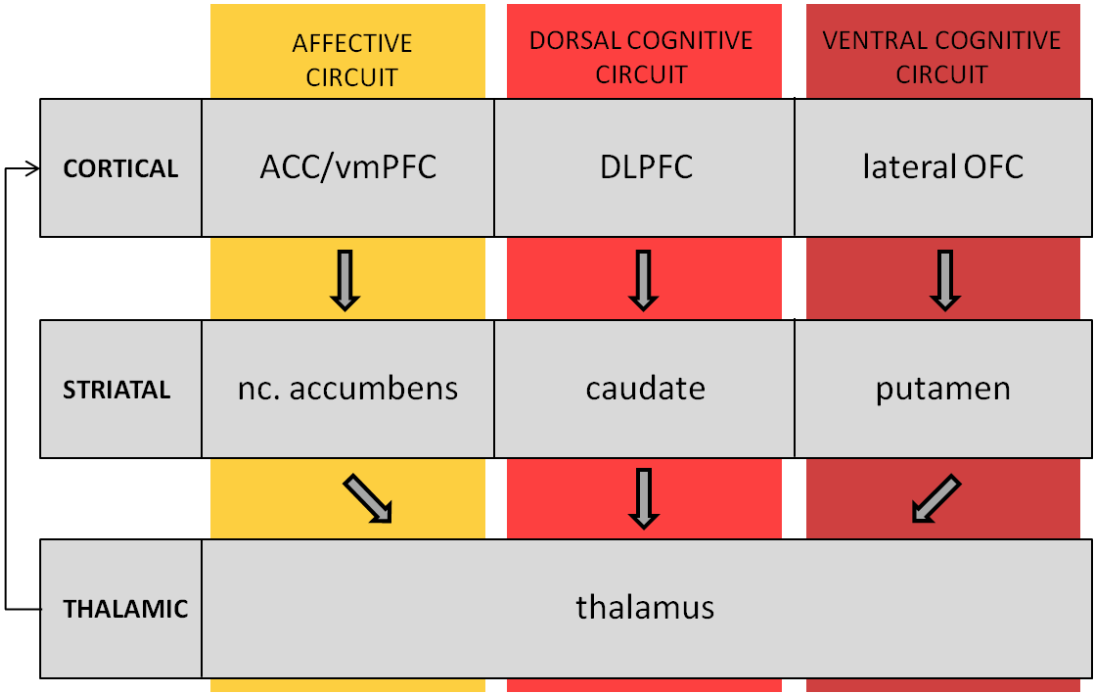

Figure 1. Illustration of components and pathways implicated in circuitry important for the pathophysiology of obsessive-compulsive disorder. Abbreviations: ACC, anterior cingulate cortex. DLPFC, dosrolateral prefrontal cortex. nc. accumbens, nucleus accumbens. OFC, orbitofrontal cortex. vmPFC, ventromedial prefrontal cotex. Modified from Milad & Rauch (2012).

One main aspect highlighted by Milad and Rauch (2012) refers to apparently differential functional aspects of OFC. Even though findings are somewhat contradictory regarding the directionality of activity alterations, i.e. hyper- vs. hypoactivity, the authors nevertheless posit, that lateral OFC (lOFC) and medial OFC (mOFC) are most likely involved in different functional impairments in OCD. Additionally, the ACC has been described as a region important for error monitoring (Bush et al., 2002; van Veen & Carter, 2002) and conflict detection (Gehring, Himle, & Nisenson, 2000). In OCD patients, a hyperactivity has been described during tasks assessing interference processing indicating abnormal error processing capabilities that may mediate decision making (Schlosser et al., 2010). Furthermore, the ACC has been implicated in fear conditioning processes, i.e. activity in dorsal ACC was reported to correlate with galvanic skin response during fear conditioning. Here, galvanic skin response is taken as a physiologic proxy for fear learning (Linnman et al., 2011; Milad et al., 2007). Finally, Milad and Rauch (2012) suggest to further clarify the role of amygdala for pathophysiological models of OCD. This claim has gained very recent

support by a meta-analysis evaluating emotional processing in OCD (Thorsen et al., 2018). Here, the authors identified fMRI- as well as PET-based studies assessing differences in responses between emotionally valenced and neutral stimulation. Compared with healthy controls, in OCD patients, an increase in activity was reported for bilateral amygdala, with stronger activation in unmedicated patients. Furthermore, activation in OFC, ACC and precuneus was related to symptom severity while comorbidity with mood and anxiety disorders was related to higher activation in amygdala, putamen, as well as insula and decreased activation in left amygdala and right ventro-medial prefrontal cortex (vmPFC). Taken together, while there is no doubt regarding the general involvement of CSTC circuits in the pathophysiology of OCD, different accounts that emphasize slightly varying structures and functional relationships have been put forward over the years (Aouizerate et al., 2004; Baxter et al., 1996; Del Casale et al., 2011; Huey et al., 2008; Insel, 1988; Kwon et al., 2009; Menzies et al., 2008; Milad & Rauch, 2012; Modell et al., 1989; Rapoport & Wise, 1988; Saxena, Bota, & Brody, 2001; Saxena et al., 1998; Saxena & Rauch, 2000). The current trend appears to facilitate research efforts aiming at elucidating the role of brain regions outside the classical CSTC circuits. This is for example reflected in a recent proposal of a neurobiological model for compulsive behavior put forward by van den Heuvel et al. (2016). Here a total of five circuits are proposed. Three of them are in accordance with the model proposed by Milad and Rauch (2012), namely the dorsal and ventral cognitive circuit as well as the affective circuit. As an extension, van den Heuvel et al. (2016) incorporate two additional circuits, i.e. a sensorimotor circuit connecting SMA, putamen and thalamus that is supposed to subserve stimulus-response based habitual behavior and a fronto-limbic circuit incorporating the amygdala and connections to vmPFC and thalamus, assumed to be important for processes of extinction.

In the past, OCD has also been discussed as a disorder featuring a neurodevelopmental component (Huyser et al., 2009; Rosenberg & Keshavan, 1998). As the development of gyrification has been shown to occur largely between the last two trimesters of gestation until about one year of age (Armstrong et al., 1995), measures thereof appear to be potentially useful markers of neurodevelopment. In line with this assumption, several studies provided evidence of alterations of gyrification in disorders associated with a neurodevelopmental component such as autism spectrum disorder (Ecker et al., 2016) and schizophrenia (Palaniyappan & Liddle, 2012; Palaniyappan et al., 2016; Palaniyappan et al., 2015). Evidence for alterations of gyrification in OCD is however somewhat heterogeneous

with many studies reporting hypogyrification (Rus et al., 2017; Shim et al., 2009; Wobrock et al., 2010) while others report hypergyrification (Fan et al., 2013).

1.2.3 Structure – Symptom Relationship in OCD

There is now accumulating evidence for structural brain alterations in OCD. For reviews and meta-analyses on white matter alterations see Fontenelle et al. (2009), Piras et al. (2013), Koch et al. (2014); for reviews on gray matter alterations see Radua and Mataix-Cols (2009), Boedhoe, Schmaal, Abe, Alonso, et al. (2017), Boedhoe, Schmaal, Abe, Ameis, et al. (2017), Hu et al. (2017); for a combined review of GM and WM alterations based on VBM studies see Piras et al. (2015). Besides descriptive findings of structural alterations, various studies assessed whether these alterations are going along with clinical measures such as symptom severity or specific symptoms. Meta-analytic results by Rotge et al. (2009) reveled a relationship between symptom severity and thalamic volumes. Alvarenga et al. (2012) report the symptom dimension “aggression” to positively correlate with GM volumes of left parietal cortex, while volumes of left insula, putamen and inferior OFC were negatively correlated. Scores for the “sexual/religious” dimension positively correlated with right lateral OFC as well as DLPFC and negatively correlated with ACC. Finally, hoarding scores positively correlated with left OFC while a negative correlation with parahippocampal gyrus was reported. Using a different instrument as well as approach to compute scores, van den Heuvel et al. (2009) similarly describe a relationship between different symptom dimensions and distinct brain regions. Here, GM volumes in caudate as well as WM volumes in parietal regions correlated with contamination/washing symptoms. Harm/checking symptoms correlated negatively, with GM and WM volumes in the temporal pole. Additionally symmetry/ordering symptoms correlated negatively with GM volume in right motor cortex, insula and parietal cortex, while a positive correlation with temporal GM and WM was found. Finally, symmetry/ordering symptoms were reported to correlate with overall GM and WM volumes. Gilbert et al. (2008) provide evidence for a negative correlation between washing symptoms and Brodman area 6, i.e. frontal cortex. Clearly, studies use different measures to assess symptoms and report various brain regions to be associated with different symptoms and additionally in sometimes contradicting directions. Also, while several studies do report such correlations (Fontenelle et al., 2011; Ha et al., 2009; Lochner et al., 2012) others do not (Nakamae et al., 2011; Zarei et al., 2011). Of note, the largest meta-analysis on subcortical volumetric

differences in OCD patients conducted to date reported alterations to be found in the hippocampus as well as pallidum (Boedhoe, Schmaal, Abe, Ameis, et al., 2017) while other subcortical regions typically assumed to play a major role in OCD were not found to display altered volumes. Additionally, no relationships between volumetric alterations and symptoms were described. In general, answering the question whether and how structural alterations are related to symptoms may be useful to identify and differentiate between state and trait markers for the disease. Trait markers are typically defined as a characteristic that allows diagnosing a disease while state markers refer to characteristics that are related to a process of a disease and reflect current severity (Davis et al., 2015). In summary, the currently available data does not allow to draw definitive conclusions on state or trait markers in OCD, nevertheless it appears promising to conduct further research, taking into consideration different approaches in order to disentangle potential relationships between structure and symptoms.

1.3 Methodological Considerations

Neuroimaging methods such as CT, MRI, and diffusion weighted imaging (DWI) are representatives of only one class of methods available to study brain morphology. Their main strength clearly stems from the human *in-vivo* applicability. However, in its current form, these methods are only able to provide information on the macro- and mesoscopic level of brain structure with rather limited capabilities to indirectly infer regionally specific information on microstructure (Lerch et al., 2017). Thus, this limitation should be considered when interpreting data and drawing conclusions. Apart from issues regarding the acquisition and meaning of measured signals, a major component of studying brain morphology involves complex analyses techniques, e.g. reconstruction algorithms as well as statistical concepts. The following section addresses three aspects: firstly, it will provide a brief overview of selected measures and analysis strategies typically employed to study brain morphology. Secondly, it introduces recent advances in studying brain morphometry in the framework of network science and graph theoretical concepts. For the following sections, the focus will be mainly on data derived from *in-vivo* human MR-imaging. Thirdly, a brief overview of the measures and methods used to study brain morphometry in the current studies will be presented.

1.3.1 Classical Approaches to Study Brain Morphology

1.3.1.1 Volume and Surface Based Methods

To date, the most prevalent approaches to examine MRI-based morphology and alterations thereof can be differentiated into volume and surface based methods (Clarkson et al., 2011). Brain data derived from MRI is typically stored in three dimensional matrices. Each element of such a matrix is considered a voxel, i.e. the three dimensional analog to a pixel, that represents information about some anatomically relevant parameter. Voxel-based methods directly operate on the elements of this matrix. Though transformations (linear as well as nonlinear) are common, the “units” being analyzed will always remain voxels. As an example, in the framework of voxel-based morphometry (VBM), images are spatially normalized into a common space using linear and nonlinear transformations, segmented into various tissue classes and spatially smoothed before computing statistics on the voxel level (Ashburner & Friston, 2000; Whitwell, 2009). Similarly, when working with surface based methods, processing of data involves creating surface models and

deriving brain morphological parameters in three dimensional space (Dale, Fischl, & Sereno, 1999; Fischl, Sereno, & Dale, 1999). Instead of voxels, the “units” being analyzed are vertices. Nevertheless, analyses will typically be conducted on individual data points reflecting an anatomical property. Examples of surface based morphometry can be found in studies of cortical thickness (Fischl & Dale, 2000), a measure that is computed vertex-wise from the distance between two surfaces, i.e. gray / white matter boundary and gray matter / cerebrospinal fluid boundary.

1.3.1.2 Commonly Used Statistical Analysis Framework

The most prevalent statistical framework used to assess and compare morphological properties, derived either from volume or surface based methods, is the GLM, i.e. general linear model (Christensen, 2011). This statistical approach yields information about local morphological properties only, since one linear regression model is fitted to every single voxel or vertex, thus resulting in statistical maps with parameters / p-values for each voxel within a volume, or vertex for each surface. For both, volume as well as surface based approaches, the interrelation between measures from different voxels or vertices is not specifically considered. While these approaches are entirely valid in its own right and have provided many new insights into structural brain alterations associated with OCD (Piras et al., 2013; Piras et al., 2015) as well as other disorders (Whitwell, 2009), they nevertheless do not allow to draw inferences about the interplay between various anatomical regions. Especially in light of neurobiological models of OCD pathopyhsiology that emphasize a circuit character with interdependent anatomical regions, a framework that has the capacity to explicitly model such interdependencies could potentially be very fruitful and informative.

1.3.1.3 Assessing Relationships Between Symptoms and Morphological Alterations

The majority of studies conducted in OCD aimed at establishing a relationship between structural alterations and different symptoms and/or symptom severity. In general, various measures, e.g. cortical thickness, volume etc., are typically correlated with scores from questionnaires aiming at identifying significant correlations. Two slightly different approaches are commonly used in this regard. One possibility is correlating the severity on a specific symptom scale, e.g. washing or checking, with a morphological parameter. Here,

each symptom is treated as an independent quantity and the interrelation between various symptom types is not further addressed (Carmona et al., 2007; Matsumoto et al., 2010; Park & Jeong, 2015; Tang et al., 2015; Zarei et al., 2011). Another way is to use information either from questionnaires that specifically aim at deriving information about symptom dimensions (Rosario-Campos et al., 2006) such as contamination, aggression or symmetry, or to combine information from various subscales into symptom dimensions, for example symmetry/ordering or harm/checking (Mataix-Cols et al., 1999; Okada et al., 2015; van den Heuvel et al., 2009). In both cases, the focus is on individual symptoms or symptom dimensions. However, it is conceivable that the entire symptom profile of a patient may be related to morphological alterations. Hence, taking into consideration interrelations between the various symptoms/symptom dimensions might be of value.

1.3.2 Network-science Inspired Approaches to Study Brain Morphology

In 2005, several researchers independently proposed to use the term 'connectome' to refer to a comprehensive map of all structural elements and their connections, together forming the human brain (Hagmann, 2005; Sporns, Tononi, & Kotter, 2005). This conceptualization as an underlying foundational principle sparked tremendous research interest eventually leading to the field of connectomics. As mentioned above, frameworks that have the capacity to model networks of anatomical (and functional) relationships are highly desirable. With rapid progress in the field of complex network analysis and the impact of network science as a transdisciplinary theory (Boccaletti et al., 2006; Newman, 2010), translation of principles and practices to the study of brain networks are appearing rapidly while constantly increasing in scope and size (Bullmore & Sporns, 2009). The translation of concepts was dramatically simplified by conceptualizing human brain networks in terms of connectivity matrices[1], therefore allowing to directly apply concepts that were developed in the mathematical framework of graph theory and largely based on working with matrices. The main workhorse for network-based analyses of brain data is therefore the mathematical framework of graph theory, which is briefly introduced below. Additionally, general approaches to graph definition and assessment of brain networks are addressed and the clinical impact of network-based studies is outlined.

[1] Here, a connectivity matrix is a square matrix in which each element A_{ij} indicates the presence or absence of a connection between the structural elements *i* and *j*.

1.3.2.1 General Framework

Conceptualizing the brain as a network and applying graph theoretical concepts for analyses requires the definition of graphs, i.e. a set of nodes and edges. Nodes are the basic building blocks of the network, while edges represent some form of connection between the nodes, together resulting in an abstract representation of the network in question using matrix notation. This framework is rather flexible as the definition of nodes can range all the way from single cells, or even smaller, up to macroscopically defined anatomical regions such as gyri. Likewise, the definition of edges can be based for example on synaptic connectivity derived from tracing studies, measures of structural association derived from DWI-based fiber tracking, or even correlation between blood-oxygen-level dependent (BOLD) signals indicating a statistical association of functional coupling between nodes (for a thorough introduction to the framework as well as applications to brain network analyses see Sporns (2012); for a comprehensive and more technical introduction see Fornito, Zalesky, and Bullmore (2016).

1.3.2.2 Construction of Brain Networks

In light of the explosion of research conducted on brain function and the ever increasing applications of network-based analyses to functional networks, it nevertheless remains vital to also study structural brain networks spanning all levels from molecular to the macro scale. In the end “structural connectivity provides an obligatory foundational model for understanding functional localization at molecular, cellular, systems, and behavioral organization levels” (Swanson & Bota, 2010). In case of MR-derived structural networks, multiple approaches are commonly used for graph construction (Griffa et al., 2013). Nodes are typically defined on the basis of parcellated high resolution anatomical imaging data according to predefined atlas-based regions of interest. Atlases in turn are commonly based on either anatomical landmarks such as sulci and gyri, or cytoarchitectonic maps. Recent developments aim at parcellating the brain based not only on anatomical landmarks or cytoarchitecture, but to provide a multi-modal parcellation scheme incorporating landmarks and cytoarchitecture, as well as prior knowledge of function and connectivity (Glasser et al., 2016). The way in which an edge is defined, in turn determines what kind of graph is constructed and thus what type of analyses methods and algorithms can be applied. The most commonly defined graphs are either undirected or directed and the connections are either weighted or unweighted (Rubinov & Sporns, 2010). For

example, edges defined as synaptic connections, i.e. at the microscopic level, inherently carry information about the directionality of a connection, whereas edges defined on the basis of tractography only carry undirected information. Similarly, a graph can contain information about the connection strength, e.g. number and type of synapses, rendering it to be weighted, or can simply indicate whether a connection is present or not, rendering it binary. The definition of edges, measuring some form of connectivity, can be broadly separated into two approaches, though other approaches exist. Firstly, it is possible to derive measures of connectivity on the basis of the concept of structural covariance (Alexander-Bloch et al., 2013). Structural covariance refers to the observation that in populations, quantification of specific morphological properties within one brain region typically covaries with the same property in other brain regions, e.g. cortical thickness values measured in Broca's area across subjects covary with cortical thickness values in Wernicke's area (Lerch et al., 2006). Secondly, structural connectivity can be inferred from DWI by applying tractography algorithms for example to model a tensor (as is done in DTI, see Mori and Zhang (2006)) that yields information on the directionality of diffusion within a specific voxel, thus allowing the reconstruction of main fiber bundles in the brain (Soares et al., 2013). In order to derive a proxy for structural connectivity between two brain regions, a fiber tracking algorithm may be initiated from a parcellated brain region, i.e. node of the graph, following the principle diffusion direction indicated by the tensor in each voxel. If there is a continuous connection between the initial node and some other node in question, the two regions are assumed to be connected (Lazar, 2010). Repeating this approach for every possible combination of nodes allows to reconstruct a macroanatomical whole brain connectivity matrix (Guye et al., 2010). The resolution is directly related to the parcellation scheme, i.e. a fine-grained parcellation increases the resolution while a gross parcellation scheme decreases resolution. The major difference between networks based on structural covariance and those based on diffusion weighted imaging, is the fact that structural covariance can be only measured across a group of subjects, while diffusion weighted imaging allows to infer connectivity within a single subject. This limits the possibility to use structural covariance to derive subject-specific, individual parameters (Alexander-Bloch et al., 2013).

1.3.2.3 Assessment of Brain Networks

Historically, two seemingly opposing concepts regarding the functional principles of the brain have been widely discussed. On the one hand, proponents of localizationism emphasize that in the brain, specific functions are localized in specific modules, e.g. Broca's region is functionally specialized for speech production. On the other hand, the standpoint of holisms, conceptualizes the brain as a system that in its entirety is important for producing behavior and in which a function cannot be assigned exclusively to one region alone (Kanwisher, 2010; Northoff, 2014). Interestingly, these approaches can be related to organizational properties that are simultaneously found in the brain, namely functional segregation, and functional integration (Sporns et al., 2005; Tononi, Sporns, & Edelman, 1994). Following these two fundamental organizational principles, a wide array of measures has been developed to quantitatively assess brain network topology in terms of functional segregation and integration. Measures of segregation are aiming at the quantification of groups or modules that are densely interconnected, thus allowing for a high degree of specialization, for example the clustering coefficient that can be computed for nodes as well as for an entire network. Measures of integration are typically based on finding shortest paths, i.e. the shortest number of steps needed to traverse between two specific nodes (Rubinov & Sporns, 2010). Relating both measures in terms of a ratio yields a global metric called small-worldness, a concept that was introduced by Watts and Strogatz (1998). In their seminal work they described a graph to possess the attribute of small-worldness if many nodes are not direct neighbors but rather cluster together, i.e. average clustering is rather high, while at the same time, every node can be reached via few steps, in other words the path length is rather low. The principle of small-worldness was shown to apply to a myriad of networks (Newman, 2010) including the brain (Bassett & Bullmore, 2006). Taken together, the brain is an organ inherently combining two fundamental organization principles, namely functional segregation as well as functional integration in order to allow for flexibility in cognition as well as behavior (Deco et al., 2015). A vast number of measures have been used to characterize various properties of segregation and integration capabilities of brain networks (Rubinov & Sporns, 2010; Sporns, 2013b) as well as other organizational principles (Fornito et al., 2016).

1.3.2.4 Clinical Impact of Network-based Studies

In general, the assessment of structural brain networks can be conducted in healthy brains in order to infer patterns of connectivity and also inform underlying relationships with patterns of brain dynamics (Sporns, 2013a). Furthermore, the same methods can be applied to examine psychiatric populations or patients suffering from neurological disorders. Traditionally, studies examining structural as well as functional brain imaging data in psychiatric populations often report changes in a multitude of different, discrete brain regions. However, interpreting focal changes in isolation may ignore important and relevant relationships between regions, especially in light of the massive interconnectedness of brain regions resulting in complex circuitry (Hulshoff Pol & Bullmore, 2013). In this regard, network-based approaches allow us to draw conclusions about brain organization and pathological mechanisms that extend beyond treating regions in isolation with the potential to derive new theories about aetiopathology (Fornito & Bullmore, 2015). An ever increasing body of literature suggests that brain disorders indeed go along with alterations in structural as well as functional large-scale brain networks (Fornito, Zalesky, & Breakspear, 2015; Griffa et al., 2013; Wen, He, & Sachdev, 2011). Consequently, recent endeavors led to the foundation of pathoconnectomics, i.e. the mapping of abnormal brain networks, under the assumption that psychiatric disorders are in fact disorders that manifest on the level of networks and therefore require an examination of network level organization (Rubinov & Bullmore, 2013). In order to better understand the underlying pathogenetic principles and meachnisms of psychiatric disorders, different perspectives can be utilized to examine networks. More precisely, networks can be interrogated at the circuit level, on the level of topology or by employing hypothesis-free, data-driven approaches on a connectome-wide basis (Fornito & Bullmore, 2015). As an example of the circuit level perspective, Seeley et al. (2009) could show that specific dementia syndromes differentially target functional connectivity networks. Regarding network topology, interesting results regarding the importance of hubs and their implication in a broad range of different brain disorders were provided by (van den Heuvel & Sporns, 2013), while the data-driven approach taken in connectome-wide studies allows for unbiased assessment of global network characteristics. As an example, Zalesky et al. (2011) could show that white matter network efficiency in schizophrenia was not associated with performance regarding intellectual ability while it was associated in healthy control subjects.

1.3.3 Methods and Measures used in Current Studies

The following section briefly describes the methods used to construct the brain graphs analyzed in Project 1 and 2 as well as the measure used in project 3. Of note, the descriptions are conceptual and several intermediate steps are not explicitly mentioned. All three projects described in this thesis strongly draw on Freesurfer, a software suite designed to allow processing and analysis of brain imaging data (Dale et al., 1999; Fischl et al., 1999). In short, a high resolution structural T1-weighted image (Figure 2A) was used to identify gray/white matter (Figure 2B, colored in red) as well as gray matter/pial boundaries (Figure 2B, colored in green). Based on these boundaries, two corresponding surfaces were reconstructed for each subject (Figure 2C). Subsequently the brain was parcellated according to an atlas into discrete cortical and subcortical brain regions (Figure 2D). In case of Project 3, hippocampus volumes were computed for each subject based on subcortical volumetric data (lower part of Figure 2D). For Project 1 and 2, the parcellated brain regions were defined as the nodes thus allowing the derivation of connectivity matrices (Figure 2E). Figure 3 illustrates the derivation of the connectivity measure used within Project 1 and 2. In both cases, the resulting connectivity matrices were depicting undirected, weighted graph.

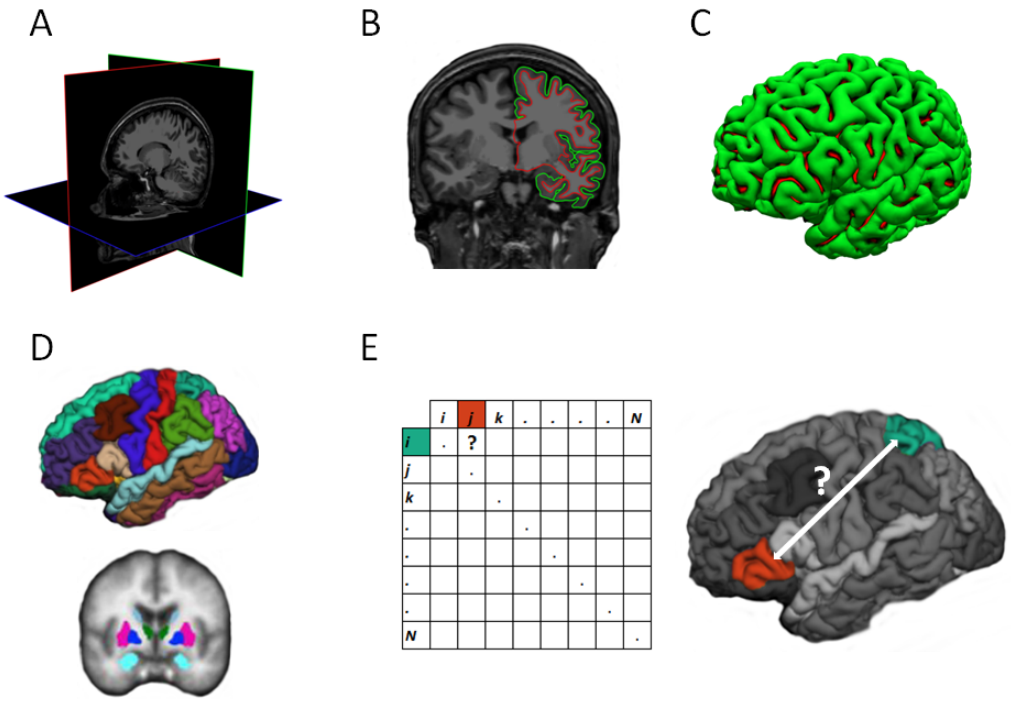

Figure 2: Illustration of node derivation
A) T1-weighted MR image. B) Identification of gray matter/white matter boundary, depicted in red, and white matter/pial boundary, depicted in green. C) Reconstructed surface representation. D) Atlas-based parcellation into descrete cortical and subcortical brain regions. E) Arrangement of nodes in form of an adjacency matrix.

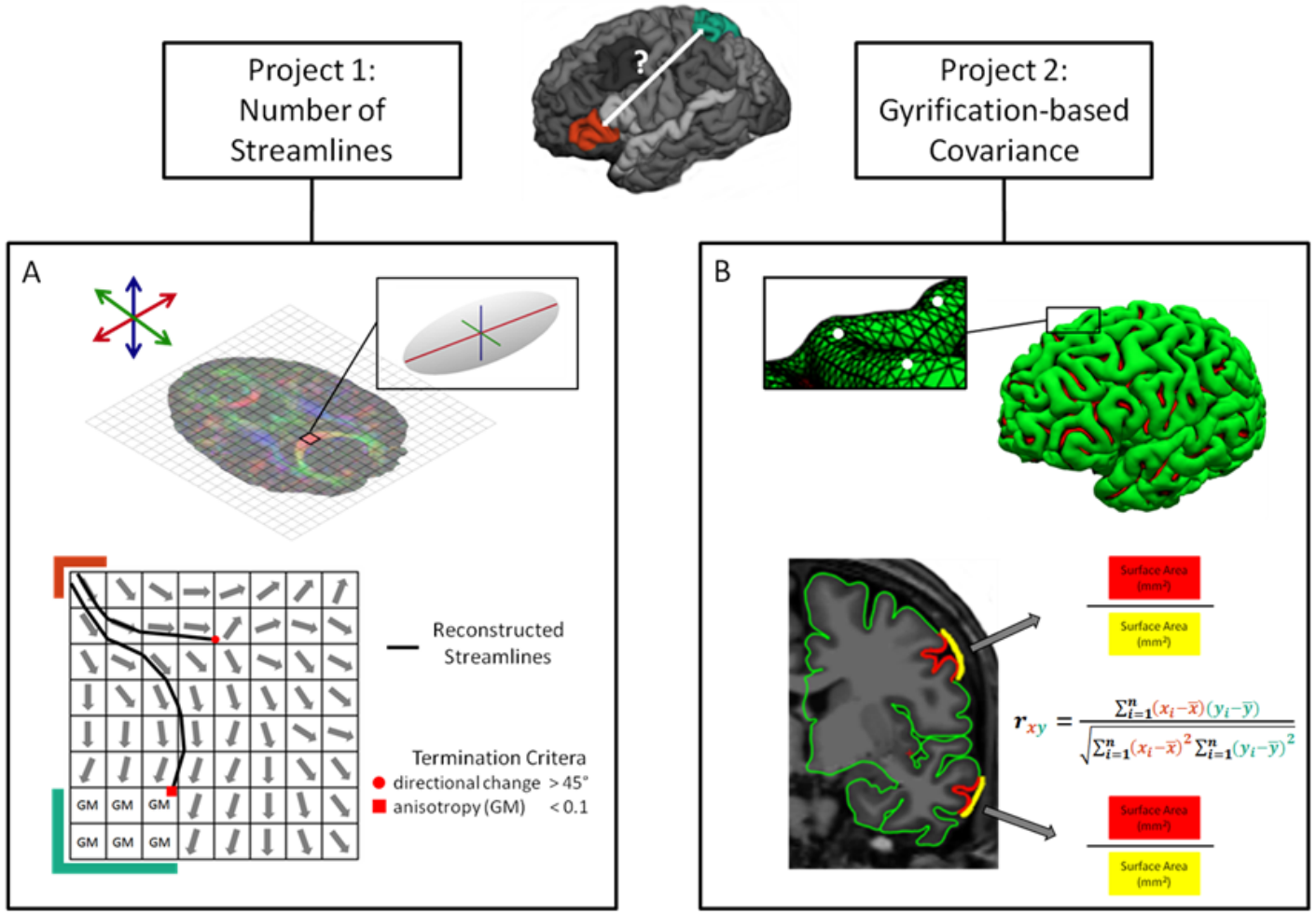

Figure 3: Illustration of measures used to define edge weights.

A) Based on diffusion weighted imaging data, one tensor is calculated for each voxel and its principle diffusion direction is used to re-construct streamlines by following the direc-tion until specific termination criteria are met. Here, termination occured in case of abrupt directional changes (>45°), FA values < 0.1 or in case of reaching limits imposed by the brain mask. The number of reconstructed streamlines between two regions is used as the edge weight. B) Based on reconstructed pial surfaces, the ratio of the pial surface area (depicted in red) below evenly spaced regions of interests adjacent to the outer pial surface (depicted in yellow) is computed for every node resulting in a local gyrification index for for each region of interest. Sub-sequently, the local gyrification indices of two regions are correlated to derive the edge weight.

For Project 1, the edge weights were defined on the basis of fiber tracking algorithms that derive information about white matter tracts on the basis of DWI data. More specifically, for every possible combination of nodes, an algorithm is initiated that follows the principle diffusion direction derived by fitting a tensor to each voxel's FA data and tracking is stopped in accordance with various termination criteria (Figure 3A). For Project 2, the edge weights were defined on the basis of local gyrification indices (lGI). The index is computed by dividing the pial surface area under a ROI that is adjacent to the pial surface by the size of the ROI itself (Schaer et al., 2008). Thus, a large index indicates that the surface area below the ROI is large when compared to the ROI itself, pointing towards stronger cortical convolution, i.e. gyrification (Figure 3B). lGIs were computed for evenly spaced vertices (white dots in top row of Figure 3B) over the cortical surface, and subsequently averaged within nodes. After acquiring the lGIs and adjusting their values for the effects of various covariates, a correlation between every possible pair of nodes was computed and subsequently used as the edge weight (Figure 3B).

1.4 Aims of the Thesis

The overall goal was two-fold. Firstly, to employ innovative brain network modeling and analyses techniques to examine how alterations in MRI-derived structural brain networks may inform pathophysiological models of OCD as well as aiming at generating new hypotheses that can potentially be examined using other morphological techniques. To this end, connectome-wide anatomical networks were constructed based on parcellations of high resolution T1-weighted MRI sequences and two different measures of structural connectivity. In the first project, connectivity networks were derived from DTI tractography allowing to draw inferences about macroanatomical, white matter structural connectivity differences as well as topological properties. In the second project, the framework of structural covariance was applied using a network based approach in conjunction with local gyrification indices as a measure related to neurodevelopmental aspects. Probing whether alterations in gyrification based networks exist can potentially inform neurobiological models of OCD in this regard. Secondly, in light of recent findings regarding hippocampal volume alterations in OCD (see section 1.2.3) it was examined whether the consideration of symptom profiles allowed to identify relationships between hipopcampal volumes and symptom related parameters that extend beyond simple associations found between isolated symptoms and morphological alterations.

Chapter 2

Project 1: “Connectomics-based structural network alterations in obsessive-compulsive disorder”

The current chapter includes the research article “Connectomics-based structural network alterations in obsessive-compulsive disorder”. This article provides evidence for an involvement of mainly temporo-limbic regions in OCD that are typically associated with emotion processing by analyzing brain networks derived from structural T1-weighted MRI data in conjunction with (DTI). It thus provides further support of the need to revise the classical model of pathophysiology. The article was published in Translational Psychiatry in 2016.

Contributions:

Authors: *Tim Jonas Reess, Oana Georgiana Rus, Ruben Schmidt, Marcel A. de Reus, Michael Zaudig, Gerd Wagner, Claus Zimmer, Martijn P. van den Heuvel, Kathrin Koch*

The author of this thesis is the first author of the manuscript. **T.J.R.**, K.K., O.G.R., with the help of M.Z., C.Z., and G.W. conceived the experiment. **T.J.R.** and O.G.R. recruited participants and conducted data acquisition. **T.J.R.**, R.S., M.A.D.R, M.P.v.d.H performed analyses and contributed analytic tools. **T.J.R.** wrote the manuscript in consultation with O.G.R., R.S., M.A.d.R., M.Z., G.W., C.Z., M.P.v.d.H., K.K. All authors discussed the results and revised the final manuscript.

OPEN

Citation: Transl Psychiatry (2016) **6**, e882; doi:10.1038/tp.2016.163

www.nature.com/tp

ORIGINAL ARTICLE

Connectomics-based structural network alterations in obsessive-compulsive disorder

TJ Reess[1,2], OG Rus[1,2], R Schmidt[3], MA de Reus[4], M Zaudig[5], G Wagner[6], C Zimmer[1], MP van den Heuvel[4,7] and K Koch[1,2,7]

Given the strong involvement of affect in obsessive-compulsive disorder (OCD) and recent findings, the current cortico-striato-thalamo-cortical (CSTC) model of pathophysiology has repeatedly been questioned regarding the specific role of regions involved in emotion processing such as limbic areas. Employing a connectomics approach enables us to characterize structural connectivity on a whole-brain level, extending beyond the CSTC circuitry. Whole-brain structural networks of 41 patients and 42 matched healthy controls were analyzed based on 83×83 connectivity matrices derived from cortical and subcortical parcellation of structural T1-weighted magnetic resonance scans and deterministic fiber tracking based on diffusion tensor imaging data. To assess group differences in structural connectivity, the framework of network-based statistic (NBS) was applied. Graph theoretical measures were calculated to further assess local and global network characteristics. The NBS analysis revealed a single network consistently displaying decreased structural connectivity in patients comprising orbitofrontal, striatal, insula and temporo-limbic areas. In addition, graph theoretical measures indicated local alterations for amygdala and temporal pole while the overall topology of the network was preserved. To the best of our knowledge, this is the first study combining the NBS with graph theoretical measures in OCD. Along with regions commonly described in the CSTC model of pathophysiology, our results indicate an involvement of mainly temporo-limbic regions typically associated with emotion processing supporting their importance for neurobiological alterations in OCD.

Translational Psychiatry (2016) **6,** e882; doi:10.1038/tp.2016.163; published online 6 September 2016

INTRODUCTION

Obsessive-compulsive disorder (OCD) is a psychiatric disorder characterized by recurrent, persistent and intrusive thoughts or images typically causing distress or anxiety (that is, obsessions), and repetitive behaviors aimed at reducing the feeling of anxiety (that is, compulsions).[1] Traditionally, alterations in cortico-striato-thalamo-cortical (CSTC) circuitry have been associated with the pathophysiology of OCD.[2] The CSTC model differentiates between affective and cognitive circuits, reflecting an impact of associated structures on emotional and cognitive functioning. However, it has recently been pointed out that the prevailing model does not specifically take into account the involvement of other structures such as amygdala and hippocampus and their interactions with frontal areas in mediating anxiety.[2] Likewise, Menzies *et al.*[3] concluded that several brain regions outside of the classical CSTC model may play a role in the pathophysiology. Based on a review of voxel-based morphometry (VBM) studies in OCD and in line with the aforementioned studies, Piras *et al.*[4] similarly state an involvement of structural alterations in regions outside of the CSTC loops such as temporo-limbic regions to be relevant in OCD. Taken together, there is emerging evidence suggesting several brain regions other than fronto-thalamo-cortical areas to play a major role in the pathophysiology of OCD.

Progress has been made in identifying structural alterations in a broad range of psychiatric diseases using various methods such as VBM,[5] and diffusion-weighted imaging.[6] With the advent of connectomics, it is now feasible to shift the view from a regional perspective toward a network perspective based on the integration of various forms of anatomical data to assess connectivity of networks in brain disease,[7] including psychiatric disorders.[8–10] The conceptualization of the brain as a complex network calls for different approaches in modeling and analysis to infer information from brain magnetic resonance (MR) images and the mathematical framework of graph theory has proven to be especially useful in the analysis of such data.[11] A broad range of measures can be calculated to assess topological properties of underlying brain graphs.[12] Assessing these measures, one can potentially derive information about fundamental organizational properties in a specific group or compute differences between groups[13] (for example, healthy controls vs psychiatric populations).[14]

To date, most studies addressing network alterations in OCD have focused on functional networks derived from resting-state functional magnetic resonance imaging (rs-fMRI).[15–18] Within a control network comprising frontal, parietal and cingulate cortex, as well as precuneus, thalamus and cerebellum, patients displayed alterations in small-world parameters.[15] A recent study[18] found decreased connectivity within the limbic system (amygdala and hippocampus) potentially related to problems with implicit learning and emotion processing observable in OCD patients. In addition, the same study reported an increase in connectivity within the executive/attention network in OCD possibly related to

[1]Department of Neuroradiology & TUM-Neuroimaging Center (TUM-NIC), Klinikum rechts der Isar, Technische Universität München, Munich, Germany; [2]Graduate School of Systemic Neurosciences GSN, Ludwig-Maximilians-Universität, Biocenter, Munich, Germany; [3]Department of Neurology, Brain Center Rudolf Magnus, University Medical Center Utrecht, Utrecht, The Netherlands; [4]Department of Psychiatry, Brain Center Rudolf Magnus, University Medical Center Utrecht, Utrecht, The Netherlands; [5]Windach Institute and Hospital of Neurobehavioural Research and Therapy (WINTR), Windach, Germany and [6]Department of Psychiatry and Psychotherapy, Jena University Hospital, Jena, Germany. Correspondence: TJ Reess, Department of Neuroradiology & TUM-Neuroimaging Center (TUM-NIC), Klinikum rechts der Isar, Technische Universität München, Ismaninger Strasse 22, München 81675, Germany.
E-mail: tim.reess@tum.de
[7]These authors contributed equally to this work.
Received 9 November 2015; revised 11 July 2016; accepted 18 July 2016

Table 1. Demographic and clinical sample characteristics

Characteristics	*OCD* (n = *41*)	*HC* (n = *42*)	P-*value*
	n *(%) or Mean* ± *s.d. (range)*	n *(%) or Mean* ± *s.d. (range)*	
Female	27 (65.9%)	24 (57.1%)	$P = 0.42$
Age (Years)	32.5 ± 10.0 (20–63)	31.8 ± 8.3 (20–57)	$P = 0.73$
Age of onset	15.9 ± 6.40	—	
Disease duration	16.8 ± 10.6	—	
Y-BOCS total	22.0 ± 5.4 (15–36)	—	
Obsession	11.4 ± 3.2 (4–17)	—	
Compulsions	10.6 ± 3.5 (0–19)	—	
OCI-R total	25.2 ± 9.2 (9–47)	—	
Hoarding	2.6 ± 2.9 (0–11)	—	
Checking	5.9 ± 3.2 (1–12)	—	
Ordering	3.5 ± 3.7 (0–12)	—	
Neutralizing	1.9 ± 2.6 (0–10)	—	
Washing	4.6 ± 3.7 (0–11)	—	
Obsessing	6.8 ± 3.0 (1–12)	—	
BDI	18.1 ± 11.4 (0–53)	—	
Comorbidities	22 (53.7%)	—	
Depression	12 (29.3%)	—	
Anxiety	3 (7.3%)	—	
Depression and anxiety	3 (7.3%)	—	
Personality disorder	1 (2.4%)	—	
Eating disorder	1 (2.4%)	—	
Depression, anxiety, ADHD	1 (2.4%)	—	
Depression, eating disorder, personality disorder	1 (2.4%)	—	
Medication	29 (70.7%)	—	
SSRI	16 (55.2%)	—	
TCA	4 (13.8%)	—	
SSRI+antipsychotic	3 (10.3%)	—	
SSRNI	2 (6.9%)	—	
SSRI+methylphenidate	1 (3.4%)	—	
SSNRI+methylphenidate	1 (3.4%)	—	
NDRI+SSNRI	1 (3.4%)	—	
Benzodiazepine+antipsychotic	1 (3.4%)	—	

Abbreviations: ADHD, attention deficit hyperactivity disorder; BDI, Beck Depression Inventory; HC, healthy controls; NDRI, norepinephrine-dopamine reuptake inhibitor; OCD, obsessive-compulsive disorder; OCI-R, Obsession-Compulsion Inventory revisited; SSNRI, selective serotonin–norepinephrine reuptake inhibitor; SSRI, selective serotonin reuptake inhibitor; TCA, tricyclic antidepressant; Y-BOCS, Yale-Brown Obsessive-Compulsive Scale.

excessive monitoring and impairments in coping with threat/uncertainty. Only very few studies have examined alterations in structural networks in OCD using the method of connectomics. One study[19] focused on cortical thickness and due to the nature of the specific measure had to disregard subcortical structures assumed to be of major importance in OCD. The only study[20] defining structural networks based on diffusion data, reports disrupted topological organization in OCD as well as reduced nodal efficiency in frontal and parietal regions as well as the caudate.

An important question is whether functional alterations observed across studies have a structural correlate. Thus far, no study to date has focused on structural network alterations in OCD using/adopting a network-based statistic (NBS) approach.[14] The current study aims at examining differences in the structural connectome in a fairly large sample of 41 OCD patients and 42 healthy controls based on the combination of anatomical and fiber tracking data derived from high-resolution structural MR scans and diffusion tensor imaging. Two approaches are used: NBS is applied to assess differences in specific topological features of networks, effectively controlling for the multiple comparison problem. Second, graph theoretical measures are applied to further identify potential changes in topologic properties. Since there is accumulating evidence for an involvement of regions outside the CSTC circuits in OCD, we expected to find structural alterations in areas not limited to CSTC loops. More specifically, due to the nature of the disease we expected an involvement of areas implicated in anxiety and emotion processing.

MATERIALS AND METHODS

Participants

A total of $n = 41$ patients with OCD as the primary diagnosis according to DSM-IV criteria were included in the study. All diagnoses were made by an experienced psychiatrist from the Windach Institute and Hospital of Neurobehavioural Research and Therapy specialized in the treatment of OCD. As a control group $n = 42$ age- and gender-matched healthy subjects were included (for demographic and clinical characteristics see Table 1).

Exclusion criteria for both groups were a history of clinically important head injuries, seizures or neurological diseases. There were no significant differences between healthy controls and OCD patients regarding age (t-test; $P = 0.73$) and gender (χ^2-test; $P = 0.42$). At time of the study, $n = 12$ patients were drug-naive or medication-free for at least 3 weeks. No patients were excluded due to comorbidities and $n = 22$ patients had one or more comorbid diagnoses. Healthy controls with a history of psychiatric illness were excluded. All patients and controls were right-handed as assessed by Annett´s handedness inventory.[21] The patients were recruited from the Windach Institute and Hospital of Neurobehavioural Research and Therapy, Germany. To assess clinical severity of obsessive-compulsive

symptoms, patients were handed the self-rated version of the Yale-Brown Obsessive-Compulsive Scale (Y-BOCS)[22–24] as well as the Obsession-Compulsion Inventory revisited (OCI-R).[25,26] In addition, the Beck Depression Inventory (BDI)[27,28] was used to assess depressive symptoms. The study was approved by the local Ethics Committee of the Klinikum rechts der Isar, München.

Image acquisition

MRI was conducted on a 3 T Philips Ingenia (Philips Healthcare, Best, the Netherlands) using a 12-channel (SENSE) head coil. Structural imaging consisted of a T1-weighted 3D MPRAGE sequence (170 slices, sagittal orientation, 240 × 240 matrix, 1 mm isotropic resolution, TR = 9 ms, TE = 4 ms, flip angle = 8°), and a diffusion-weighted imaging sequence (60 slices, 112 × 112 matrix, 2 mm isotropic resolution, TR = 9000 ms, TE = 57 ms, flip angle = 90°, 32 diffusion directions, *b*-value = 1000 s mm^{-2}, two $b = 0$ images).

Image processing

Based on the high-resolution T1-weighted structural image, the cortical and subcortical structures as well as the brain stem were parcellated using Freesurfer (V5.1., http://surfer.nmr.mgh.harvard.edu/). Processing included automatic segmentation into gray and white matter tissue compartments followed by parcellation of the gray matter mask into distinct brain regions based on a normalized template. The resulting parcellation consisted of a total of 83 distinct brain regions of which 68 were cortical (34 per hemisphere), 14 subcortical (7 per hemisphere: thalamus, caudate, putamen, pallidum, hippocampus, amygdala, nucleus accumbens) and 1 represented the brainstem[29–31] (see Supplementary Figure 1 for illustration of nodes). This parcellation scheme comprises several nodes that are thought to play an important role in the pathophysiology of OCD. Of special interest are several subcortical (for example, caudate, putamen, nucleus accumbens, amygdala, thalamus), as well as cortical regions (rostral middle frontal, medial orbital frontal, insula). In addition, this scheme is in line with studies examining other psychiatric diseases[8,32] and may thus facilitate comparison of results across diagnostic categories.

Diffusion data were corrected for movement and eddy-current distortions by realigning all diffusion-weighted images to the diffusion unweighted ($b = 0$) scan. A tensor was fitted to each voxel's individual diffusion profile by applying a robust fitting method.[33] Based on the fitted tensors, FA values as well as the preferred direction of diffusion (represented by the principal eigenvector) were calculated for each voxel.

Tractography

Reconstruction of white matter tracts was based on Fiber Assignment by Continuous Tracking (FACT).[34–36] To initiate tracking, eight seeds were placed in every voxel assigned to be white matter tissue based on the brain mask. Starting from each seed, tracking proceeded along the main diffusion direction propagating from voxel to voxel. Fiber tracking was terminated if the FA-value in a given voxel was < 0.1, the angle between the preferred diffusion direction of two subsequent voxels exceeded 45° or the streamline exceeded the brain mask.

Graph construction

A graph is the representation of a network in mathematical terms and is defined by a set of nodes, and a collection of edges describing the interactions between the nodes. To perform network analysis, a graph representing the structural connectivity network was constructed individually for each participant. Each node was assigned a specific brain region derived from the previous parcellation step. For every possible pair of nodes (N_i,N_j) it was determined whether a connection, that is a continuous streamline between N_i and N_j, was present or not. If present, the value of the connection was assigned the value of the number of streamlines (NOS) as indicated by the fiber tracking results. If a connection was absent, the connectivity value was set to zero. In this manner, for every participant, a single undirected, NOS-weighted graph was constructed. To avoid the influence of spurious connections, all edges with a streamline count of < 2 were set to zero. A group threshold was applied to balance the influences of false-positive and false-negative reconstructions of tracts.[37] In a first step, for each group separately, edges that were present in at least 60% of all group members were retained while all other edges were set to zero. In a second step, all edges that were present in at least 60% of the entire sample were retained. All subsequent analyses were conducted using the output from applying the 60% threshold within the entire sample. To check the stability of results, we additionally thresholded all matrices with varying thresholds, ranging from 30 to 90% with 5% increments and repeated all analysis (see Supplementary Tables 7 and 8).

NBS analysis

Group differences between structural connectivity matrices were examined using the framework of the NBS introduced by Zalesky *et al.*[14] NBS is a recently developed nonparametrical method to avoid the multiple comparison problem encountered when conducting mass univariate significance testing in graphs. Statistical significance is established for specific subsets of nodes that are mutually connected in topological rather than physical space. The first step in the analysis requires the calculation of a test statistic (here *t*-statistic) for each individual edge based on the differences in connectivity values (that is, NOS) between groups. Second, a primary component-forming threshold (here $P < 0.01$, uncorrected) is applied to identify all edges displaying potential differences in connectivity strength. Third, all subthreshold edges are assessed for mutual connections forming clusters in topological space that may point toward the existence of non-chance clusters. Permutation testing is then applied to compute *P*-values for every component previously identified. To this end, steps 1 through 3 are repeated for each of the 5000 random permutations of group assignments (that is, patient or control), with noting the maximum cluster sizes of components resulting in a null distribution for the largest component size. The final hypothesis test is then carried out for the empirically determined components by comparing their sizes with the proportion of permutations yielding a component with equal or greater size. The final result controls the family-wise error rate at cluster level with $P < 0.05$. Visualization of NBS networks was conducted using graphViz V2.3 (www.graphviz.org).[38]

Graph theoretical analyses

All measures were calculated on the individual structural connectivity matrices using the Brain Connectivity Toolbox (http://www.brain-connectivity-toolbox.net/)[12] under Matlab (R2014a, http://mathworks.com) and subsequently compared between groups. The following graph metrics were calculated for global description of the networks: (1) normalized global weighted clustering (γ), (2) normalized characteristic weighted path length (λ), (3) global strength, (4) total fiber counts. To calculate γ and λ, for every participant's brain network a set of 1000 random networks with identical degree sequence was formed. Subsequently for each of these networks, the weighted clustering coefficient and characteristic weighted path length were calculated and used for normalization. For description of nodal properties, the following node-specific (that is, region specific) graph metrics were calculated: (1) weighted clustering coefficient, (2) shortest weighted path length, (3) nodal strength. All comparisons involving graph measures were tested using permutation-based testing (10 000 permutations) corrected for multiple comparisons using false discovery rate (FDR)-correction[39] if applicable.

Analysis of nodal volumes

Volume differences on a nodal level can in principle lead to differences in the number of reconstructed streamlines and thus drive parts of the results. To check for such influences, a group comparison for the volumes of all nodes was conducted using permutation testing (10 000 permutations) and FDR-correction.

Correlations

Potential relationships between clinical scores (Y-BOCS, OCI-R, BDI) and network measures were assessed including the NOS of edges comprising a significantly different cluster in the NBS analysis, as well as graph measures, displaying significant differences on a local and global scale. All correlations were corrected for multiple comparisons using FDR-correction.

Influence of medication status

To assess the influence of medication status on results, we separately compared the subgroup of patients receiving medication with all healthy controls. This decision was based on the fact that the subsample of patients not receiving any medication ($n = 12$) was likely to cause a lack of power in the statistical analysis. Instead, using the above mentioned

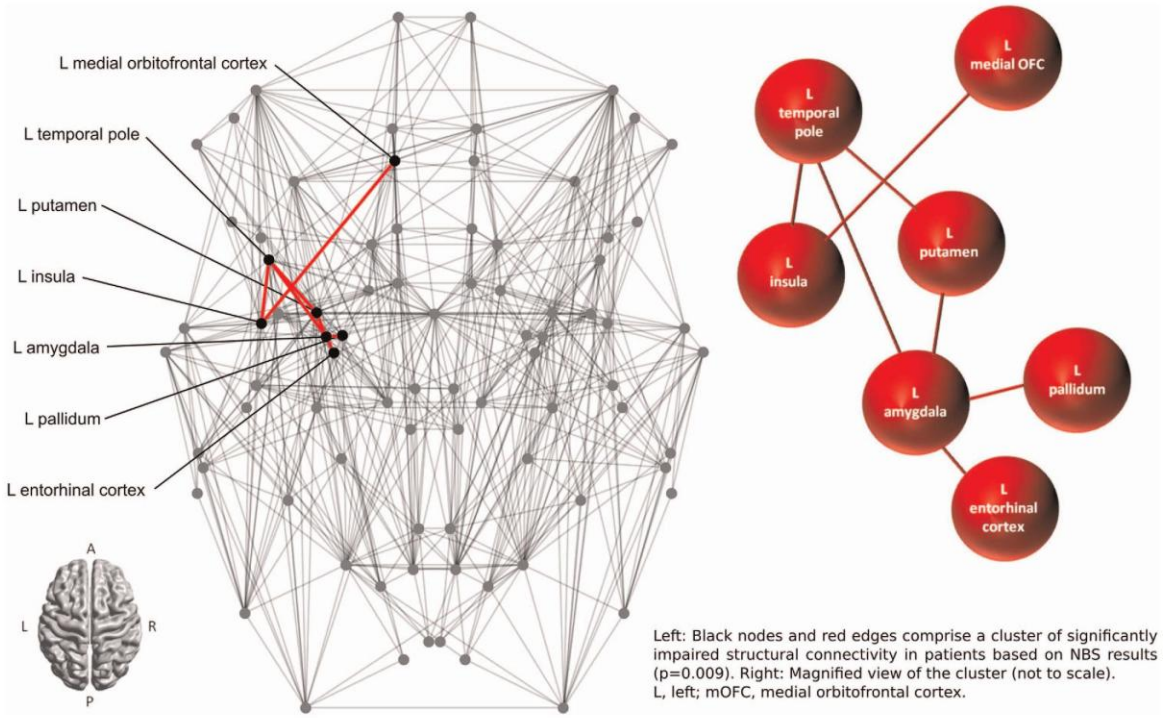

Figure 1. Connectome map representing nodes (circles) and edges (lines) of the structural network for the whole group. L, left; NBS, network-based statistic; OFC, orbitofrontal cortex.

approach, it was assessed whether the effects under consideration increased or decreased in magnitude, indicating a possible influence of medication status.

RESULTS

NBS of structural connectivity alterations in OCD

NBS analysis revealed a single network of decreased structural connectivity in OCD as compared with healthy controls ($P=0.009$). The network comprised a total of seven nodes connected by seven edges. The entire network was confined to the left hemisphere and included the following nodes: medial orbitofrontal cortex (mOFC), putamen, pallidum, amygdala, entorhinal cortex, insula and temporal pole (see Figure 1 for a depiction of the entire network structure). All connections between nodes were impaired in patients, that is, for each edge within the cluster, the NOS was consistently reduced in patients (see Table 2). For illustration purposes see Figure 2 depicting the aggregated streamline trajectories comprising the edges within the significantly impaired cluster for patients and healthy controls.

The analyses results obtained by varying the initial thresholds are presented in Supplementary Table 7. Overall, the NBS results were stable with only minor differences in cluster size for the most extreme thresholds (80–90%).

Graph analysis

The overall topology of the networks was found to be in the small-world regime for both groups with the normalized global clustering coefficient $\gamma>1$ (mean ± s.d.; patients: $\gamma=3.0604\pm0.2456$; controls: $\gamma=3.0016\pm0.1324$; $P=0.183$) and the normalized characteristic global path length $\lambda\sim1$ (patients: $\lambda=1.2125\pm0.0891$; controls: $\lambda=1.2052\pm0.1085$; $P=0.748$). There was a trend for a reduced global degree strength in patients (mean ± s.d.; patients: 3986.2 ± 771.0; controls: 4281.0 ± 651.7; $P=0.056$), as well as a trend for a reduced total fiber count in patients (mean ± s.d.; patients: 165 430 ± 31 996; controls: 177 660 ± 27 044; $P=0.063$). For local topological measures, the following significant differences were found: (1) decreased weighted clustering coefficients of left amygdala ($P<0.001$, FDR-corrected), left temporal pole ($P<0.001$, FDR-corrected) and right temporal pole ($P=0.002$, FDR-corrected); (2) increased shortest weighted path length of left amygdala ($P<0.001$, FDR-corrected), (3) decreased nodal strength of left amygdala ($P<0.001$, FDR-corrected). For nodes with significant differences based on uncorrected results see Supplementary Table 1. Regarding the stability of graph measure results, all results for amygdala are stable across the entire range of thresholds. There is some minor variation in significant differences for the weighted clustering coefficients and shortest weighted path lengths (see Supplementary Table 8). For a depiction of the global graph measures plotted as a function of connectivity matrix density see Supplementary Figure 2.

Analysis of nodal volumes

Analysis of nodal volumes yielded no significant differences ($P>0.05$, FDR-corrected) for any of the nodes derived from cortical parcellation. See Supplementary Table 2 for details regarding the volume comparisons of all nodes comprising the NBS cluster.

Correlation between clinical scores and connectivity parameters

There were no significant correlations between clinical scores and connections found to be impaired in the NBS analysis or for global and local graph measures (see Supplementary Tables 4–6 for reports of trend correlations between clinical scores and graph measures).

Table 2. Number of streamlines of edges comprising the network displaying significant group differences based on NBS analysis

Network edges	*NOS-value OCD mean ± s.d.*	*NOS-value HC mean ± s.d.*	P-*value/t-statistic*
L putamen–L amygdala	414.1 ± 224.3	656.4 ± 249.6	$P < 0.001$, $t = 4.13$
L pallidum–L amygdala	166.9 ± 151.2	317.6 ± 231.9	$P < 0.001$, $t = 3.65$
L putamen–L temporal pole	239.7 ± 140.5	365.7 ± 212.6	$P = 0.002$, $t = 3.18$
L amygdala–L temporal pole	393.0 ± 169.0	533.0 ± 246.7	$P = 0.003$, $t = 3.01$
L temporal pole–L insula	110.4 ± 116.4	204.3 ± 168.8	$P = 0.004$, $t = 2.99$
L mOFC–L insula	51.9 ± 62.2	126.8 ± 136.8	$P = 0.005$, $t = 2.94$
L amygdala–L entorhinal cortex	138.6 ± 104.0	223.4 ± 162.3	$P = 0.006$, $t = 2.83$

Abbreviations: HC, healthy controls; L, left; mOFC, medial orbitofrontal cortex; NBS, network-based statistic; NOS, number of streamlines; OCD, obsessive-compulsive disorder. Mean ± s.d. for the number of streamlines for each edge within the NBS cluster.

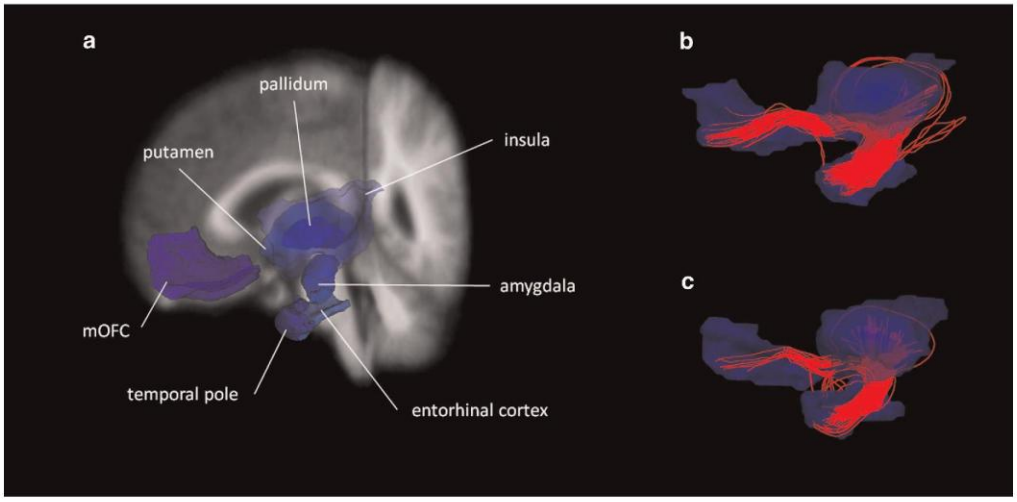

Figure 2. Illustration of the streamline trajectories comprising the edges of the significant NBS component. (**a**) For better anatomical reference, the nodes within the NBS component were extracted from the fsaverage segmentation and projected on the fsaverage anatomical T1-weighted image image. Fiber tracking results show aggregrated streamlines within the NBS component over all (**b**) controls and over all (**c**) patients. Aggregate fiber clouds have been downsampled to streamline counts representative of the subject groups. mOFC, medial orbitofrontal cortex; NBS, network-based statistic.

Influence of medication status

The NBS results obtained from comparing healthy subjects with patients receiving medication yielded one significant cluster ($P = 0.047$, corrected). It comprised a total of five nodes connected by five edges. The entire network was confined to the left hemisphere and included the following nodes: putamen, pallidum, amygdala, insula, and temporal pole. All connections between nodes were impaired in patients, that is, for each edge within the cluster, the NOS was consistently reduced in patients (see Supplementary Table 3).

For local topological measures, the following significant differences were found: (1) decreased weighted clustering coefficients of left amygdala ($P < 0.002$) and left temporal pole ($P < 0.002$); (2) increased shortest weighted path length of left amygdala ($P < 0.001$), (3) decreased nodal strength of left amygdala ($P < 0.001$).

DISCUSSION

The current study reports on NBS-based structural connectome differences between OCD patients and healthy controls, as well as graph theoretical analysis parameters. The NBS analysis revealed a single network with decreased structural connectivity in OCD. The affected subnetwork was lateralized to the left side and consisted of connections between mOFC, putamen, pallidum, amygdala, entorhinal cortex, insula and temporal pole. Several of these nodes are commonly implicated in the classical CSTC model of OCD such as the mOFC, putamen and pallidum providing evidence of the involvement of altered structural connectivity between these areas in the pathophysiology of OCD.

Interestingly, the connections between several nodes within the NBS cluster resemble a fronto-temporal pattern connecting mOFC, insula, temporal pole, amygdala and entorhinal cortex. Widespread anatomical connectivity between the aforementioned areas has been described in the literature. A major connection between the orbital and temporal gyrus is provided through the uncinate fasciculus (UF)[40] which is commonly regarded as forming part of the limbic system due to connectivity and topology.[41] Fibers are originating in the parahippocampal area, including the entorhinal cortex and temporal pole, reaching the orbital cortex after passing the amygdala and the limen insula.[41] Some authors also describe an extension of the UF to the amygdala.[42] Using a diffusion tensor imaging fiber tracking approach in humans, the anterior insula has been demonstrated to contain fibers connecting orbital/inferior frontal areas and temporal areas with parts of the fibers overlapping with the UF.[43]

Several studies using DWI measures and Tract-based Spatial Statistics (TBSS) have reported microstructural alterations within

the UF in OCD, among others a decrease in FA values in left and right UF, as well as a reduced mean diffusivity in left UF in patients receiving medication[44] and an increase in axial diffusivity in left and right UF in a pediatric sample of OCD patients.[45] Regarding our results, a potential involvement of the UF seems possible as the connections between the aforementioned nodes are mainly provided through fibers that closely resemble the trajectory of the UF (also see Figure 2). Unlike TBSS, the connectomics approach taken in the current analysis does not focus on voxel-wise white matter alterations within a skeleton of the main fiber tracts but rather on the NOS between nodes. However, it is remarkable that there might be a convergence between results derived using various methods such as TBSS and NBS. Our results are also in line with a recent review/meta-analysis[46] that comes to the conclusion that reductions in UF structural connectivity might be interpreted as the correlate of processing deficits in the emotional domain observed in neuropsychological research conducted with OCD patients.

A large body of evidence points toward wide-spread alterations in cortical volumes in OCD patients[4] with changes mainly affecting frontal, temporal, thalamic and temporo-limbic areas. In addition, a recent multicenter study[47] including over 400 patients, found a relative decrease of gray matter volume in the inferior frontal cortex extending to the anterior insula in OCD patients. As mentioned above, volume differences can lead to differences in the number of reconstructed streamlines and therefore influence results. The analysis of volume differences yielded no significant results between patients and controls for any of the nodes in the NBS cluster. This indicates that differences in the number of reconstructed streamlines are most likely not due to regional changes in volume but may rather indicate a correlate of underlying pathology. Note that the absence of volumetric differences in our sample does not necessarily contradict the findings from meta-analyses as they generally possess a higher statistical power to detect even subtle differences.

The importance of the amygdala is not specifically considered in the traditional CSTC model even though there is accumulating evidence indicating an involvement of this structure in the disease[48–52] and an ongoing debate about its role in the pathophysiology of OCD.[2] The NBS result clearly indicates an involvement of the amygdala. Specifically, within the impaired NBS cluster it is also the node displaying the highest binary degree (for example, the highest number of direct neighbors), providing a link between temporal and striatal areas. The important role is further underlined by results from graph theoretical measures indicating a decreased weighted clustering coefficient, a decrease in weighted degree strength, as well as an increased shortest path length for left amygdala. The clustering coefficient measures how strongly connected the neighbors of amygdala are and a decrease in clustering may thus point toward a decreased structural connectivity among the directly connected neighbors of the amygdala. This result might be interpreted such that in OCD, information normally traversing rather directly between immediate neighbors in healthy subjects may be more prone to be mediated via connections involving the amygdala, thus allowing it to exert an increased control over information flow between neighbors. As a measure of integration reflecting information about the connectivity between amygdala and all remaining nodes, the increase in shortest path length further indicates that amygdala is not as efficiently connected as in healthy controls. Taken together, there might be an additive effect in the sense that information is not only more prone to travel through amygdala, but also the connectivity between amygdala and its neighbors, as well as other brain regions is not as efficient.

Considering anxiety to be a core phenomenon of OCD, the finding of altered structural connectivity of limbic areas (such as OFC and amygdala) is especially striking since these areas are commonly thought to be central to emotion processing and behavioral regulation[53,54] with amygdala playing a central role for fear and anxiety. Hence, the alterations found in graph measures substantiate current discussions about the relevance of the amygdala for OCD and may represent the structural substrate of the pronounced feelings of anxiety preceding or accompanying patients´ obsessive thoughts and compulsive actions.

Similar to left amygdala, both temporal poles also exhibited a decreased weighted clustering coefficient. The temporal pole has been implicated in various domains such as memory,[55] as well as emotional processing, coupling sensory stimulation to emotional responses.[56,57] There is first evidence of an involvement of altered temporal pole structure and function in OCD. Van den Heuvel *et al.*[58] found a negative correlation between checking symptoms and gray matter and white matter volume. Furthermore, the level of functional activation in the anterior temporal pole and amygdala during symptom provocation is reported to be associated with better subsequent treatment response to cognitive behavioral therapy.[59] Taken together, previous and current findings provide support for the notion of structural alterations in amygdala and temporal pole in OCD which may be clinically relevant and may go along with an increase in functional activation. The association between increased functional activation in these limbic core regions and subsequent responsivity to treatment is in line with the emotional processing theory by Foa,[60] which assumes that activation of limbic (and predominantly amygdala) regions during the experience of clinical symptoms is a prerequisite for successful exposure-based treatments for anxiety disorders. Whether there is a direct association between functional and structural alterations, as well as an analog association in OCD between structural alterations in these regions and individual treatment responsivity remains to be elucidated. To date there is only one study examining structural white matter network characteristics in OCD from a network perspective reporting several alterations in global and local graph measures.[20] Their main findings are a reduction in global efficiency, as well as an increase in shortest path length, as well as γ and λ in patients. In addition, they report a significant correlation between λ and the Y-BOCS obsession score. There are, however, considerable methodological differences in comparison to our study that might have caused divergent findings. First and foremost, the composition of the sample differs regarding the number of patients ($n = 41$ vs $n = 26$), as well as other characteristics (with all patients being unmedicated with no comorbidities in the study by Zhong *et al.*[20]). Second, several parameters directly influencing the number of reconstructed streamlines differed substantially, such as the parcellation scheme which affects the volume of nodes and thus influences the number of voxels within each ROI to initialize tracking from. Furthermore, the tracking was initialized from one seed within each voxel in the study by Zhong *et al.* compared with eight seeds in the current study. In addition, we applied a more liberal threshold (FA-value < 0.1 vs FA-value < 0.2 used by Zhong *et al.*) as termination criteria for fiber tracking. Finally, we applied a 60% threshold to all connectivity matrices to find a good balance between false-positive and false-negative connections (see Materials and methods section). Taken together, the combination of differences in sample composition and choices influencing the number of reconstructed streamlines might explain divergent findings.

Apart from examinations of structural connectivity, there is an increasing number of studies using functional MRI to further elucidate the neurobiological basis of OCD. Göttlich *et al.*[18] report a decrease in connectivity between limbic (amygdala, hippocampus and parahippocampal gyrus) and basal ganglia, as well as the default mode and executive/attention network in patients. In addition, the connectivity within the limbic network was reported to be impaired. Similarly, Jung *et al.*[61] found an increased functional connectivity between nucleus accumbens and lateral orbitofrontal cortex during rest and a decrease in functional

connectivity between nucleus accumbens and amygdala during incentive processing in patients. These results were interpreted as evidence in favor of abnormalities in modulatory influence of affective/motivational states on functional network connections in patients. Keeping in mind that the concept of functional connectivity is based on statistical associations and that the relationship between alterations in function and structure is not a straight-forward one-to-one mapping but rather complicated,[62] there still seems to be an overlap between regions implicated in structural networks displaying alterations as shown in this study (amygdala, mOFC, striatal and temporal regions) and findings from altered functional connectivity between fronto-striato-temporal networks. It seems plausible that the structural alterations especially of connections between limbic regions might contribute to the proposed abnormalities in modulatory influence of affective/motivational states.

The current study has several limitations. Despite being fairly large, the examined sample comprised a certain proportion of patients with comorbid disorders, as well as a mix of medicated and unmedicated patients. Previous reports indicate an influence of selective serotonin reuptake inhibitor treatment on brain structure and function.[63,64] Nevertheless, the analysis of the subgroup of patients receiving medication is in good accordance with the primary analysis comparing healthy controls with all patients. The NBS analysis yielded one significant cluster that was only slightly varying in size. The magnitude of the differences in NOS-values increased for all edges in the NBS cluster of the medicated patients. This effect might be due to true differences in medication status. Alternatively, the connectivity differences could be related to differences in symptom severity. On average, the patient group receiving medication had a higher total Y-BOCS score than the unmedicated patients though formal statistical significance was not reached (medicated patients: 22.93 ± 5.16 vs unmedicated patients: 19.83 ± 3.16; $P = 0.095$). The results of the graph measures computed for the subgroup of medicated patients were also rather similar to the results obtained from the original analysis with only the local clustering for the right temporal pole not reaching statistical significance. This again could be related to the above mentioned differences. Regarding the fact that selective serotonin reuptake inhibitors are the first line of treatment in OCD, influences of medication should be more rigorously assessed in future studies preferably comparing non-medicated and medicated groups with healthy controls separately.

Due to various limitations inherent to the method of fiber tracking, the accuracy of retrieved streamlines poses an issue in terms of false-positive and negative connections. To account for this fact, we applied a group threshold previously shown to strike a balance between erroneously assigning tracts.[37] In the present study, a parcellation scheme commonly used in the Freesurfer suite was applied to increase comparability of results. Furthermore, the symptom heterogeneity typically found in OCD patients poses an issue. There is accumulating evidence that specific symptom dimensions in OCD can go along with specific alterations in neural processing, as well as structural alterations.[48,58,65] Thus, it seems reasonable to explicitly consider the heterogeneity of symptom dimensions in future studies by trying to group patients according to symptom profile or predominant symptom dimension. Clearly, this approach would call for even bigger sample sizes to reach sufficient statistical power.

In summary, applying a network-based analysis strategy comparing structural brain networks of OCD patients and healthy controls we demonstrate impairments in a specific subnetwork in patients. Parts of the network overlap with regions commonly described in the CSTC model of the disease. However, several implicated regions and their connections are concentrated on a fronto-temporal axis indicating limbic structures to play a role in pathology.

CONFLICT OF INTEREST

The authors declare no conflict of interest.

ACKNOWLEDGMENTS

This study was supported by German Research Foundation (DFG) grants to KK (DFG KO 3744/2-1) and GW (DFG WA 3001/3-1). TR received a travel stipend from the Graduate School of Systemic Neurosciences, Ludwig-Maximilians-Universität München, to conduct part of the research at the Department of Psychiatry, Brain Center Rudolf Magnus, University Medical Center Utrecht. The funding agencies had no influence on the design and conduct of the study including collection, management, analysis and interpretation of the data, as well as preparation, review or approval of the manuscript.

REFERENCES

1 American Psychiatric A. *Diagnostic and Statistical Manual of Mental Disorders*. Text Revision (DSM-IV-TR). American Psychiatric Association: Washington, DC, 2000.
2 Milad MR, Rauch SL. Obsessive-compulsive disorder: beyond segregated cortico-striatal pathways. *Trends Cogn Sci* 2012; **16**: 43–51.
3 Menzies L, Chamberlain SR, Laird AR, Thelen SM, Sahakian BJ, Bullmore ET. Integrating evidence from neuroimaging and neuropsychological studies of obsessive-compulsive disorder: the orbitofronto-striatal model revisited. *Neurosci Biobehav Rev* 2008; **32**: 525–549.
4 Piras F, Piras F, Chiapponi C, Girardi P, Caltagirone C, Spalletta G. Widespread structural brain changes in OCD: a systematic review of voxel-based morphometry studies. *Cortex* 2015; **62**: 89–108.
5 Goodkind M, Eickhoff SB, Oathes DJ, Jiang Y, Chang A, Jones-Hagata LB *et al.* Identification of a common neurobiological substrate for mental illness. *JAMA Psychiatry* 2015; **72**: 305–315.
6 White T, Nelson M, Lim KO. Diffusion tensor imaging in psychiatric disorders. *Top Magn Reson Imaging* 2008; **19**: 97–109.
7 Griffa A, Baumann PS, Thiran JP, Hagmann P. Structural connectomics in brain diseases. *Neuroimage* 2013; **80**: 515–526.
8 Korgaonkar MS, Fornito A, Williams LM, Grieve SM. Abnormal structural networks characterize major depressive disorder: a connectome analysis. *Biol Psychiatry* 2014; **76**: 567–574.
9 van den Heuvel MP, Mandl RC, Stam CJ, Kahn RS, Hulshoff Pol HE. Aberrant frontal and temporal complex network structure in schizophrenia: a graph theoretical analysis. *J Neurosci* 2010; **30**: 15915–15926.
10 Narr KL. Leaver AM. Connectome and schizophrenia. *Curr Opin Psychiatry* 2015; **28**: 229–235.
11 Bullmore ET, Bassett DS. Brain graphs: graphical models of the human brain connectome. *Annu Rev Clin Psychol* 2011; **7**: 113–140.
12 Rubinov M, Sporns O. Complex network measures of brain connectivity: uses and interpretations. *Neuroimage* 2010; **52**: 1059–1069.
13 Fornito A, Zalesky A, Breakspear M. Graph analysis of the human connectome: promise, progress, and pitfalls. *Neuroimage* 2013; **80**: 426–444.
14 Zalesky A, Fornito A, Bullmore ET. Network-based statistic: identifying differences in brain networks. *Neuroimage* 2010; **53**: 1197–1207.
15 Zhang T, Wang J, Yang Y, Wu Q, Li B, Chen L *et al.* Abnormal small-world architecture of top-down control networks in obsessive-compulsive disorder. *J Psychiatry Neurosci* 2011; **36**: 23–31.
16 Shin DJ, Jung WH, He Y, Wang J, Shim G, Byun MS *et al.* The effects of pharmacological treatment on functional brain connectome in obsessive-compulsive disorder. *Biol Psychiatry* 2014; **75**: 606–614.
17 Hou JM, Zhao M, Zhang W, Song LH, Wu WJ, Wang J *et al.* Resting-state functional connectivity abnormalities in patients with obsessive-compulsive disorder and their healthy first-degree relatives. *J Psychiatry Neurosci* 2014; **39**: 304–311.
18 Gottlich M, Kramer UM, Kordon A, Hohagen F, Zurowski B. Decreased limbic and increased fronto-parietal connectivity in unmedicated patients with obsessive-compulsive disorder. *Hum Brain Mapp* 2014; **35**: 5617–5632.
19 Kim SG, Jung WH, Kim SN, Jang JH, Kwon JS. Disparity between dorsal and ventral networks in patients with obsessive-compulsive disorder: evidence revealed by graph theoretical analysis based on cortical thickness from MRI. *Front Hum Neurosci* 2013; **7**: 302.
20 Zhong Z, Zhao T, Luo J, Guo Z, Guo M, Li P *et al.* Abnormal topological organization in white matter structural networks revealed by diffusion tensor tractography in unmedicated patients with obsessive-compulsive disorder. *Prog Neuropsychopharmacol Biol Psychiatry* 2014; **51**: 39–50.
21 Annett M. A classification of hand preference by association analysis. *Br J Psychol* 1970; **61**: 303–321.

22 Goodman WK, Price LH, Rasmussen SA, Mazure C, Fleischmann RL, Hill CL *et al.* The Yale-Brown Obsessive Compulsive Scale. I. Development, use, and reliability. *Arch Gen Psychiatry* 1989; **46**: 1006–1011.
23 Hand I, Büttner-Westphal H. Die Yale-Brown Obsessive Compulsive Scale (Y-BOCS): ein halbstrukturiertes interview zur beurteilung des schweregrades von denk- und handlungszwängen. *Verhaltenstherapie* 1991; **1**: 223–225.
24 Steketee G, Frost R, Bogart K. The Yale-Brown Obsessive Compulsive Scale: interview versus self-report. *Behav Res Ther* 1996; **34**: 675–684.
25 Foa EB, Huppert JD, Leiberg S, Langner R, Kichic R, Hajcak G *et al.* The obsessive-compulsive inventory: development and validation of a short version. *Psychol Assess* 2002; **14**: 485–496.
26 Gonner S, Leonhart R, Ecker W. The Obsessive-Compulsive Inventory-Revised (OCI-R): validation of the German version in a sample of patients with OCD, anxiety disorders, and depressive disorders. *J Anxiety Disord* 2008; **22**: 734–749.
27 Beck AT, Steer RA, Brown G. *Manual for the Beck Depression Inventory-II*. Psychological Corporation: San Antonio, TX, USA, 1996.
28 Hautzinger M, Keller F, Kühner C, BDI-II. *Beck-Depressions-Inventar Revision*. 2. Auflage (ed.). Pearson Assessment: Frankfurt am Main, Germany, 2009.
29 Fischl B, Sereno MI, Dale AM. Cortical surface-based analysis. II: Inflation, flattening, and a surface-based coordinate system. *Neuroimage* 1999; **9**: 195–207.
30 Fischl B, van der Kouwe A, Destrieux C, Halgren E, Segonne F, Salat DH *et al.* Automatically parcellating the human cerebral cortex. *Cereb Cortex* 2004; **14**: 11–22.
31 Desikan RS, Segonne F, Fischl B, Quinn BT, Dickerson BC, Blacker D *et al.* An automated labeling system for subdividing the human cerebral cortex on MRI scans into gyral based regions of interest. *Neuroimage* 2006; **31**: 968–980.
32 van den Heuvel MP, Sporns O, Collin G, Scheewe T, Mandl RC, Cahn W *et al.* Abnormal rich club organization and functional brain dynamics in schizophrenia. *JAMA Psychiatry* 2013; **70**: 783–792.
33 Chang LC, Jones DK, Pierpaoli C. RESTORE: robust estimation of tensors by outlier rejection. *Magn Reson Med* 2005; **53**: 1088–1095.
34 Mori S, van Zijl PC. Fiber tracking: principles and strategies—a technical review. *NMR Biomed* 2002; **15**: 468–480.
35 Mori S, Crain BJ, Chacko VP, van Zijl PC. Three-dimensional tracking of axonal projections in the brain by magnetic resonance imaging. *Ann Neurol* 1999; **45**: 265–269.
36 Mori S, Kaufmann WE, Davatzikos C, Stieltjes B, Amodei L, Fredericksen K *et al.* Imaging cortical association tracts in the human brain using diffusion-tensor-based axonal tracking. *Magn Reson Med* 2002; **47**: 215–223.
37 de Reus MA, van den Heuvel MP. Estimating false positives and negatives in brain networks. *Neuroimage* 2013; **70**: 402–409.
38 Gansner ER, North SC. An open graph visualization system and its applications to software engineering. *Software Pract Exper* 2000; **30**: 1203–1233.
39 Benjamini Y, Hochberg Y. Controlling the false discovery rate - a practical and powerful approach to multiple testing. *J R Stat Soc Ser B Stat Methodol* 1995; **57**: 289–300.
40 Ebeling U, von Cramon D. Topography of the uncinate fascicle and adjacent temporal fiber tracts. *Acta Neurochir (Wien)* 1992; **115**: 143–148.
41 Von Der Heide RJ, Skipper LM, Klobusicky E, Olson IR. Dissecting the uncinate fasciculus: disorders, controversies and a hypothesis. *Brain* 2013; **136**: 1692–1707.
42 Thiebaut de Schotten M, Dell'Acqua F, Valabregue R, Catani M. Monkey to human comparative anatomy of the frontal lobe association tracts. *Cortex* 2012; **48**: 82–96.
43 Cloutman LL, Binney RJ, Drakesmith M, Parker GJ, Lambon Ralph MA. The variation of function across the human insula mirrors its patterns of structural connectivity: evidence from in vivo probabilistic tractography. *Neuroimage* 2012; **59**: 3514–3521.
44 Benedetti F, Giacosa C, Radaelli D, Poletti S, Pozzi E, Dallaspezia S *et al.* Widespread changes of white matter microstructure in obsessive-compulsive disorder: effect of drug status. *Eur Neuropsychopharmacol* 2013; **23**: 581–593.
45 Jayarajan RN, Venkatasubramanian G, Viswanath B, Janardhan Reddy YC, Srinath S, Vasudev MK *et al.* White matter abnormalities in children and adolescents with obsessive-compulsive disorder: a diffusion tensor imaging study. *Depress Anxiety* 2012; **29**: 780–788.
46 Piras F, Piras F, Caltagirone C, Spalletta G. Brain circuitries of obsessive compulsive disorder: a systematic review and meta-analysis of diffusion tensor imaging studies. *Neurosci Biobehav Rev* 2013; **37**: 2856–2877.
47 de Wit SJ, Alonso P, Schweren L, Mataix-Cols D, Lochner C, Menchon JM *et al.* Multicenter voxel-based morphometry mega-analysis of structural brain scans in obsessive-compulsive disorder. *Am J Psychiatry* 2014; **171**: 340–349.
48 Via E, Cardoner N, Pujol J, Alonso P, Lopez-Sola M, Real E *et al.* Amygdala activation and symptom dimensions in obsessive-compulsive disorder. *Br J Psychiatry* 2014; **204**: 61–68.
49 Simon D, Adler N, Kaufmann C, Kathmann N. Amygdala hyperactivation during symptom provocation in obsessive-compulsive disorder and its modulation by distraction. *Neuroimage Clin* 2014; **4**: 549–557.
50 Cardoner N, Harrison BJ, Pujol J, Soriano-Mas C, Hernandez-Ribas R, Lopez-Sola M *et al.* Enhanced brain responsiveness during active emotional face processing in obsessive compulsive disorder. *World J Biol Psychiatry* 2011; **12**: 349–363.
51 Simon D, Kaufmann C, Musch K, Kischkel E, Kathmann N. Fronto-striato-limbic hyperactivation in obsessive-compulsive disorder during individually tailored symptom provocation. *Psychophysiology* 2010; **47**: 728–738.
52 van Velzen LS, de Wit SJ, Curcic-Blake B, Cath DC, van Vries FE, Veltman DJ *et al.* Altered inhibition-related frontolimbic connectivity in obsessive-compulsive disorder. *Hum Brain Mapp* 2015; **36**: 4064–4075.
53 Phelps EA, LeDoux JE. Contributions of the amygdala to emotion processing: from animal models to human behavior. *Neuron* 2005; **48**: 175–187.
54 Dolan RJ. The human amygdala and orbital prefrontal cortex in behavioural regulation. *Philos Trans R Soc Lond B Biol Sci* 2007; **362**: 787–799.
55 Simmons WK, Martin A. The anterior temporal lobes and the functional architecture of semantic memory. *J Int Neuropsychol Soc* 2009; **15**: 645–649.
56 Olson IR, Plotzker A, Ezzyat Y. The Enigmatic temporal pole: a review of findings on social and emotional processing. *Brain* 2007; **130**: 1718–1731.
57 Blaizot X, Mansilla F, Insausti AM, Constans JM, Salinas-Alaman A, Pro-Sistiaga P *et al.* The human parahippocampal region: I. Temporal pole cytoarchitectonic and MRI correlation. *Cereb Cortex* 2010; **20**: 2198–2212.
58 van den Heuvel OA, Remijnse PL, Mataix-Cols D, Vrenken H, Groenewegen HJ, Uylings HB *et al.* The major symptom dimensions of obsessive-compulsive disorder are mediated by partially distinct neural systems. *Brain* 2009; **132**: 853–868.
59 Olatunji BO, Ferreira-Garcia R, Caseras X, Fullana MA, Wooderson S, Speckens A *et al.* Predicting response to cognitive behavioral therapy in contamination-based obsessive-compulsive disorder from functional magnetic resonance imaging. *Psychol Med* 2014; **44**: 2125–2137.
60 Foa EB, McNally RJ. Mechanisms of change in exposure therapy. In:Rapee RM (ed). *Current Controversies in the Anxiety Disorders*. Guilford Press: New York, NY, USA, 1996, pp 329–343.
61 Jung WH, Kang DH, Kim E, Shin KS, Jang JH, Kwon JS. Abnormal corticostriatal-limbic functional connectivity in obsessive-compulsive disorder during reward processing and resting-state. *Neuroimage Clin* 2013; **3**: 27–38.
62 Wang Z, Dai Z, Gong G, Zhou C, He Y. Understanding structural-functional relationships in the human brain: a large-scale network perspective. *Neuroscientist* 2015; **21**: 290–305.
63 Hoexter MQ, de Souza Duran FL, D'Alcante CC, Dougherty DD, Shavitt RG, Lopes AC *et al.* Gray matter volumes in obsessive-compulsive disorder before and after fluoxetine or cognitive-behavior therapy: a randomized clinical trial. *Neuropsychopharmacology* 2012; **37**: 734–745.
64 Kraus C, Ganger S, Losak J, Hahn A, Savli M, Kranz GS *et al.* Gray matter and intrinsic network changes in the posterior cingulate cortex after selective serotonin reuptake inhibitor intake. *Neuroimage* 2014; **84**: 236–244.
65 Harrison BJ, Pujol J, Cardoner N, Deus J, Alonso P, Lopez-Sola M *et al.* Brain corticostriatal systems and the major clinical symptom dimensions of obsessive-compulsive disorder. *Biol Psychiatry* 2013; **73**: 321–328.

Supplementary Information accompanies the paper on the Translational Psychiatry website (http://www.nature.com/tp)

Supplementary Information

Reess TJ, Rus OG, Schmidt R, de Reus MA, Zaudig M, Wagner G, Zimmer C, van den Heuvel MP, Koch K. Connectomics-based structural network alterations in obsessive-compulsive disorder.

Supplementary Table 1. Group differences for local graph measures significant at a level of p<0.05, uncorrected.

Weigthed Connectivity Strength	**p-value**	**Weighted Clustering Coefficient**	**p-value**
Subcortical structures		*Subcortical structures*	
L pallidum	p = 0.032; HC > OCD	R putamen	p = 0.022; HC > OCD
R putamen	p = 0.021; HC > OCD	R n. accumbens	p = 0.024; HC > OCD
R pallidum	p = 0.002; HC > OCD		
R n. accumbens	p = 0.005; HC > OCD		
Cortical structures		*Cortical structures*	
L entorhinal cortex	p = 0.016; HC > OCD	L hippocampus	p = 0.043; HC > OCD
L pericalcarine	p = 0.024; OCD > HC	L entorhinal cortex	P = 0.019; HC > OCD
L precuneus	p = 0.046; HC > OCD		
L temporal pole	p = 0.007; HC > OCD		
R entorhinal cortex	p = 0.041; HC > OCD		
R rostral middle frontal cortex	p = 0.011; HC > OCD		
R superior parietal cortex	p = 0.027; HC > OCD		
R temporal pole	p = 0.040; HC > OCD		
R insula	p = 0.041; HC > OCD		
brain stem	p = 0.013; HC > OCD		

HC, healthy controls; OCD, obsessive-compulsive disorder; L, left; R, right; all tests are permutation based with 10000 permutations

Supplementary Table 1 (continued)

Shortest Path Length	p-value	Shortest Path Length	p-value
Subcortical structures		*Subcortical structures*	
L thalamus	p = 0.007; HC < OCD	R caudate	p = 0.039; HC < OCD
L caudate	p = 0.030; HC < OCD	R putamen	p = 0.018; HC < OCD
L putamen	p = 0.040; HC < OCD	R pallidum	p = 0.008; HC < OCD
L pallidum	p = 0.008; HC < OCD	R amygdala	p = 0.018; HC < OCD
L hippocampus	p = 0.021; HC < OCD	R n. accumbens	p = 0.037; HC < OCD
Cortical structures		*Cortical structures*	
L entorhinal cortex	p = 0.001; HC < OCD	R postcentral	p = 0.032; HC < OCD
L isthmuscingulate cortex	p = 0.043; HC < OCD	R precentral	p = 0.020; HC < OCD
L superior parietal cortex	p = 0.021; HC < OCD	R precuneus	p = 0.047; HC < OCD
L temporal pole	p = 0.006; HC < OCD	R rostral middle frontal cortex	p = 0.012; HC < OCD
		R superior parietal cortex	p = 0.015; HC < OCD
		R supramarginal gyrus	p = 0.040; HC < OCD
		R temporal pole	p = 0.008; HC < OCD
		R transversetemporal	p = 0.031; HC < OCD
Brain stem	p = 0.020; HC < OCD		

HC, healthy controls; OCD, obsessive-compulsive disorder; L, left; R, right; all tests are permutation based with 10000 permutations

Supplementary Table 2. Group comparison of volumes (mm^3) for nodes comprising the NBS network.

Node	**Volume (mm^3) OCD** mean ± SD	**Volume (mm^3) HC** mean ± SD	**p-value**	**Cohen's d [95% - confidence interval]**
L putamen	6562.1 ± 809.9	6436.1 ± 765.9	p = 0.476	- 0.16 [-0.59 – 0.27]
L pallidum	1736.0 ± 233.7	1804.6 ± 231.8	p = 0.192	0.30 [-0.14 – 0.73]
L temporal pole	2656.1 ± 397.0	2702.3 ± 433.1	p = 0.594	0.11 [-0.32 – 0.54]
L insula	6484.3 ± 779.6	6633.9 ± 809.3	p = 0.408	0.19 [-0.24 – 0.62]
L amygdala	1730.2 ± 251.2	1786.6 ± 228.9	p = 0.292	0.24 [-0.20 – 0.67]
L mOFC	4555.0 ± 647.0	4698.4 ± 767.9	p = 0.357	0.20 [-0.23 – 0.63]
L entorhinal cortex	1807.8 ± 297.8	1908.6 ± 357.4	p = 0.168	0.31 [-0.13 – 0.74]

HC, healthy controls; OCD, obsessive-compulsive disorder; L, left; mOFC, medial orbitofrontal cortex; SD, standard deviation

Supplementary Table 3. Number of streamlines of edges comprising the network displaying significant group differences based on NBS analysis of only medicated patients (n=29).

Network edges	**NOS-value** $OCD_{medicated}$ **Mean ± SD**	**NOS-value HC Mean ± SD**	**p-value / t-statistic**
L putamen – L amygdala	440.2 ± 232.9	656.4 ± 249.6	$p < 0.001$, $t = 3.76$
L pallidum – L amygdala	173.5 ± 204.3	317.6 ± 231.9	$p = 0.003$, $t = 3.14$
L putamen – L temporal pole	236.3 ± 186.8	365.7 ± 212.6	$p = 0.006$, $t = 2.87$
L amygdala – L temporal pole	384.3 ± 211.4	533.0 ± 246.7	$p = 0.005$, $t = 2.91$
L temporal pole – L insula	109.1 ± 148.1	204.3 ± 168.8	$p = 0.008$, $t = 2.76$

Mean ± standard deviation for the number of streamlines for each edge within the NBS cluster. NOS, number of streamlines; L, left; SD, standard deviation

Supplementary Table 4. Correlations between significantly impaired edges from the NBS cluster and clinical scores. Only trend correlations ($p < 0.1$) are reported.

Network Eedges (NOS)	**clinical score / demographic information**	**p-value / pearson correlation coefficient**
L putamen – L amygdala	age of onset	$p = 0.079$, $r = 0.288$
L pallidum – L amygdala	washing (OCI-R)	$p = 0.080$, $r = -0.284$
L putamen – L temporal pole	obsessing (OCI-R)	$p = 0.059$, $r = -0.297$
	obsession (Y-BOCS)	$p = 0.087$, $r = -0.270$
	total (Y-BOCS)	$p = 0.091$, $r = -0.268$

NOS: number of streamlines; All reported p-values are uncorrected

Supplementary Table 5. Correlations between total degree strength and clinical scores. Only trend correlations ($p < 0.1$) are reported.

Global Graph Measures	**clinical score / demographic information**	**p-value, correlation coefficient**
Global degree strength	disease duration	p = 0.004, r = -0.443* p = 0.416, r = -0.132‡

* pearson correlation coefficient; ‡ partial correlation coefficient [controlling for age]

Supplementary Table 6. Correlations between significantly different local graph measures and clinical scores. Only trend correlations ($p < 0.1$) are reported.

Local Graph Measures	**clinical score / demographic information**	**p-value, correlation coefficient**
Amygdala – clustering	obsessing (OCI-R)	p = 0.082, r = 0.275*
Amygdala – shortest path length	disease duration	p = 0.055, r = 0.302* p = 0.397, r = -0.138‡
R temporal pole – clustering	hoarding (OCI-R)	p = 0.016, r = -0.374*
	checking (OCI-R)	p = 0.056, r = 0.301*
	washing (OCI-R)	p = 0.050, r = -0.308*

* pearson correlation coefficient; ‡ partial correlation coefficient [controlling for age]

Supplementary Table 7. NBS results of analysis conducted with various group-thresholds.

% threshold	density (%)	cluster size	p-value
30	25.51 %	7	0.019
35	23.63 %	7	0.016
40	22.51 %	7	0.015
45	20.86 %	7	0.014
50	19.54 %	7	0.013
55	17.95 %	7	0.010
60	17.34 %	7	0.009
65	14.96 %	7	0.009
70	13.69 %	7	0.005
75	11.99 %	7	0.005
80	10.11 %	6	0.008
85	8.96 %	6	0.006
90	7.49 %	6	0.005
All NBS analyses were conducted with 5000 permutations			

The significantly impaired cluster for the NBS analysis is essentially stable for the various thresholds. Only for the 80%, 85%, and 90% threshold the cluster size is reduced by one with the connection between mOFC and insula not being part of the cluster.

Supplementary Table 8. Results for differences in local graph measures and global degree strength computed for various group thresholds.

% threshold	weighted clustering	Shortest weighted path	nodal strength	Global degree strength	density (in %)
30	no differences	L amygdala	L amygdala	p = 0.081	25.51 %
35	no differences	L amygdala L entorhinal	L amygdala	p = 0.080	23.63 %
40	L amygdala	L amygdala L entorhinal	L amygdala	p = 0.080	22.51 %
45	L amygdala	L amygdala L entorhinal	L amygdala	p = 0.080	20.86 %
50	L amygdala	L amygdala	L amygdala	p = 0.070	19.54 %
55	L amygdala L temporal pole	L amygdala L entorhinal	L amygdala	p = 0.063	17.95 %
60	L amygdala L temporal pole R temporal pole	L amygdala	L amygdala	p = 0.056	17.34 %
65	L amygdala L temporal pole R temporal pole	L amygdala L entorhinal	L amygdala	p = 0.054	14.96 %
70	L amygdala L temporal pole R temporal pole	L amygdala L entorhinal	L amygdala	p = 0.047	13.69 %
75	L amygdala L temporal pole	L amygdala L entorhinal	L amygdala	p = 0.044	11.99 %
80	L amygdala L temporal pole	L amygdala L entorhinal	L amygdala L temporal pole	p = 0.051	10.11 %
85	L amygdala L temporal pole	L amygdala L entorhinal	L amygdala L temporal pole	p = 0.045	8.96 %
90	L amygdala L temporal pole R temporal pole	L amygdala	L amygdala	P = 0.034	7.49 %

all tests are permutation based with 10000 permutations

All reported nodes were significantly different regarding the graph measure in question, based on FDR-corrected, permutation based testing with 5000 permutations

Supplementary Figure 1. Illustration of the parcellation scheme used for defining the nodes.

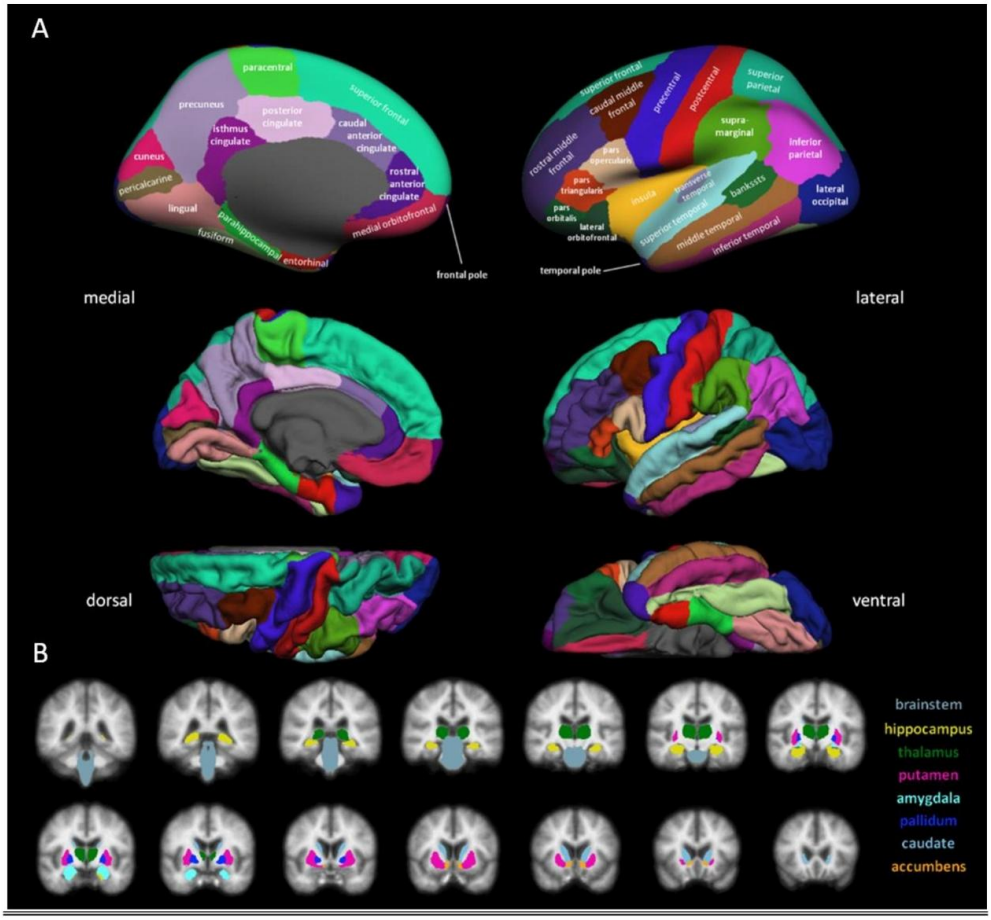

A. Top row: Illustration of all cortical labels used to define cortical nodes, overlayed on the inflated fsaverage brain. Middle and bottom rows: Same as above with labels being overlayed on the reconstructed fsaverage brain. B. Illustration of all subcortical labels used to define subcortical nodes, overlayed on the fsaverage brain. Bankssts: bank of the superior temporal sulcus

Supplementary Figure 2. Global graph measures and small-worldness plotted as a function of connectivity matrix densities.

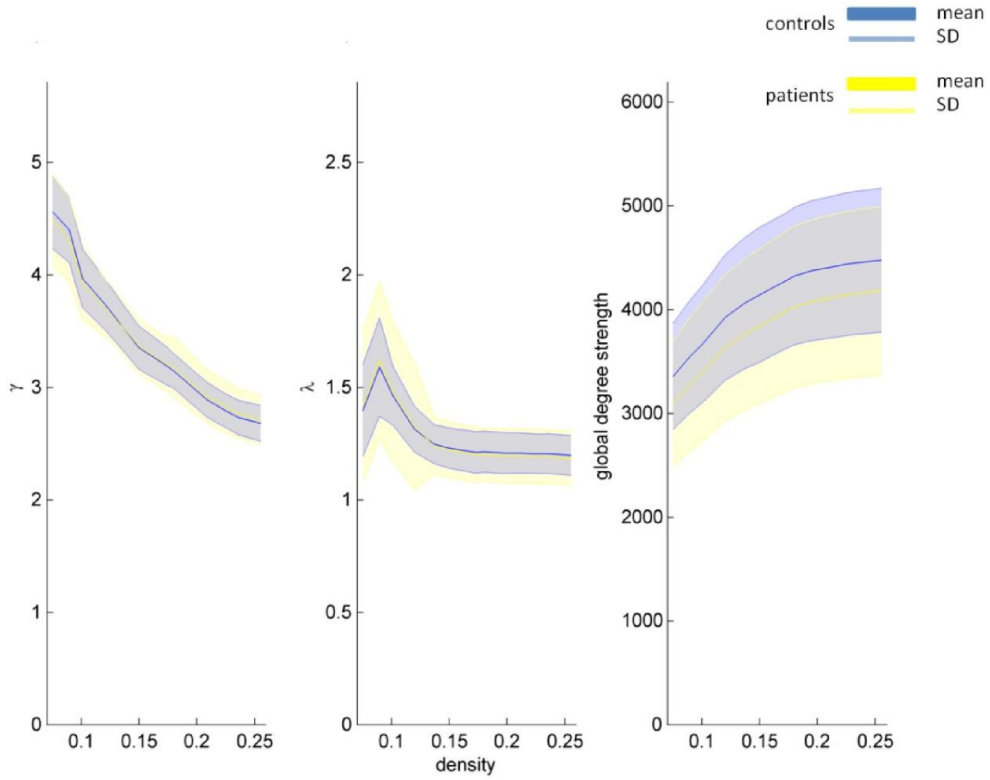

Chapter 3

Project 2: “Network-based decoupling of local gyrification in obsessive-compulsive disorder”

The current chapter includes the research article “Network-based decoupling of local gyrification in obsessive-compulsive disorder”. This article, for the first time, aimed at analyzing gyrification-based structural covariance networks in OCD. Results indicated widespread alterations in OCD that are potentially related to time-locked neurodevelopmental periods. The manuscript was published in Human Brain Mapping in 2018.

Contributions:

Authors: *Tim Jonas Reess, Oana Georgiana Rus, Deniz A. Gürsel, Benita Schmitz-Koep, Gerd Wagner, Götz Berberich, Kathrin Koch*

The author of this thesis is the first author of the manuscript. **T.J.R.** and K.K. with the help of G.W. and G.B. conceived the experiment. **T.J.R.**, O.G.R., B.S.K., and D.A.G recruited participants and conducted the data acquisition. G.W. contributed data. **T.J.R.** performed analyses. **T.J.R.** wrote the manuscript in consultation with O.G.R., G.W., and K.K. All authors discussed the results and revised the final manuscript.

Received: 18 September 2017 | Revised: 7 March 2018 | Accepted: 23 March 2018

DOI: 10.1002/hbm.24071

RESEARCH ARTICLE

WILEY

Network-based decoupling of local gyrification in obsessive-compulsive disorder

Tim Jonas Reess[1,2] | Oana Georgiana Rus[1,2] | Deniz A. Gürsel[1] | Benita Schmitz-Koep[1] | Gerd Wagner[3] | Götz Berberich[4] | Kathrin Koch[1,2]

[1]Department of Neuroradiology & TUM-Neuroimaging Center (TUM-NIC), Klinikum rechts der Isar, Technische Universität München, Ismaninger Straße 22, Munich, 81675, Germany

[2]Graduate School of Systemic Neurosciences GSN, Ludwig-Maximilians-Universität, Biocenter, Großhaderner Strasse 2, Munich, 82152, Germany

[3]Department of Psychiatry and Psychotherapy, Jena University Hospital, Philosophenweg 3, Jena, 07743, Germany

[4]Windach Institute and Hospital of Neurobehavioural Research and Therapy (WINTR), Schützenstr. 100, Windach, 86949, Germany

Correspondence
Tim Jonas Reess, Department of Neuroradiology, Ismaninger Straße. 22, 81675 München.
Email: tim.reess@tum.de

Funding information
Grant Sponsor: German Research Foundation (DFG), Grant/Award Numbers: DFG KO 3744/7-1 and DFG WA 3001/3-1

Abstract

Gyrification is associated with cortical maturation and closely linked to neurodevelopmental processes. Obsessive-compulsive disorder has previously been associated with neurodevelopmental risk factors. Using graph theoretical modeling we examined structural covariance patterns to assess potential disruptions in processes associated with neurodevelopment in OCD. In total 97 patients and 92 healthy controls underwent magnetic resonance imaging. Structural covariance networks based on local gyrification indices were constructed using an atlas-based parcellation scheme. Network properties were assessed using the network-based statistic as well as global and local graph theoretical measures. Correlations between gyrification and symptom severity as well as age of disease onset were examined. Network-based statistic analysis revealed one cluster with significantly decreased structural covariance in patients comprising mainly ventral brain regions ($p = .041$). Normalized characteristic path length was found to be impaired in patients ($p = .051$). On a nodal level, left middle frontal sulcus displayed a significantly decreased local clustering coefficient ($p < .001$). Finally, gyrification in several inferior frontal nodes significantly correlated with age of onset but not symptom severity. The decrease in a gyrification-based covariance network in OCD appears to be mostly confined to ventral areas in which gyrification starts the latest during development. This pattern may indicate that alterations taking place during development are potentially time locked to specific periods. Correlations between gyrification in inferio-frontal nodes and age of onset potentially indicate a structural trait rather than state marker for OCD. Finally, a trend in impaired global integration capabilities may point towards potentially widespread global alterations during neurodevelopment in patients.

KEYWORDS
connectome, gyrification, MRI, network, OCD

1 | INTRODUCTION

The processes leading to the characteristic differentiation of the brain's surface into sulci and gyri, called gyrification, have been studied across various species employing a broad range of experimental techniques (Zilles, Palomero-Gallagher, & Amunts, 2013). Different theoretical accounts have been put forward to explain gyrification (Fernandez, Llinares-Benadero, & Borrell, 2016; Ronan & Fletcher, 2015; Sun & Hevner, 2014) with a common assumption that it increases efficiency regarding metabolic cost via shorter axons and thus increased information processing speed (Striedter, Srinivasan, & Monuki, 2015; White, Su, Schmidt, Kao, & Sapiro, 2010). Further evidence also indicates a potential relationship between structural connectivity and cortical folding (Takahashi, Folkerth, Galaburda, & Grant, 2012; Van Essen, 1997). Additionally, several studies have revealed a structure-cognition

Abbreviations: FDR, false discovery rate; HC, healthy controls; *lGI*, *local* gyrification index; NaSSA, noradrenergic and specific serotonergic antidepressant; NBS, network-based statistic; NDRI, norepinephrine-dopamine reuptake inhibitor; OCD, obsessive-compulsive disorder; SSNRI, selective serotonin-norepinephrine reuptake inhibitor; SSRI, selective serotonin reuptake inhibitor; TCA, tricyclic antidepressant; Y-BOCS, Yale-Brown Obsessive-Compulsive Scale.

relationship in healthy subjects in terms of associations between local gyrification and cognitive performance in working memory and mental flexibility tasks (Gautam, Anstey, Wen, Sachdev, & Cherbuin, 2015) as well as attention and semantic verbal fluency tasks (Jockwitz et al., 2017). Interestingly, gyrification has been demonstrated to mainly occur between the last two trimesters of gestation up to approximately one year (Armstrong, Schleicher, Omran, Curtis, & Zilles, 1995; White et al., 2010), thus making it a potential marker for early neurodevelopment. In line with the fact that gyrification is clearly associated with neurodevelopment, there has been accumulating evidence of alterations in diseases featuring a neurodevelopmental component such as autism spectrum disorder (Ecker et al., 2016), depression (Han et al., 2017) and schizophrenia (Palaniyappan & Liddle, 2012; Palaniyappan et al., 2016; Palaniyappan, Park, Balain, Dangi, & Liddle, 2015). Recent evidence points towards altered gyrification patterns to be also found in obsessive-compulsive disorder (OCD) which has previously been discussed as a disorder with neurodevelopmental risk factors (Huyser, Veltman, de Haan, & Boer, 2009; Rosenberg & Keshavan, 1998). However, results regarding alterations in cortical folding in OCD are somewhat heterogeneous with the majority of studies reporting hypogyrification (Rus et al., 2016; Shim et al., 2009; Wobrock et al., 2010) or gender-specific hypogyrification (Venkatasubramanian et al., 2012), and others reporting hypergyrification (Fan et al., 2013). Thus far, analyses of gyrification patterns were typically based on univariate (i.e., region of interest) or mass-univariate (e.g., whole-brain, vertex-wise) approaches yielding information on local changes. While being entirely valid in their own right, it has recently become feasible to additionally infer information at a network level employing connectomics-based methods. Here, the focus is shifted from observing purely local differences towards observing changes in the covariance between morphological properties within brain regions (Alexander-Bloch, Giedd, & Bullmore, 2013). Thus far, the evaluation of structural as well as functional brain alterations employing a network level perspective has revealed important new results that have the potential to further inform neurobiological models of OCD by providing additional information on disease specific alterations in selected parameters of network complexity (Feusner et al., 2015; Jung et al., 2017; Moreira et al., 2017; Reess et al., 2016; Shin et al., 2014; Vaghi et al., 2017). To date numerous studies of anatomical covariance based networks (mainly using measures of cortical thickness or volume) have been conducted (Evans, 2013) and first studies of gyrification-based networks in schizophrenia have recently been published (Palaniyappan et al., 2016; Palaniyappan et al., 2015). The aim of our study is to extend recent local findings of altered gyrification in OCD to the network level, via examination of gyrification-based covariance networks. To this end we based our analysis on data previously described in Rus et al. (Rus et al., 2016) but further increased the sample size by adding an independent set of another 42 subjects (OCD = 24, healthy controls = 18) resulting in total sample sizes of $n = 97$ patients and $n = 92$ healthy controls. To the best of our knowledge, to date no study has examined gyrification-based networks in OCD employing a connectomics approach. Given the previously described alterations found in local measures of gyrification, it seems likely to also find changes in structural covariance on the network level. However, this is not a necessity since differences in gyrification derived from local examination do not have to map closely to differences derived from network analyses examining covariance between regions, and vice versa. We therefore propose two alternative scenarios regarding the results. The absence of alterations in gyrification-based networks regarding global topological measures might speak in favor of changes that are locally confined (i.e., hardly tractable by assessing global network measures), and may thus be interpreted as potentially independent in mechanism, therefore resulting in rather focal changes. Alternatively, alterations in global network topology may be indicative of impairments in the development of the system as a whole. More specifically, changes in measures of segregation might be indicative of developmental changes on a modular level, whereas changes in measures of integration might point towards a potentially common mechanism affecting neurodevelopment on a rather global level and/or time span. A second line of questioning addresses potential relationships between gyrification and the age of disease onset as well as symptom severity. Correlations with age of onset may further point towards altered gyrification being a neurodevelopmental risk factor in OCD.

2 | MATERIALS AND METHODS

2.1 | Participants

The study sample comprised three different samples examined at two centers. A total of $n = 97$ patients with OCD as the primary diagnosis were included in the study. Patients of two samples (M1_ocd, $n = 39$; M2_ocd, $n = 25$), both scanned at the Klinikum rechts der Isar, Technische Universität München, Germany were recruited from the Windach Institute and Hospital of Neurobehavioral Research and Therapy (WINTR), an institution specialized in the treatment of OCD. The third sample (J1_ocd, $n = 33$) was recruited and scanned at the University Hospital for Psychiatry and Psychotherapy, Jena, Germany. All subjects were in-house patients, diagnosed by an experienced psychiatrist according to DSM-IV criteria. As a control group $n = 92$ age and gender-matched healthy subjects were included (M1_hc, $n = 41$; M2_hc, $n = 19$; J1_hc, $n = 32$). Exclusion criteria for all subjects were a history of clinically important head injuries, seizures or neurological diseases. There were no significant differences between healthy controls and OCD patients regarding age (two-sample t test, two-tailed; $t_{187} = -0.667$, $p = .505$) and gender (Chi-Square test; $\chi^2_{102} = 107.79$, $p = .281$). For demographical and clinical sample characteristics, see Table 1.

At the time of the study, $n = 36$ patients were drug-naïve or medication free for at least 3 weeks. No patients were excluded due to comorbidities and $n = 30$ patients had one or more comorbid diagnosis. Prior to scanning, patients were handed the Yale-Brown Obsessive-Compulsive Scale (Y-BOCS) to assess clinical severity of obsessive-compulsive symptoms. The study was approved by the local Ethics Committee of the Klinikum rechts der Isar, München and the Ethics Committee of the University Hospital Jena. The study protocol was in compliance with the Declaration of Helsinki.

TABLE 1 Demographic and clinical sample characteristics

Characteristics	OCD (n = 97) n (%) or mean ± SD (range)	HC (n = 92) n (%) or mean ± SD (range)
Female	65 (67.0%)	54 (58.7%)
age (years)	32.5 ± 9.1 (19–62)	30.2 ± 9.6 (18–57)
age of onset	17.3 ± 6.4	–
Y-BOCS total	20.9 ± 6.2 (9–38)	–
Obsession	10.5 ± 4.0 (0–20)	–
Compulsions	10.6 ± 3.5 (0–19)	–
comorbidities	31 (32.0%)	–
depression	21	–
anxiety disorders	10	–
personality disorder	4	–
eating disorder	2	–
ADHD	2	–
medication	56 (57.7%)	–
SSRI	43	–
SSNRI	8	–
neuroleptic	5	–
TCA	4	–
methylphenidate	2	–
benzodiazepine	1	–
NDRI	1	–
NaSSA	1	–

Note that multiple comorbid diagnosis as well as different medication types can be present in a single patient.
Abbreviations: HC, healthy controls; NaSSA, noradrenergic and specific serotonergic antidepressant; NDRI, norepinephrine-dopamine reuptake inhibitor; OCD, obsessive-compulsive disorder; SSNRI, selective serotonin-norepinephrine reuptake inhibitor; SSRI, selective serotonin reuptake inhibitor; TCA, tricyclic antidepressant; Y-BOCS, Yale-Brown Obsessive-Compulsive Scale.

2.2 | Image acquisition

Structural magnetic resonance imaging (MRI) at the Munich site was conducted on a 3T Philips Ingenia (Philips Healthcare, Best, The Netherlands) using a 12-channel (SENSE) head coil (M1_ocd, M1_hc) or a 32-channel (SENSE) head coil (M2_ocd, M2_hc). MRI at the Jena site was conducted on a 3T Siemens MAGNETOM (Siemens Medical Solutions, Erlangen, Germany) using a 12-channel receive-only head matrix coil (J1_ocd, J1_hc). Details regarding image acquisition parameters are given in the Supporting Information.

2.3 | Image processing

Cortical surface reconstruction was conducted using FreeSurfer's (V5.3.0 http://surfer.nmr.mgh.harvard.edu/) standard processing pipeline (Dale, Fischl, & Sereno, 1999; Fischl et al., 2002; Fischl, Sereno, & Dale, 1999). After reconstruction, *local* Gyrification Index (*l*GI) was computed based on the method developed by Schaer et al. (2008). In short, the algorithm provides a ratio between the pial surface area and cortical sheet surface area, sampled over regions of interest that are spread over cortex. This approach results in a continuous vertex-based measure of local gyrification index over the entire cortical surface. For subsequent graph construction, Freesurfer's Destrieux brain parcellation scheme was applied (Destrieux, Fischl, Dale, & Halgren, 2010) and all reconstructed brain data were parcellated accordingly yielding a total of 74 regions within each hemisphere. Quality control was performed using the ENIGMA cortical quality control protocols (http://enigma.ini.usc.edu/protocols/imaging-protocols/). Destrieux based parcellations were additionally overlayed on reconstructed surfaces and visually checked after running the QA Tools provided on the Freesurfer webpage (https://surfer.nmr.mgh.harvard.edu/fswiki/QATools).

2.4 | Graph construction

In a first step, the averaged *l*GI values within each parcellated brain region were adjusted for age, sex, scan sequence, and total intracranial volume using multiple regression in line with He, Chen, and Evans, (2007). The residuals were subsequently used as a proxy for subjects' *l*GI. Each brain region derived from the Destrieux parcellation was assigned as a node. An edge represented the correlation between the adjusted *l*GIs of two nodes. Correlations for every possible pair of nodes (N_i, N_j) were computed, resulting in a 148 × 148 symmetric graph, representing a gyrification-based structural covariance network. To avoid the influence of spurious relationships, significance of correlations was tested and only edges surviving FDR-correction ($p < .05$) were retained. Subsequently, to perform network analysis, a graph was constructed for each group (i.e., OCD patients and healthy controls) and all edges previously identified as exceeding the FDR-corrected threshold were set to zero. These FDR-corrected correlation matrices were subsequently used to conduct a network-based statistic (NBS) analysis. For computation of graph measures the connectivity matrices were thresholded over a range of connection densities (see Graph theoretical analysis below) in order to preserve the same number of edges in each group.

2.5 | Network-based statistic analysis

Group differences between *l*GI based networks were examined using the framework of the NBS introduced by Zalesky et al. (Zalesky, Fornito, & Bullmore, 2010). NBS is a nonparametrical method to deal with the multiple comparison problem encountered in conducting mass univariate significance testing in graphs. Statistical significance is established for specific subsets of nodes that are mutually connected in topological rather than physical space. The first step requires the computation of a test statistic, in this case the difference in Fishers *z*-transformed group-based correlation coefficients. Second, a primary component forming threshold ($p < .001$, two sided test) is applied to identify all edges displaying potential differences in *l*GI correlations. Third, all subthreshold edges are assessed for mutual connections forming clusters in topological space that may point towards the existence of non-chance clusters. Permutation testing is then applied to

compute p values for every component previously identified. For each of 10,000 permutations, group labels are randomly shuffled resulting in two new groups with sample sizes being equal to the original groups. Within each, correlation coefficients between nodes are determined and subsequently Fisher z-transformed. For each edge the difference in z-transformed correlation coefficients between groups is computed. Based on these matrices steps two and three are repeated with noting the maximum cluster size of components resulting in a null distribution for largest component size. The final hypothesis test is then carried out for the empirically determined components by comparing their sizes with the proportion of permutations yielding a component with equal or greater size. The final result controls the family-wise error rate at cluster level with $p < .05$. Visualization of NBS networks was conducted using BrainNet Viewer (V1.53; Xia, Wang, & He, 2013).

2.6 | Graph theoretical analysis

The following global graph measures were computed: normalized average clustering coefficient gamma (γ) to assess segregation, as well as normalized average path length lambda (λ) to assess integration. Finally sigma ($\sigma = \frac{\gamma}{\lambda}$) was used as an index of small-worldness. Normalization of network measures was based on dividing the empirically found measure by the respective measure computed over a total of 1,000 null networks created using a rewiring algorithm that preserves the degree distribution. As a local measure of segregation, node-based normalized local clustering coefficients were computed. As a local measure of integration, node-based normalized local efficiencies were computed. Statistical comparisons for all measures were based on permutation testing with 1,000 permutations. Subject data was randomly sampled and assigned to a group while preserving the original group sizes (healthy controls and OCD). For each resampling, the resulting correlation matrices were binarized and thresholded. As the computation of graph measures is strongly influenced by fragmented connectivity matrices (Fornito, Zalesky, & Bullmore, 2016) the measures were computed for a range of densities (0.1–0.5 with increments of 0.05) over which no fragmentation of graphs occurred. Subsequently, the empirically found group differences for global and local graph measures were compared with the distribution of group differences constructed from computing the graph measures across all resampled connectivity matrices. Computing each measure over the given range of densities results in a curve for each measure that is finally compared between groups over the entire threshold range using functional data analysis (Ramsay, 2005), effectively accounting for the multiple comparison problem. Simultaneously taking into account the values over the entire threshold range effectively avoids the multiple comparison problem typically encountered if comparing the differences over various density values. All results were tested at $p < .05$ based on a two-sided test. For local graph measures, results are reported at $p < .05$, using FDR-correction. For formulas regarding the computation of network measure see Rubinov & Sporns (Rubinov & Sporns, 2010). All measures were calculated on the group based connectivity matrices using the Graph Analysis Toolbox (GAT, V1.3.32; Hosseini, Hoeft, & Kesler, 2012) which draws on algorithms provided in the Brain Connectivity Toolbox (BCT) using Matlab (R2013a, The MathWorks, Inc., Natick, MA).

2.7 | Correlations with clinical scores

Potential relationships between clinically relevant information (Y-BOCS, age of onset) and node-based *l*GIs were assessed using Pearson correlation coefficients based on data adjusted for age, sex, scanner, and total intracranial volume. All correlations were corrected for multiple comparisons using FDR-correction at $p < .05$.

2.7.1 | Assessment for group x age interaction effects

Several studies have revealed differential age trajectories for structural brain measures such as cortical thickness (Fouche et al., 2017) and volume (de Wit et al., 2014) between OCD patients and healthy controls. To examine whether similar effects are present in the current sample, a separate model assessing group x age interaction effects, controlling for sex, total intracranial volume, as well as scan sequence was computed.

2.7.2 | Exploratory subgroup analyses

In order to assess potential effects of medication and comorbidity, exploratory subgroup analyses were performed. To this end, the patient group was split into patients with and without medication as well as with and without comorbidity. Subsequently, three comparisons for medication effects as well as for effects of comorbidity were conducted: (1) between patient groups only, (2) patients with medication or comorbidity vs. healthy controls, and (3) patients without medication or comorbidity versus healthy controls. Subgroup analyses comprised NBS as well as graph measures. We additionally performed NBS analyses to evaluate the influence of early versus late onset by splitting the patient sample using various thresholds (for details see Supporting Information).

3 | RESULTS

3.1 | NBS of gyrification based network alterations in OCD

NBS analysis revealed a single network of consistently reduced structural covariances in OCD patients as compared with healthy controls ($p = .041$, corrected, see Figure 1). The network comprised a total of 31 nodes (see Table 2) connected by 34 edges (see Table 3) and was distributed throughout both hemispheres (see Figure 1).

3.2 | Graph measures describing global and local network properties

Networks of both groups were found to be in the small-world regime indicated by γ-values > 1 and λ-values ~ 1 with σ exceeding one (see Table 4). No significant differences were found for σ as well as γ. However, the normalized average characteristic path length (λ) was different between groups at trend level ($p = .0510$) with OCD patients displaying a higher λ compared with healthy controls. For plots of group differences for each graph measure as a function of density see Figure 2.

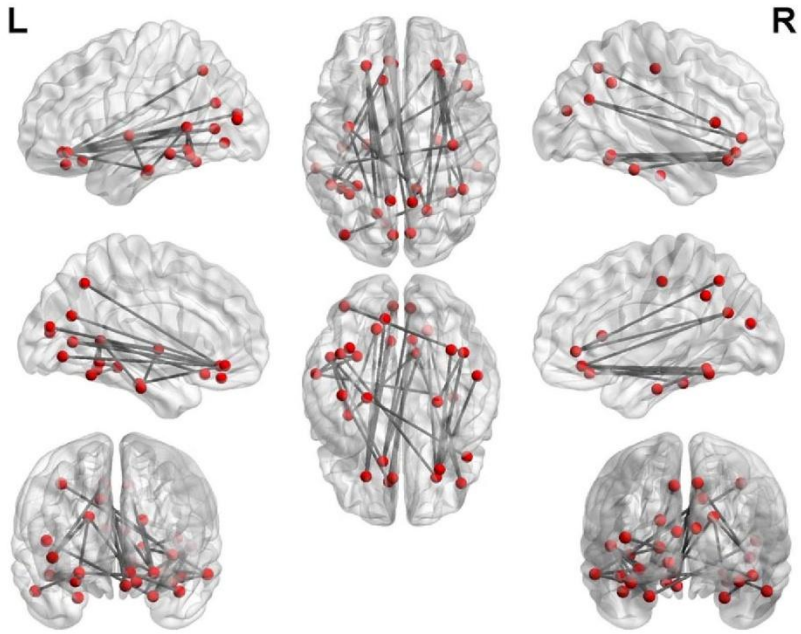

FIGURE 1 Network-based statistic analysis results. Visualization of the significantly altered gyrification-based structural covariance network (i.e., decreased covariance) in OCD based on network-based statistic analysis ($p = .041$). Red dots indicate nodes comprising the cluster, gray lines indicate edges between nodes [Color figure can be viewed at wileyonlinelibrary.com]

3.3 | Local measures

A significant decrease in local clustering within left middle frontal sulcus was found in patients ($p < .001$, corrected). No significant differences were found for any other nodes regarding local clustering or local efficiency measures.

3.4 | Correlations with clinical scores

A total of five nodes revealed significant correlations (FDR-corrected) between *l*GI values and age of onset (see Table 5 and Supporting Information Table S1 for correlations at $p < .05$, uncorrected). All correlations were positive indicating that later age of onset was associated with larger *l*GIs. There were no significant correlations between *l*GI values and YBOCS-scores for any of the nodes in question.

3.5 | Group × age interaction effects

While age was significantly correlated with *l*GI values across widespread areas within each group separately (see Supporting Information Figure S1), there were no group x age interaction effects within the current sample.

3.6 | Exploratory subgroup analyses

3.6.1 | Effects of medication, comorbidity, and early versus late onset

There were no significant differences between medicated and unmedicated patients in the NBS analysis ($p = .199$). Comparison of medicated patients vs. healthy controls ($p = .116$) as well as unmedicated patients versus healthy controls ($p = .799$) did not yield significant differences. There were no significant differences between patients with and without comorbidity ($p = .930$). Comparison of patients with comorbidity versus healthy controls ($p = .189$) as well as without comorbidities versus healthy controls ($p = .213$) did not yield significant differences. There were also no significant differences in NBS results regarding early versus late onset splits (see Supporting Information for more details).

4 | DISCUSSION

The current study reports on structural connectome differences in gyrification-based covariance networks between OCD patients and healthy controls. The results can be broadly split into three aspects: (1) NBS results assessing differences in the overall topology of the networks, (2) results from graph measures assessing differences in global as well as local characteristics in network structure, and (3) relationships between gyrification and the age of onset. Firstly, applying the framework of the NBS, one cluster with consistently decreased structural coupling in gyrification was identified in OCD. A striking feature in the pattern of this cluster is the asymmetry of decreased structural covariances towards rather ventral brain regions. More precisely, nodes found within the cluster can be broadly assigned to three categories: (a) inferior-frontal as well as (b) occipito-temporal regions, together accounting for ~80% of all nodes, and c) parieto-occipital regions in conjunction with parts of insula accounting for the remaining ~20% of nodes in the cluster. Interestingly, in OCD patients, Kim, Jung, Kim,

TABLE 2 Nodes comprising the significantly different network. based statistic cluster in obsessive-compulsive disorder

Region	Node	Left	Right
Inferior-frontal	Orbital sulci	×	×
	Gyrus rectus	×	
	Medial orbital sulcus	×	
	Suborbital sulcus	×	
	Orbital gyrus		×
	Lateral orbital sulcus		×
	Horizontal ramus of ant. segment of lateral sulcus		×
Occipito-temporal	Cuneus	×	×
	Lateral occipito-temporal gyrus	×	×
	Parahippocampal gyrus	×	×
	Lateral occipito-temporal sulcus	×	×
	Lingual gyrus	×	
	Middle occipital gyrus	×	
	Middle temporal gyrus	×	
	Superior temporal sulcus	×	
	Medial occipito-temporal sulcus and lingual sulcus	×	
	Anterior transverse collateral sulcus	×	
	Calcarine sulcus	×	
	Inferior temporal gyrus		×
Parietal	Precuneus	×	×
	Subparietal sulcus		×
Parieto-occipital	Parieto-occipital sulcus	×	×
Fronto-parietal	Central sulcus		×
Insula	Long insular gyrus and central sulcus of the insula	×	

Jang, and Kwon, (2013) found measures of nodal efficiency to be decreased in ventral and increased in dorsal nodes of brain networks constructed on the basis of cortical thickness. However, results are not directly comparable as it was demonstrated by Gautam et al. (2015) that cortical thickness and gyrification are typically negatively correlated in a rather unspecific, largely distributed pattern with the exception of aspects of medial frontal regions that are also negatively correlated but cover a rather large area and are more pattern-like. Additionally, local measures of efficiency are computed on a nodal basis and are related to clustering coefficients. Nevertheless, first evidence from Kim et al. (2013) indicates alterations that are following a dorsal/ventral gradient. Our findings also point to a dorsal/ventral imbalance based on another anatomical measure, that is, gyrification covariance networks. Typically, an imbalance in dorsal/ventral fronto-striatal circuitry appears to be associated especially with cognitive inflexibility (Gu et al., 2008), with reduced dorsal circuit activity leading to disinhibition and thus increased activity in ventral fronto-striatal circuits. Additionally, ventral fronto-striatal circuits have been associated especially with altered reward processing and the regulation of affect in OCD (Milad & Rauch, 2012). There is accumulating evidence that networks constructed on the basis of structural covariance, that is, cortical thickness as well as gray matter volume, are indicating synchronized developmental changes (Alexander-Bloch et al., 2013; Khundrakpam et al., 2013; Zielinski, Gennatas, Zhou, and Seeley, 2010). Regarding the developmental trajectory of gyrification, it has been proposed that its starting point lies within dorsal parieto-occipital areas and over the course of development proceeds to *superior* frontal and temporal regions before finally continuing to *inferior* frontal and temporal regions (Takahashi et al., 2012). The spatial pattern of differences found in the NBS analysis might be indicative of an impairment that may be time locked to late stages in neurodevelopment as most of the affected nodes are located in inferior frontal and inferior temporo-occipital areas in which gyrification starts latest. Therefore, these ventrally located alterations in gyrification-based covariance networks in OCD patients may potentially be attributable to a common, yet still unknown, mechanism or cause related to a rather late period in neurodevelopment and may indicate a risk factor for the development of OCD. A similar pattern of alterations in grey matter volumes of mostly ventrally located brain regions such as the thalamus, hippocampus, OFC, posterior cingulate cortex and centrum semiovale can be observed in preterm birth (Ball et al., 2012). Additionally, there appears to be an overlap between grey matter alterations of ventral brain structures and associated intrinsic connectivity in preterm born adults as well (Bauml et al., 2015). Surprisingly, two recent studies have identified preterm birth and low birth weight (among others) to be risk factors for developing OCD (Brander et al., 2016; Fevang, Hysing, Markestad, & Sommerfelt, 2016). Given that *l*GI values for nodes did not correlate with symptom severity, alterations may potentially be interpreted as a trait instead of state marker in line with the notion of gyrification being a measure that is rather stable over time and revealed no group x age interaction effects in our sample. One striking feature, further illustrating the value of connectome based approaches in general, is the difference in results between the current study and the findings presented by Rus et al. (2016). Though in both studies the measure being analyzed is lGI, findings are somewhat different. Rus et al. (2016) report alterations mainly in insula and dorsal regions (i.e. inferior and superior parietal, post- and precentral as well as superior frontal areas) that are confined to the right hemisphere without revealing significant differences concentrating on ventral regions. This discrepancy in finding is, however, not surprising as both analyses essentially measure something potentially very different. In one case, it

TABLE 3 Edges comprising the significantly different NBS cluster in obsessive-compulsive disorder

Side	Edge connecting	
Left–left	Long insular gyrus/central sulcus of the insula	Parahippocampal gyrus
	Lateral occipito-temporal gyrus	Middle temporal gyrus
	Long insular gyrus/central sulcus of the insula	Calcarine sulcus
	Middle temporal gyrus	Med. occipito-temporal sulcus/lingual sulcus
	Cuneus	Orbital sulci
	Lingual gyrus	Orbital sulci
	Precuneus	Orbital sulci
	Calcarine sulcus	Orbital sulci
	Parieto-occipital sulcus	Orbital sulci
	Anterior transverse collateral sulcus	Suborbital sulcus
	Long insular gyrus/central sulcus of the insula	Superior temporal sulcus
	Lateral occipito-temporal gyrus	Superior temporal sulcus
	Parahippocampal gyrus	Superior temporal sulcus
	Med. occipito-temporal sulcus/lingual sulcus	Superior temporal sulcus
	Medial orbital sulcus	Superior temporal sulcus
Left–right	Medial orbital sulcus	Cuneus
	Gyrus rectus	Precuneus
	Medial orbital sulcus	Precuneus
	Suborbital sulcus	Precuneus
	Parahippocampal gyrus	Horiz. ramus of ant. segment of lateral sulcus
	Middle temporal gyrus	Central sulcus
	Middle occipital gyrus	Lateral occipito-temporal sulcus
	Lateral occipito-temporal sulcus	Orbital sulci
	Medial orbital sulcus	Parieto-occipital sulcus
	Long insular gyrus/central sulcus of the insula	Subparietal sulcus
right–right	Lateral occipito-temporal gyrus	Orbital gyrus
	Parahippocampal gyrus	Lateral occipito-temporal sulcus
	Orbital gyrus	Lateral occipito-temporal sulcus
	Precuneus	Lateral orbital sulcus
	Lateral occipito-temporal gyrus	Orbital sulci
	Inferior temporal gyrus	Orbital sulci
	Lateral occipito-temporal sulcus	Orbital sulci
	Lateral orbital sulcus	Parieto-occipital sulcus
	Orbital sulci	Parieto-occipital sulcus

is a vertex-by-vertex comparison of *l*GIs between groups while in the other case it is the comparison of mutual correlation between *l*GIs of different brain regions between groups. However, there is also some overlap regarding correlations with age at onset. Comparing the correlation between *l*GI and age at onset reported in Rus et al. (2016) with correlations between average node-wise *l*GI with age at onset from the current study reveals a substantial overlap. It should be kept in mind, however, that correlations in the current study are significantly correlated at an uncorrected threshold of $p < .05$ which, on the other hand, is likely due to the need for multiple comparison adjustment which in case of network based studies is typically quite extensive. Finally, the overlap in correlations is not surprising as a large proportion of the sample is essentially based on the same subjects. Secondly, the overall network topology assessed by measuring small-worldness showed no

TABLE 4 Global topological measures of gyrification-based structural covariance networks

	Healthy controls	Obsessive-compulsive disorder	Functional data analysis based permutation test (*p* values)
Small-world index (σ)	1.5019 (0.5029)	1.6104 (0.4589)	0.5480
Normalized average clustering coefficient gamma (γ)	1.6492 (0.7182)	1.8363 (0.7910)	0.3460
Normalized average characteristic path length (λ)	1.0730 (0.0847)	1.1060 (0.1371)	0.0510

All indices mean ± *SD*.

significant abnormalities in patients. This finding is in line with other studies employing graph based analysis strategies in schizophrenia using gyrification based networks (Palaniyappan et al., 2016; Palaniyappan et al., 2015) as well as various other structural outcome measures in OCD (Kim et al., 2013; Reess et al., 2016; Zhong et al., 2014). However, the normalized average characteristic path length (λ) was found to be decreased in patients at trend level ($p = .051$) potentially indicating a decreased global integration capability in patients. Considering that nodes within the impaired network found using NBS analysis are mainly distributed ventrally, one might try to probe whether the trend effect in normalized average characteristic path length is mainly driven by alterations between ventral nodes. This type of analysis would however be circular if conducted within the same data set. The only node displaying significant differences (FDR-corrected) regarding local clustering was found to be the left middle frontal sulcus. In OCD, this node's clustering coefficient was decreased, indicating that its topological neighbors are less well connected with each other than in healthy controls. This is a potentially relevant finding given the anatomy and functionality of the middle frontal sulcus. The middle frontal sulcus is buried within middle frontal gyrus (Destrieux et al., 2010) and overlaps with dorso-lateral prefrontal cortex (DLPFC), a region that has previously been associated with planning abilities. Interestingly, van den Heuvel et al. (2005) report a decreased activity in left DLPFC-striatal responsiveness in obsessive compulsive disorder to go along with

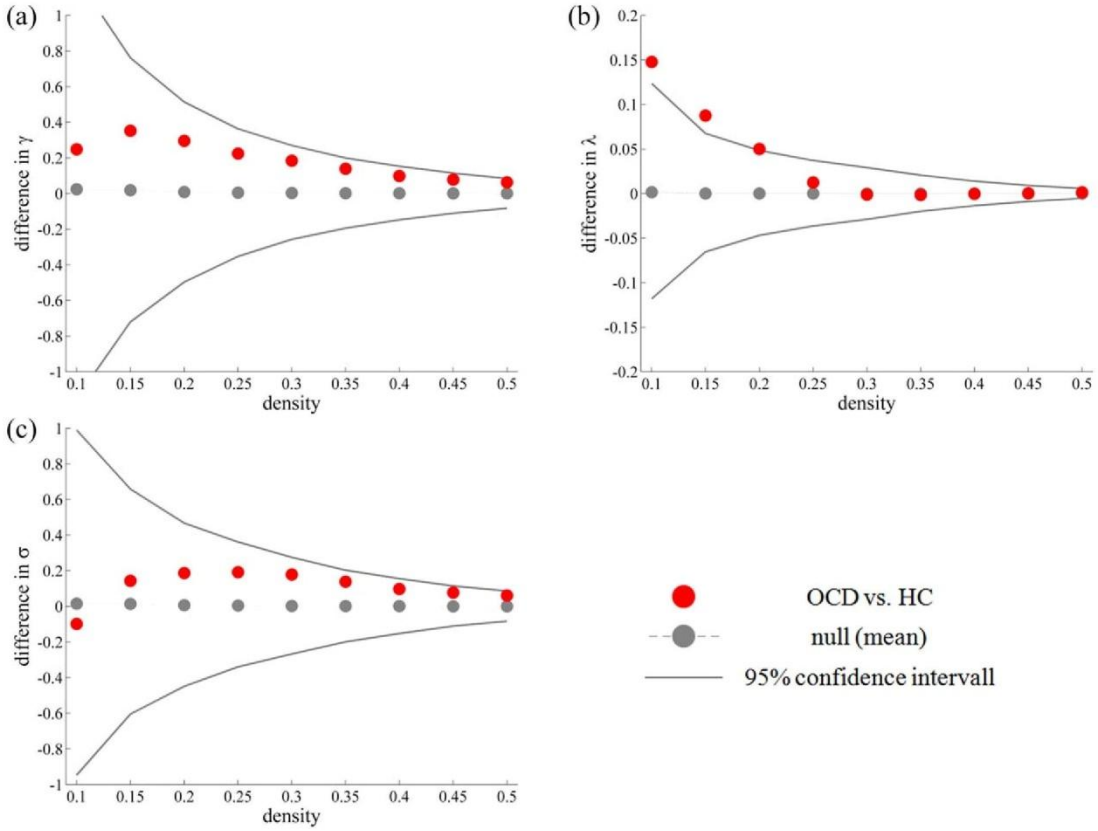

FIGURE 2 Global graph-measures as a function of density. (a) Between-group differences in normalized average clustering coefficients, γ. (b) Between-group differences in normalized average characteristic path length, λ. (c) Between-group differences in small-world index, σ [Color figure can be viewed at wileyonlinelibrary.com]

TABLE 5 Correlations between node-based local gyrification and age of onset

	r	*p* (FDR-corrected)
lh gyrus rectus	0.328	$p = .001$
lh suborbital sulcus	0.355	$p < .001$
rh gyrus rectus	0.346	$p < .001$
rh subcallosal gyrus	0.318	$p = .002$
rh medial orbital sulcus	0.372	$p < .001$

Abbreviations: lh, left hemisphere; rh, right hemisphere; *r*, Pearson correlation coefficient; FDR, false discovery rate.

impaired task performance during a Tower of London Task assessing planning abilities. Furthermore, Kaller, Rahm, Spreer, Weiller, and Unterrainer (2011), similarly employing a Tower of London Task, found a dissociation between left and right DLPFC function with stronger activations in the left DLPFC correlating with higher demands on goal hierarchy in healthy subjects. This is interpreted as a stronger involvement of left DLPFC during goal extraction for a given problem. Hence, the decreased clustering coefficient of the left middle frontal sulcus indicating a reduced connectivity among its neighbors may constitute the structural basis of impaired planning abilities in OCD. However, it should be noted that a further study reported impairments in DLPFC activity related to impaired task performance not only for OCD but also other diagnostic categories including panic disorder and hypochondriasis (van den Heuvel et al., 2011). The authors therefore concluded that a common, disease-unspecific mechanism may underlie the impairments in planning ability. Thirdly, we report significant positive correlations between *l*GI's in several inferior frontal nodes and age of onset indicating that smaller *l*GI values are accompanied by earlier age of disease onset. The lack of group × age interactions may speak in favor of differences in gyrification networks indicating a potential early neurodevelopmental risk factor that appears to be independent of age related developmental trajectories. Additionally, the significant association with age of onset suggests that age of onsets itself seems to further influence these early alterations. However, due to the cross-sectional study design it is not possible to draw strong conclusions about these alterations to be best interpreted as trait markers. Nevertheless, the present findings might be used to generate hypotheses and spark further research into the subject-matter ideally applying longitudinal study designs. Additionally, it may be interesting to try to assess whether patients were born pre-term when studying structural brain alterations in general and gyrification in particular. Previous studies revealed a relationship between measures of integration and segregation with therapy outcomes in schizophrenia (Palaniyappan et al., 2016). Future work might therefore use gyrification-based network measures to examine relationships between gyrification and therapy outcome (responder, nonresponder) in OCD as well. Additionally, it would be of interest to conduct analyses based on sub-graphs that are binned into phases (e.g., early, mid, late) according to the developmental scheme of gyrification. Furthermore, comparing the relationship between *l*GI values in OCD patients, their first-degree relatives, and healthy control subjects might shed more light on the importance of gyrification as a potential structural endophenotype.

5 | LIMITATIONS

Combining data from various centers using different acquisition protocols in order to substantially increase sample sizes may introduce systematic biases. This issue was addressed by adjusting *l*GI values for the scan sequence and thus coil type used. Nevertheless, some bias that cannot be removed using the applied statistical tools might remain and should be acknowledged. Due to the cross-sectional nature of the study design, it is not possible to draw strong conclusions regarding the idea of ascribing alterations in covariance patterns to time locked, sensitive periods. Additionally, very recent evidence by Cao et al. (2017) indicates that patients with various psychiatric disorders (major depression disorder, schizophrenia, and bipolar disorder I) display deviating gyrification trajectories over age when compared with healthy controls. However, the group x age interaction analyses revealed no such differences within the current sample implying a similar trajectory within OCD and healthy controls. This, in turn, speaks against a disease-related neurodegenerative or progressive process and supports our hypothesis of early neurodevelopmental alterations. Furthermore, the sample in the current study is age-matched and *l*GI values were adjusted for age-effects prior to computing correlation matrices. Another limiting factor lies within the rather heterogeneous sample regarding medication status as well as presence of comorbidities. To the best of our knowledge, there are no studies to date, that systematically examine the relationship between medication and gyrification. Additionally, previous work from our group (Rus et al., 2016) revealed that taking medication status as well as comorbidities into consideration did not significantly affect gyrification differences between OCD patients and healthy controls. Conducting exploratory sub group analyses of medicated/unmedicated patients as well as patients with and without comorbidity revealed no significant differences in the NBS results. However, a lack of significant differences does not necessarily imply a lack of relationship. Therefore, potential relationships should still be investigated in the future preferably using substantially larger sample sizes.

FINANCIAL DISCLOSURE

This study was supported by German Research Foundation (DFG) grants to K. K. (DFG KO 3744/7-1) and G. W. (DFG WA 3001/3-1). The funding agencies had no influence on the design and conduct of the study including collection, management, analysis and interpretation of the data, as well as preparation, review or approval of the manuscript. The authors reported no biomedical financial interests or potential conflicts of interest.

ORCID

Tim Jonas Reess http://orcid.org/0000-0002-6030-9769

REFERENCES

Alexander-Bloch, A., Giedd, J. N., & Bullmore, E. (2013). Imaging structural co-variance between human brain regions. *Nature Reviews Neuroscience*, *14*(5), 322–336.

Armstrong, E., Schleicher, A., Omran, H., Curtis, M., & Zilles, K. (1995). The ontogeny of human gyrification. *Cerebral Cortex (New York, N.Y.: 1991)*, *5*(1), 56–63.

Ball, G., Boardman, J. P., Rueckert, D., Aljabar, P., Arichi, T., Merchant, N., … Counsell, S. J. (2012). The effect of preterm birth on thalamic and cortical development. *Cerebral Cortex*, *22*(5), 1016–1024.

Bauml, J. G., Daamen, M., Meng, C., Neitzel, J., Scheef, L., Jaekel, J., … Sorg, C. (2015). Correspondence between aberrant intrinsic network connectivity and gray-matter volume in the ventral brain of preterm born adults. *Cerebral Cortex*, *25*(11), 4135–4145.

Brander, G., Rydell, M., Kuja-Halkola, R., Fernandez de la Cruz, L., Lichtenstein, P., Serlachius, E., … Mataix-Cols, D. (2016). Association of perinatal risk factors with obsessive-compulsive disorder: A population-based birth cohort, sibling control study. *JAMA Psychiatry*, *73*(11), 1135–1144.

Cao, B., Mwangi, B., Passos, I. C., Wu, M. J., Keser, Z., Zunta-Soares, G. B., … Soares, J. C. (2017). Lifespan gyrification trajectories of human brain in healthy individuals and patients with major psychiatric disorders. *Scientific Reports*, *7*(1), 511.

Dale, A. M., Fischl, B., & Sereno, M. I. (1999). Cortical surface-based analysis. I. Segmentation and surface reconstruction. *Neuroimage*, *9*(2), 179–194.

de Wit, S. J., Alonso, P., Schweren, L., Mataix-Cols, D., Lochner, C., Menchon, J. M., … van den Heuvel, O. A. (2014). Multicenter voxel-based morphometry mega-analysis of structural brain scans in obsessive-compulsive disorder. *American Journal of Psychiatry*, *171*(3), 340–349.

Destrieux, C., Fischl, B., Dale, A., & Halgren, E. (2010). Automatic parcellation of human cortical gyri and sulci using standard anatomical nomenclature. *Neuroimage*, *53*(1), 1–15.

Ecker, C., Andrews, D., Dell'Acqua, F., Daly, E., Murphy, C., Catani, M., … Murphy, D. G. (2016). Relationship between cortical gyrification, white matter connectivity, and autism spectrum disorder. *Cerebral Cortex*, *26*(7), 3297–3309.

Evans, A. C. (2013). Networks of anatomical covariance. *NeuroImage*, *80*, 489–504.

Fan, Q., Palaniyappan, L., Tan, L., Wang, J., Wang, X., Li, C., … Liddle, P. F. (2013). Surface anatomical profile of the cerebral cortex in obsessive-compulsive disorder: A study of cortical thickness, folding and surface area. *Psychological Medicine*, *43*(05), 1081–1091.

Fernandez, V., Llinares-Benadero, C., & Borrell, V. (2016). Cerebral cortex expansion and folding: What have we learned? *The Embo Journal*, *35*(10), 1021–1044.

Feusner, J. D., Moody, T., Lai, T. M., Sheen, C., Khalsa, S., Brown, J., … O'Neill, J. (2015). Brain connectivity and prediction of relapse after cognitive-behavioral therapy in obsessive-compulsive disorder. *Frontiers in Psychiatry*, *6*, 74.

Fevang, S. K., Hysing, M., Markestad, T., & Sommerfelt, K. (2016). Mental health in children born extremely preterm without severe neurodevelopmental disabilities. *Pediatrics*, *137*(4), e20153002.

Fischl, B., Salat, D. H., Busa, E., Albert, M., Dieterich, M., Haselgrove, C., … Dale, A. M. (2002). Whole brain segmentation: Automated labeling of neuroanatomical structures in the human brain. *Neuron*, *33*(3), 341–355.

Fischl, B., Sereno, M. I., & Dale, A. M. (1999). Cortical surface-based analysis. II: Inflation, flattening, and a surface-based coordinate system. *Neuroimage*, *9*(2), 195–207.

Fornito, A., Zalesky, A., & Bullmore, E. (2016). *Fundamentals of Brain Network Analysis*. Cambridge, MA: Academic Press.

Fouche, J. P., Du Plessis, S., Hattingh, C., Roos, A., Lochner, C., Soriano-Mas, C., … van den Heuvel, O. A. (2017). Cortical thickness in obsessive-compulsive disorder: Multisite mega-analysis of 780 brain scans from six centres. *British Journal of Psychiatry*, *210*(01), 67–74.

Gautam, P., Anstey, K. J., Wen, W., Sachdev, P. S., & Cherbuin, N. (2015). Cortical gyrification and its relationships with cortical volume, cortical thickness, and cognitive performance in healthy mid-life adults. *Behavioural Brain Research*, *287*, 331–339.

Gu, B. M., Park, J. Y., Kang, D. H., Lee, S. J., Yoo, S. Y., Jo, H. J., … Kwon, J. S. (2008). Neural correlates of cognitive inflexibility during task-switching in obsessive-compulsive disorder. *Brain*, *131*(1), 155–164.

Han, K. M., Won, E., Kang, J., Kim, A., Yoon, H. K., Chang, H. S., … Ham, B. J. (2017). Local gyrification index in patients with major depressive disorder and its association with tryptophan hydroxylase-2 (TPH2) polymorphism. *Human Brain Mapping*, *38*(3), 1299–1310.

He, Y., Chen, Z. J., & Evans, A. C. (2007). Small-world anatomical networks in the human brain revealed by cortical thickness from MRI. *Cerebral Cortex*, *17*(10), 2407–2419.

Hosseini, S. M., Hoeft, F., & Kesler, S. R. (2012). GAT: A graph-theoretical analysis toolbox for analyzing between-group differences in large-scale structural and functional brain networks. *PLoS One*, *7*(7), e40709.

Huyser, C., Veltman, D. J., de Haan, E., & Boer, F. (2009). Paediatric obsessive-compulsive disorder, a neurodevelopmental disorder? Evidence from neuroimaging. *Neuroscience & Biobehavioral Reviews*, *33*(6), 818–830.

Jockwitz, C., Caspers, S., Lux, S., Jutten, K., Schleicher, A., Eickhoff, S. B., … Zilles, K. (2017). Age- and function-related regional changes in cortical folding of the default mode network in older adults. *Brain Structure and Function*, *222*(1), 83–99.

Jung, W. H., Yucel, M., Yun, J. Y., Yoon, Y. B., Cho, K. I., Parkes, L., … Kwon, J. S. (2017). Altered functional network architecture in orbitofronto-striato-thalamic circuit of unmedicated patients with obsessive-compulsive disorder. *Human Brain Mapping*, *38*(1), 109–119.

Kaller, C. P., Rahm, B., Spreer, J., Weiller, C., & Unterrainer, J. M. (2011). Dissociable contributions of left and right dorsolateral prefrontal cortex in planning. *Cerebral Cortex*, *21*(2), 307–317.

Khundrakpam, B. S., Reid, A., Brauer, J., Carbonell, F., Lewis, J., Ameis, S., … Evans, A. C. (2013). Developmental changes in organization of structural brain networks. *Cerebral Cortex*, *23*(9), 2072–2085.

Kim, S. G., Jung, W. H., Kim, S. N., Jang, J. H., & Kwon, J. S. (2013). Disparity between dorsal and ventral networks in patients with obsessive-compulsive disorder: Evidence revealed by graph theoretical analysis based on cortical thickness from MRI. *Frontiers in Human Neuroscience*, *7*, 302.

Milad, M. R., & Rauch, S. L. (2012). Obsessive-compulsive disorder: Beyond segregated cortico-striatal pathways. *Trends in Cognitive Science*, *16*(1), 43–51.

Moreira, P. S., Marques, P., Soriano-Mas, C., Magalhaes, R., Sousa, N., Soares, J. M., & Morgado, P. (2017). The neural correlates of obsessive-compulsive disorder: A multimodal perspective. *Translational Psychiatry*, *7*(8), e1224.

Palaniyappan, L., & Liddle, P. F. (2012). Dissociable morphometric differences of the inferior parietal lobule in schizophrenia. *European Archives of Psychiatry and Clinical Neuroscience*, *262*(7), 579–587.

Palaniyappan, L., Marques, T. R., Taylor, H., Mondelli, V., Reinders, A. A., Bonaccorso, S., … Dazzan, P. (2016). Globally efficient brain

organization and treatment response in psychosis: A connectomic study of gyrification. *Schizophrenia Bulletin*, *42*(6), 1446–1456.

Palaniyappan, L., Park, B., Balain, V., Dangi, R., & Liddle, P. (2015). Abnormalities in structural covariance of cortical gyrification in schizophrenia. *Brain Structure and Function*, *220*(4), 2059–2071.

Ramsay, J. O. (2005). *Functional Data Analysis*. New York: Springer.

Reess, T. J., Rus, O. G., Schmidt, R., de Reus, M. A., Zaudig, M., Wagner, G., … Koch, K. (2016). Connectomics-based structural network alterations in obsessive-compulsive disorder. *Translational Psychiatry*, *6*(9), e882.

Ronan, L., & Fletcher, P. C. (2015). From genes to folds: A review of cortical gyrification theory. *Brain Structure and Function*, *220*(5), 2475–2483.

Rosenberg, D. R., & Keshavan, M. S. (1998). A.E. Bennett Research Award. Toward a neurodevelopmental model of of obsessive–compulsive disorder. *Biological Psychiatry*, *43*(9), 623–640.

Rubinov, M., & Sporns, O. (2010). Complex network measures of brain connectivity: Uses and interpretations. *Neuroimage*, *52*(3), 1059–1069.

Rus, O. G., Reess, T. J., Wagner, G., Zaudig, M., Zimmer, C., & Koch, K. (2016). Hypogyrification in obsessive-compulsive disorder. *Psychological Medicine*, 1–9.

Schaer, M., Cuadra, M. B., Tamarit, L., Lazeyras, F., Eliez, S., & Thiran, J. P. (2008). A surface-based approach to quantify local cortical gyrification. *IEEE Transactions on Medical Imaging*, *27*(2), 161–170.

Shim, G., Jung, W. H., Choi, J. S., Jung, M. H., Jang, J. H., Park, J. Y., … Kwon, J. S. (2009). Reduced cortical folding of the anterior cingulate cortex in obsessive-compulsive disorder. *Journal of Psychiatry & Neuroscience*, *34*, 443–449.

Shin, D. J., Jung, W. H., He, Y., Wang, J., Shim, G., Byun, M. S., … Kwon, J. S. (2014). The effects of pharmacological treatment on functional brain connectome in obsessive-compulsive disorder. *Biological Psychiatry*, *75*(8), 606–614.

Striedter, G. F., Srinivasan, S., & Monuki, E. S. (2015). Cortical folding: When, where, how, and why? *Annual Review of Neuroscience*, *38*, 291–307.

Sun, T., & Hevner, R. F. (2014). Growth and folding of the mammalian cerebral cortex: From molecules to malformations. *Nature Reviews. Neuroscience*, *15*(4), 217–232.

Takahashi, E., Folkerth, R. D., Galaburda, A. M., & Grant, P. E. (2012). Emerging cerebral connectivity in the human fetal brain: An MR tractography study. *Cerebral Cortex*, *22*(2), 455–464.

Vaghi, M. M., Vertes, P. E., Kitzbichler, M. G., Apergis-Schoute, A. M., van der Flier, F. E., Fineberg, N. A., … Robbins, T. W. (2017). Specific frontostriatal circuits for impaired cognitive flexibility and goal-directed planning in obsessive-compulsive disorder: Evidence from resting-state functional connectivity. *Biological Psychiatry*, *81*(8), 708–717.

van den Heuvel, O. A., Mataix-Cols, D., Zwitser, G., Cath, D. C., van der Werf, Y. D., Groenewegen, H. J., … Veltman, D. J. (2011). Common limbic and frontal-striatal disturbances in patients with obsessive compulsive disorder, panic disorder and hypochondriasis. *Psychological Medicine*, *41*(11), 2399–2410.

van den Heuvel, O. A., Veltman, D. J., Groenewegen, H. J., Cath, D. C., van Balkom, A. J., van Hartskamp, J., … van Dyck, R. (2005). Frontal-striatal dysfunction during planning in obsessive-compulsive disorder. *Archives of General Psychiatry*, *62*(3), 301–309.

Van Essen, D. C. (1997). A tension-based theory of morphogenesis and compact wiring in the central nervous system. *Nature*, *385*(6614), 313–318.

Venkatasubramanian, G., Zutshi, A., Jindal, S., Srikanth, S. G., Kovoor, J. M., Kumar, J. K., & Janardhan Reddy, Y. C. (2012). Comprehensive evaluation of cortical structure abnormalities in drug-naive, adult patients with obsessive-compulsive disorder: A surface-based morphometry study. *Journal of Psychiatric Research*, *46*(9), 1161–1168.

White, T., Su, S., Schmidt, M., Kao, C. Y., & Sapiro, G. (2010). The development of gyrification in childhood and adolescence. *Brain and Cognition*, *72*(1), 36–45.

Wobrock, T., Gruber, O., McIntosh, A. M., Kraft, S., Klinghardt, A., Scherk, H., … Moorhead, T. W. (2010). Reduced prefrontal gyrification in obsessive-compulsive disorder. *European Archives of Psychiatry and Clinical Neuroscience*, *260*(6), 455–464.

Xia, M., Wang, J., & He, Y. (2013). BrainNet Viewer: A network visualization tool for human brain connectomics. *PLoS One*, *8*(7), e68910.

Zalesky, A., Fornito, A., & Bullmore, E. T. (2010). Network-based statistic: Identifying differences in brain networks. *Neuroimage*, *53*(4), 1197–1207.

Zhong, Z., Zhao, T., Luo, J., Guo, Z., Guo, M., Li, P., … Li, Z. (2014). Abnormal topological organization in white matter structural networks revealed by diffusion tensor tractography in unmedicated patients with obsessive-compulsive disorder. *Progress in Neuropsychopharmacology & Biological Psychiatry*, *51*, 39–50.

Zielinski, B. A., Gennatas, E. D., Zhou, J., & Seeley, W. W. (2010). Network-level structural covariance in the developing brain. *Proceedings of the National Academy of Sciences of the United States of America*, *107*(42), 18191–18196.

Zilles, K., Palomero-Gallagher, N., & Amunts, K. (2013). Development of cortical folding during evolution and ontogeny. *Trends in Neurosciences*, *36*(5), 275–284.

SUPPORTING INFORMATION

Additional Supporting Information may be found online in the supporting information tab for this article.

How to cite this article: Reess TJ, Rus OG, Gürsel DA, et al. Network-based decoupling of local gyrification in obsessive-compulsive disorder. *Hum Brain Mapp*. 2018;00:1–11. https://doi.org/10.1002/hbm.24071

Supplementary material

Scan parameters for the different samples:

M1ocd / M1hc:

Structural imaging consisted of a T1-weighted 3D MPRAGE sequence (170 slices, sagittal orientation, 240x240 matrix, 1mm isotropic resolution, TR=9ms, TE=4ms, flip angle=8°). Data was acquired using a 12 channel (SENSE) head coil.

M2ocd / M2hc:

Structural imaging consisted of a T1-weighted 3D MPRAGE sequence (230 slices, sagittal orientation, 368 x 340 matrix, 0.7 x 0.75 x 0.7mm resolution, TR=11ms, TE=5.1ms, flip angle=8°). Data was acquired using a 32 channel (SENSE) head coil. Resolution of data within group was downsampled to 1 mm isotropic resolution to match the resolution of the other two samples.

J1ocd / J1hc:

Structural imaging consisted of a T1-weighted 3D MPRAGE sequence (192 slices, sagittal orientation, 256x256 matrix, 1mm isotropic resolution, TR=2300ms, TE=3.03ms, flip angle=9°). Data was acquired using a 12 channel receive-only head matrix coil.

NBS analyses of early vs. late onset splits

To evaluate the influence of early (EO) vs. late onset (LO) on NBS results we split the patient sample into early and late onset OCD. Since there is no commonly agreed upon criterion to define cutoffs for early and late onset OCD, with different studies using different criteria (see Taylor, 2011, Table 3), we applied 5 different cutoffs that naturally influence the sample size (EO <= 10 yrs, n=14; EO <= 12 yrs, n=24; EO =< 14 yrs, n= 33; EO=< 16, n=47; EO=<18 yrs, n=59). None of the NBS analyses yielded significantly different clusters between EO and LO.

Supplementary Table I. Correlations between node-based local gyrification and age of onset (uncorrected $P<0.05$)

Node	r	*P* (uncorrected)
lh fronto-marginal sulcus and gyrus	0.265	$P = 0.009$
lh subcentral sulcus and gyrus	0.212	$P = 0.037$
lh anterior cingulated gyrus and sulcus	0.219	$P = 0.031$
lh opercular part of inferior frontal gyrus	0.220	$P = 0.030$
lh orbital part of inferior fronal gyrus	0.214	$P = 0.035$
lh long insular gyrus and central sulcus of insula	0.256	$P = 0.011$
lh short insular gyri	0.250	$P = 0.013$
lh orbital gyri	0.223	$P = 0.028$
lh gyrus rectus	0.328*	$P = 0.001$
lh subcallosal gyrus	0.259	$P = 0.010$
lh anterior transverse temporal gyrus	0.226	$P = 0.026$
lh horizontal ramus of ant. segment of lat. sulcus	0.268	$P = 0.008$
lh post. ramus of lat. sulcus	0.221	$P = 0.030$
lh ant. segment of cicular sulcus of insula	0.290	$P = 0.004$
lh inf. segment of circular sulcus of insula	0.237	$P = 0.020$
lh sup. segment of circular sulcus of insula	0.256	$P = 0.011$
lh lateral orbital sulcus	0.229	$P = 0.024$
lh medial orbital sulcus	0.270	$P = 0.008$
lh suborbital sulcus	0.355*	$P < 0.001$
rh subcentral gyrus and sulci	0.216	$P = 0.034$

rh ant. part of cingulated gyrus and sulcus	0.233	$P = 0.021$
rh opercular part of inferior frontal gyrus	0.201	$P = 0.048$
rh triangular part of inferior frontal gyrus	0.238	$P = 0.019$
rh long insular gyrus and central sulcus of insula	0.227	$P = 0.025$
rh gyrus rectus	0.346*	$P < 0.001$
rh subcallosal gyrus	0.318*	$P = 0.002$
rh anterior transverse temporal gyrus	0.209	$P = 0.040$
rh vertical ramus of ant. segment of the lateral sulcus	0.205	$P = 0.044$
rh post. ramus of the lateral sulcus	0.221	$P = 0.030$
rh inf. segment of circular sulcus of insula	0.212	$P = 0.037$
rh sup. segment of circular sulcus of insula	0.231	$P = 0.023$
rh medial orbital sulcus	0.372*	$P < 0.001$
rh orbital sulci	0.257	$P = 0.011$
rh suborbital sulcus	0.302	$P = 0.003$

lh, left hemisphere; rh, right hemisphere; r, Pearson correlation coefficient computed on previously adjusted *I*GI values; * indicates correlations that are significant correcting for multiple comparisons using false-discovery rate

Supplementary Table II. p-values for subgroup analyses results for graph measures

Comparison	λ	γ	σ
HC vs. medicated OCD	0.2970	0.9040	0.7350
HC vs. unmedicated OCD	0.1600	0.1050	0.1530
Medicated OCD vs. unmedicated OCD	0.6780	0.1850	0.2020
HC vs. OCD with comorbidities	0.8440	0.2110	0.2480
HC vs. OCD without comorbidities	0.0780	0.5500	0.7300
OCD with vs. OCD without comorbidities	0.3150	0.6720	0.5730

HC: healthy controls; OCD: obsessive-compulsive disorder; γ = normalized average clustering coefficient; λ = normalized average path length; σ = small-worldness

Supplementary Figure 1. Association between IGI and age within patients and controls. There were no significant group x age interaction effects, controlling for sex, intracranial volume and scan sequence.

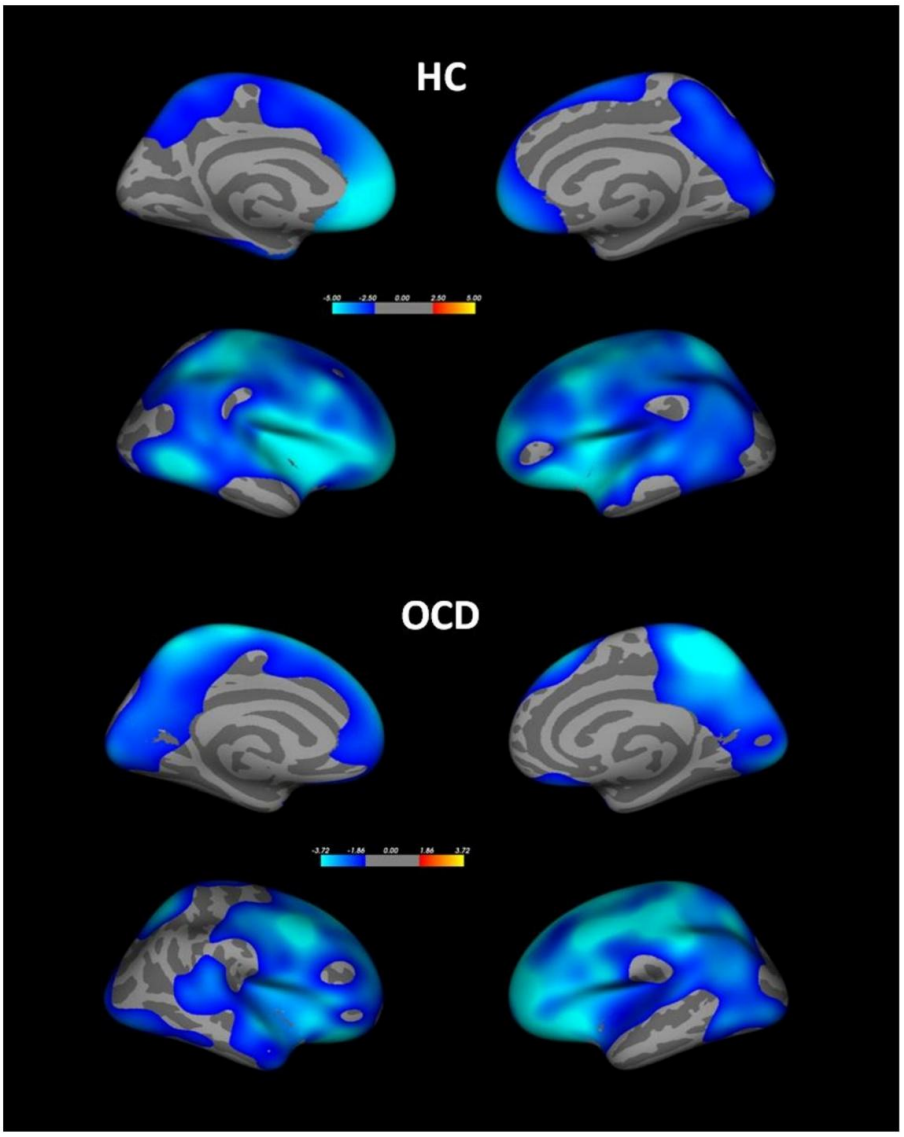

There were no significant group x age interaction effects.

References

Taylor, S. (2011) Early versus late onset obsessive-compulsive disorder: evidence for distinct subtypes. Clin Psychol Rev, 31:1083-100.

Chapter 4

Project 3: “Association between hippocampus volume and symptom profiles in obsessive-compulsive disorder”

The current chapter includes the research article “Association between hippocampus volume and symptom profiles in obsessive-compulsive disorder”. This article aimed at exploring potential relationships between symptom profiles and hippocampus volume in OCD. Employing a clustering algorithm allowed to derive symptom profile groups that were differentially associated with hippocampus volume alterations. The article was published in Neuroimaging: Clinical in 2018.

Contributions

Authors: *Tim Jonas Reess, Oana Georgiana Rus, Deniz A. Gürsel, Benita Schmitz-Koep, Gerd Wagner, Götz Berberich, Kathrin Koch*

The author of this thesis is the first author of the manuscript. **T.J.R.**, K.K., and O.G.R. together with G.W. and G.B. conceived the experiment. **T.J.R.**, O.G.R., D.A.G., and B.S.K. recruited participants and acquired data. G.W. contributed data and analytic tools. T.J.R. performed analyses. **T.J.R.** and K.K. wrote the manuscript in consultation with O.G.R., D.A.G., G.B., and G.W. All authors discussed the results and revised the final manuscript.

NeuroImage: Clinical 17 (2018) 474–480

Contents lists available at ScienceDirect

NeuroImage: Clinical

journal homepage: www.elsevier.com/locate/ynicl

Association between hippocampus volume and symptom profiles in obsessive–compulsive disorder

Tim Jonas Reess[a,b,c,*], Oana Georgiana Rus[a,b,c], Deniz A. Gürsel[a,b], Benita Schmitz-Koep[a], Gerd Wagner[d], Götz Berberich[e], Kathrin Koch[a,b,c]

[a] Department of Neuroradiology, Klinikum rechts der Isar, Technische Universität München, Ismaningerstrasse 22, 81675 Munich, Germany
[b] TUM-Neuroimaging Center (TUM-NIC), Klinikum Rechts der Isar, Technische Universität München TUM, Ismaninger Strasse 22, 81675 Munich, Germany
[c] Windach Institute and Hospital of Neurobehavioural Research and Therapy (WINTR), Windach, Schützenstraße 100, 86949 Windach, Germany
[d] Graduate School of Systemic Neurosciences GSN, Ludwig-Maximilians-Universität, Biocenter, Großhaderner Strasse 2, 82152 Munich, Germany
[e] Department of Psychiatry and Psychotherapy, Jena University Hospital, Philosophenweg 3, 07743 Jena, Germany

ARTICLE INFO

Keywords:
Hippocampus
Obsessive-compulsive
OCD
Symptom dimension
Freesurfer
MRI

ABSTRACT

Background: The hippocampus has recently been identified to play a key role in the pathophysiology of adult obsessive-compulsive disorder (OCD). Surprisingly, there is only limited evidence regarding the potential relationships with symptom dimensions. Due to the heterogeneity of symptoms in OCD, we aimed at further examining, whether hippocampal volume differences might be related to symptom profiles instead of single symptom dimensions.

Methods: In order to find out more about the potential association between clinical symptom profiles and alterations in hippocampal volume we categorized a large sample of OCD patients ($N = 66$) into distinct symptom profile groups using K-means clustering. In addition, hippocampal volumes of the different symptom profile groups were compared with hippocampal volumes in a sample of 66 healthy controls.

Results: We found significant differences in hippocampal volume between the different symptom profile groups which remained significant after correcting for age, sex, total intracranial volume, OCI-total score, depression, medication, disease duration and scanner. The patient group characterized by overall lower symptom scores and without high symptom severity in any specific domain showed the highest hippocampal volume. Finally, the comparison with healthy controls demonstrated significantly lower hippocampal volumes in those patients whose symptom profile was characterized by a high severity of ordering and checking symptoms.

Conclusions: Present results provide further confirmation for alterations in hippocampus structure in OCD and suggest that symptom profiles which take into account the multi-symptomatic character of the disorder should be given greater attention in this context.

1. Introduction

Despite increasing evidence for structural brain alterations in obsessive-compulsive disorder (OCD) the overall picture has to be considered as rather heterogeneous with findings reporting both increases and decreases in gray matter volume, thickness, surface area or gyrification (Fan et al., 2013; Kuhn et al., 2013; Nakamae et al., 2012; Piras et al., 2015; Rus et al., 2016; Shaw et al., 2015; Shin et al., 2007; Venkatasubramanian et al., 2012; Wobrock et al., 2010). In an attempt to reduce overall result heterogeneity and to filter out the most meaningful alterations, an increasing number of meta-analyses pooling data from multiple OCD sites worldwide are emerging in the OCD research community (Boedhoe et al., 2017; De Wit et al., 2014; Fouche et al., 2017). The ENIGMA consortium analysis constitutes the largest meta-analysis on structural alterations in OCD to date. Employing a coordinated and standardized analysis approach, meta- and mega-analysis of data from 1830 OCD patients ($N = 335$ children, $N = 1495$ adults) and 1759 controls was conducted to identify alterations in subcortical brain volumes in OCD patients compared to healthy controls (Boedhoe et al., 2017). As one of the main findings the analysis revealed the adult patient sample to have significantly increased pallidum and significantly smaller hippocampus volumes compared to healthy controls. The pallidum is regarded as one of the core regions within the frequently discussed cortico-striato-thalamo-cortical (CSTC) circuit. A dysbalance within this circuit is assumed to represent a central psychopathological mechanism underlying obsessions and compulsions in

* Corresponding author at: Department of Neuroradiology, Klinikum Rechts der Isar, Technische Universität München, Ismaningerstrasse 22, 81675 Munich, Germany.
E-mail address: tim.reess@tum.de (T.J. Reess).

https://doi.org/10.1016/j.nicl.2017.11.006
Received 19 June 2017; Received in revised form 13 October 2017; Accepted 7 November 2017
Available online 08 November 2017

OCD. In contrast, the hippocampus has not been the focus of OCD psychopathophysiology up to now. Its volume, however, is frequently found to be decreased in other psychiatric disorders such as depression (Frodl and O'Keane, 2013; Malykhin and Coupland, 2015) and PTSD (Ahmed-Leitao et al., 2016; O'Doherty et al., 2015). One potential mechanism underlying volumetric changes in the hippocampus seems to be uncontrollable stress (i.e., stress perceived as distress) which is one of the main characteristics of many psychiatric disorders such as PTSD. Distress has been demonstrated to change neuronal morphology, suppress neuronal proliferation, and reduce hippocampal volume (Kim et al., 2015). According to ICD-10, OCD is classified as a stress-related disorder and patients with OCD tend to report high levels of stress and anxiety independent of their specific symptoms or symptom profiles (Stein et al., 2010). Therefore, there is strong reason to assume that hippocampal volume differences may be clinically relevant in OCD as well. Of note, the ENIGMA meta-analysis identified hippocampal volume differences to be larger in medicated patients, however, no relationship with symptoms was found. The ENIGMA study related volume differences to specific symptoms as assessed by the Y-BOCS checklist. However, it should be noted that the majority of all OCD patients are multi-symptomatic and the individual symptom profiles of OCD patients are heterogeneous to the extent that two patients may display different overlapping or even non-overlapping symptom patterns (Mataix-Cols et al., 2005). Hence, instead of correlating outcome measures with specific symptoms one at a time, it may be reasonable to adopt an approach that accounts for possible interrelations of different symptom dimensions in patients. The fact that Boedhoe et al. (2017) found no significant correlations between symptom dimensions and hippocampus volumes is striking given the clear involvement of volume differences in patients found in their study. One possible explanation might be that symptom dimensions were related to structural alterations while controlling for the effects of other symptom dimensions, therefore effectively treating each symptom in isolation. To find out more about the clinical relevance of the recently reported differences in hippocampal structure, the present study employs a cluster analysis approach on dimensional symptoms to reach a differentiation into distinct symptom composition profiles, comparing hippocampal volumes between the different symptom profile groups. Thus, we aimed at exploring whether taking into account the interrelation between different symptoms, i.e., patients´ symptom composition profile, would be a valuable approach to relate structural alterations to clinically relevant features. We assumed that if the hippocampus would indeed be differentially affected in dependence on specific symptom composition profiles volume differences should be related to different symptom profiles. If hippocampus volumes would not be related to symptom profiles, this would rather speak in favor of a clinically unspecific hippocampal involvement in the disease.

2. Methods and materials

2.1. Participants

Data from two samples were combined. Sample one (S1) comprised $n = 42$ patients and $n = 46$ healthy controls and sample two (S2) comprised $n = 24$ patients and $n = 20$ healthy controls resulting in a total size of $n = 66$ patients with OCD as the primary diagnosis according to DSM-IV criteria and $n = 66$ healthy controls (see Table 1 for demographic and clinical details). Patients and controls were matched for sex and age in both samples. All patients were recruited from the Windach Institute and Hospital of Neurobehavioural Research and Therapy, Germany, and diagnoses were made by an experienced psychiatrist. Exclusion criteria for all participants were a history of clinically important head injuries, seizures or neurological diseases. At time of the study, $n = 48$ patients were drug-naive or medication free for at least 3 weeks and $n = 30$ patients had one or more comorbid diagnoses. To assess clinical severity of obsessive-compulsive symptoms, patients were administered the self-rated version of the Yale-Brown Obsessive-Compulsive Scale (Y-BOCS) (Goodman et al., 1989; Hand and Büttner-Westphal, 1991). The Obsession-Compulsion Inventory revisited (OCI-R) (Foa et al., 2002; Gonner et al., 2008) was administered to more specifically assess different symptom dimensions. Additionally, depressive symptoms were evaluated based on the Beck Depression Inventory (BDI-II) (Beck et al., 1996; Hautzinger et al., 2009) in patients of sample S1 and the Hamilton Depression Scale (HAM-D) (Hamilton, 1960) in patients of sample S2. The study was approved by the local Ethics Committee of the Klinikum rechts der Isar, München and was conducted in accordance with the Declaration of Helsinki.

Table 1
Demographic and clinical sample characteristics.

Characteristics	OCD	HC
	n	*n*
	Mean ± SD	Mean ± SD
Sample size	66	66
Female	46 (69.7%)	46 (69.7%)
Age (years)	32.4 ± 10.5	31.6 ± 10.3[‡]
Disease duration	16.0 ± 10.8	
Y-BOCS total	21.0 ± 6.2	
Obsession	11.0 ± 3.6	
Compulsions	9.9 ± 3.9	
OCI-R total	25.4 ± 10.0	
Hoarding	2.3 ± 2.6	
Checking	5.5 ± 3.6	
Ordering	3.9 ± 3.8	
Neutralizing	2.2 ± 2.9	
Washing	4.8 ± 3.9	
Obsessing	6.8 ± 3.6	
BDI (S1)	18.0 ± 11.5	
HAM-D (S2)	12.6 ± 4.9	
Comorbidities	30 (45.5%)	
Depression	23	
Anxiety disorder	10	
Personality disorder	4	
Eating disorder	2	
ADHD	2	
Medication	48 (72.7%)	
SSRI	35	
SSRNI	6	
Neuroleptic	5	
TCA	3	
Methylphenidate	1	
Benzodiazepine	1	
NDRI	1	
NaSSA	1	

Note that multiple comorbid diagnoses as well as different medication types can be present in a single patient; abbreviations for medication: NaSSA, noradrenergic and specific serotonergic antidepressant; NDRI, norepinephrine-dopamine reuptake inhibitor; SSNRI, selective serotonin-norepinephrine reuptake inhibitor; SSRI, selective serotonin reuptake inhibitor; TCA, tricyclic antidepressant.

[‡] Two-sample *t*-test ($t(130) = 0.442$, $p = 0.659$).

2.2. Image acquisition

Magnetic resonance imaging was conducted on a 3T Philips Ingenia (Philips Healthcare, Best, The Netherlands) using a 12-channel (SENSE) head coil. For sample S1, structural imaging consisted of a T1-weighted 3D MPRAGE sequence with an isotropic resolution of 1 mm (170 slices, sagittal orientation, 240 × 240 matrix, TR = 9 ms, TE = 4 ms, flip angle = 8°) while for sample S2, imaging consisted of a T1-weighted 3D MPRAGE sequence with a resolution of 0.7 × 0.75 × 0.7 mm (230 slices, sagittal orientation, 368 × 340 matrix, TR = 11 ms, TE = 5.1 ms, flip angle = 8°). Prior to analysis the 24 submillimeter data sets of sample S2 were downsampled in order for all images to have a consistent resolution of 1 mm isotropic.

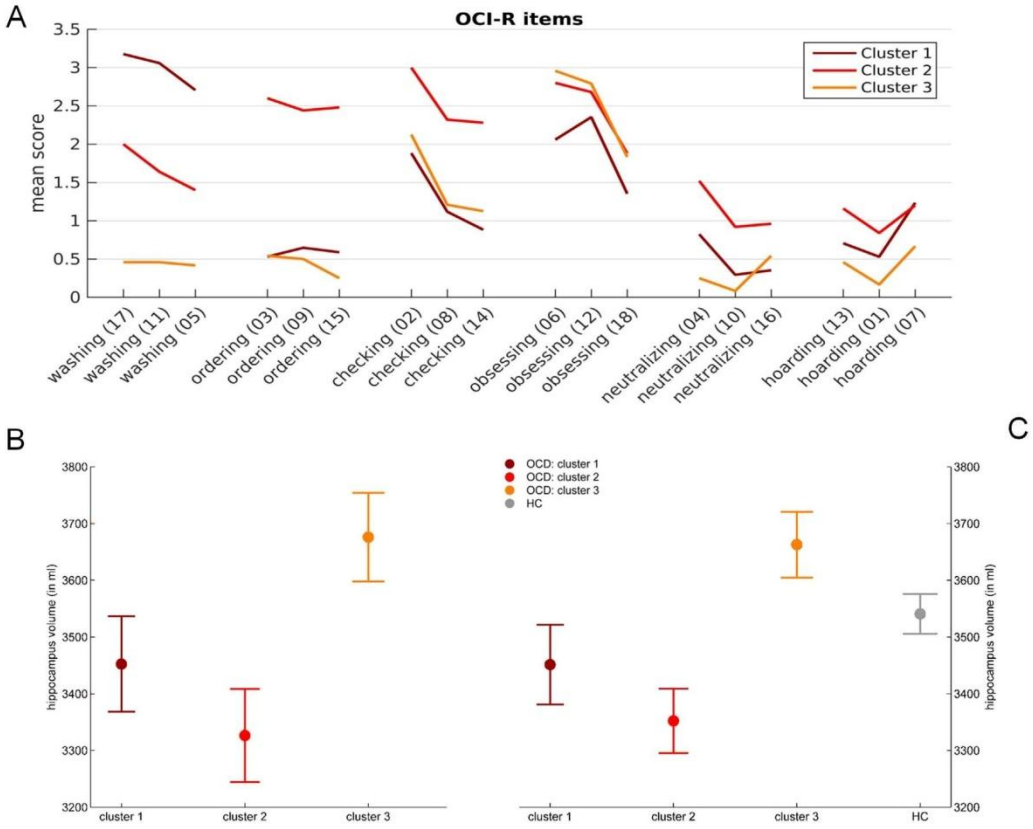

Fig. 1. Symptom profile composition and hippocampal volumes. Symptom composition analysis (A): Mean scores of each OCI-R item according to cluster membership, grouped by symptom dimensions. Numbers in parentheses indicate the number of each item in the questionnaire. Within patients analysis (B): Marginal means ± standard error. There was a significant main effect of cluster membership on global hippocampal volume while controlling for age, sex, total intracranial volume, total OCI-R score, clinically relevant depression, medication, disease duration and scanner ($F(2,55) = 3.301$, $p = 0.044$). Between groups analysis (C): Marginal means ± standard error. There was a significant main effect of cluster on global hippocampal volume while controlling for age, sex, and total intracranial volume ($F(3,125) = 4.752$, $p = 0.004$).

2.3. Image processing

Based on these T1-weighted images, cortical and subcortical structures were initially segmented and labeled using Freesurfer (Version 6.0, http://surfer.nmr.mgh.harvard.edu/) (Dale et al., 1999; Fischl et al., 2002; Fischl et al., 1999). Processing included automatic segmentation into gray and white matter tissue compartments followed by parcellation of the gray matter mask into distinct brain regions and reconstruction of brain surfaces. These results were subsequently used to initialize the labeling of hippocampi using the recently released hippocampal subfield segmentation algorithm implemented in the Freesurfer package. Compared to previous versions, the labeling rests on an atlas which was built based on ex vivo MRI data of postmortem brain tissue acquired at 7T with sub-millimeter resolution and results have been shown to be in better agreement with histological studies (Iglesias et al., 2015). Hippocampus segmentations were visually inspected and volumes were quantitatively checked for outliers.

2.4. Symptom composition analysis (SCA)

In order to partition the patients according to their symptom composition, all OCI-R items were entered into a K-means cluster analysis in SPSS (IBM Corp. Released 2016. IBM SPSS Statistics for Windows, Version 24.0. Armonk, NY: IBM Corp). This type of analysis allows to derive subgroups whose members are characterized by being rather similar in symptom composition within each subgroup while being as different as possible in symptom composition to members of other subgroups. The number of clusters (k) to be extracted was predefined to k = 3. This number was chosen in order to extract a number of clusters that allows for sufficient differentiability of patients while preserving a relatively large number of subjects per clusters (see Supplementary Fig. 1 for further details).

2.5. Statistical analysis

Demographic and clinical characteristics of subjects forming the three different clusters were compared using one-way ANOVAs with the respective demographic or clinical variable as dependent variable and cluster membership as factor with three factor levels. In line with Boedhoe et al. (2017) hippocampus volumes of the left and right hemisphere were averaged to yield a single hippocampus volume for each subject. For patients only, an ANCOVA model was fit to assess cluster-related differences in hippocampus volume while controlling for the following covariates: age, sex, total intracranial volume, OCI-total score, depression, medication, disease duration, and scanner. Controlling for OCI-total scores allows the assessment of potential effects of cluster membership irrespective of cluster-specific differences in global OCI symptom severity. Medication was entered as a dichotomous variable indicating whether patients were medication naïve or medication free for at least three weeks prior to scanning. HAM-D and BDI scores were transformed into a dichotomous variable and used as a proxy to indicate the absence or presence of clinically relevant depressive symptoms. HAM-D scores ≥ 9 and BDI scores ≥ 13 were considered to indicate the presence of relevant depressive symptoms

Table 2
Demographic and clinical sample characteristics in the three patient groups.

Characteristics	Cluster 1	Cluster 2	Cluster 3	F-statistic	*p*-Value
	Mean ± SD	Mean ± SD	Mean ± SD		
	n(%)	n(%)	n(%)		
OCI total	23.47 ± 8.65	34.12 ± 6.46	17.67 ± 6.13	34.924	< 0.001*
Age	31.38 ± 11.20	33.63 ± 11.06	31.90 ± 9.72	0.266	0.767
Disease duration	12.88 ± 6.61	18.92 ± 13.59	15.04 ± 9.58	1.742	0.184
Male	1 (5.9%)	9 (36.0%)	10 (41.7%)	3.531	0.035
Depression	9 (52.9%)	21 (84%)	17 (70.8%)	2.451	0.094
Medication	15 (88.2%)	20 (80.0%)	14 (58.3%)	2.779	0.070

* $p < 0.05$, Bonferroni-corrected for the total number of ANOVAs computed.

according to the German National Disease Management Guideline Depression (DGPPN and KBV, 2015). In a second analysis, potential cluster-related differences in hippocampus volumes between patients and healthy controls were assessed. To this end, an ANCOVA model was fit treating all healthy controls as belonging to one synthetic cluster of their own resulting in the factor cluster with four levels. Additionally, the analysis was controlled for the following covariates: age, sex, and total intracranial volume.

3. Results

3.1. Symptom composition analysis (SCA)

The mean scores of each OCI-R item according to cluster membership are depicted in Fig. 1A. Items are grouped together according to OCI symptom scales. ANOVA analyses revealed a significant main effect of cluster on OCI total score ($F(2,63) = 34.924$, $p < 0.001$, corrected). Information regarding demographic characteristics and statistical differences between each patient cluster are depicted in Table 2.

3.2. Hippocampus volume

3.2.1. Within patients analysis

There was a significant main effect of cluster on global hippocampus volume while controlling for age, sex, total intracranial volume, total OCI-R score, clinically relevant depression, medication, disease duration, and scanner ($F(2,55) = 3.301$, $p = 0.044$, $\eta^2 = 0.057$). Additionally, there was a significant main effect of sex ($F(1,55) = 6.429$, $p = 0.014$, $\eta^2 = 0.055$), total intracranial volume ($F(1,55) = 7.291$, $p = 0.009$, $\eta^2 = 0.063$), presence or absence of clinically relevant depression ($F(1,55) = 5.613$, $p = 0.021$, $\eta^2 = 0.048$) and scanner ($F(1,55) = 5.354$, $p = 0.024$, $\eta^2 = 0.017$) (see Fig. 1B as well as Table 3). Post-hoc tests indicated that hippocampus volume was significantly different between cluster 2 and 3 ($p = 0.020$, 95% CI [−562.77, −49.47]) while there was a trend significant difference between cluster 1 and 3 ($p = 0.056$, 95% CI [−432.59, 5.75]) and no significant difference between clusters 1 and 2 ($p = 0.456$, 95% CI [−154.82, 340.21]). For exploratory analyses of hippocampus subfield volumes see Supplementary Table I.

3.2.2. Between groups analysis

There was a significant main effect of cluster on global hippocampus volume while controlling for age, sex, total intracranial volume and scanner ($F(3,125) = 4.752$, $p = 0.004$, $\eta^2 = 0.071$). Additionally, there was a significant main effect of sex ($F(1,125) = 10.914$ $p = 0.001$, $\eta^2 = 0.081$), total intracranial volume ($F(1,125) = 17.758$ $p < 0.001$, $\eta^2 = 0.088$) and scanner ($F(1,125) = 6.797$ $p = 0.010$, $\eta^2 = 0.034$) (see Fig. 1C as well as Table 4). Post-hoc tests were conducted to compare each patient cluster with healthy controls (c1 vs. HC, c2 vs. HC, c3 vs. HC). For this comparison alpha was Bonferroni-corrected to be $\alpha = 0.05/3$ or $\alpha = 0.017$. Cluster 2 was found to be significantly different from HC ($p = 0.012$, 95% CI [−297.39, −37.47]). Differences between cluster 3 and healthy controls ($p = 0.063$, 95% CI [−255.23, 6.75]) as well as between cluster 1 and HC were not significant ($p = 0.366$, 95% CI [−82.68, 222.46]).

Table 3
ANCOVA model details for within patients analysis.

	Sum of squares (Typ III)	df	Mean squares	F	Significance	η^2	Partial η^2
Corrected model	5,342,274.95	10	534,227.50	6.107	< 0.001		0.526
Constant term	3,484,000.10	1	3,484,000.10	39.829	< 0.001		0.420
Cluster	577,495.26	2	288,747.63	3.301	0.044*	0.057	0.107
Age	27,210.95	1	27,210.95	0.311	0.579	0.003	0.006
Sex	562,325.53	1	562,325.53	6.429	0.014*	0.055	0.105
ICV	637,788.24	1	637,788.24	7.291	0.009*	0.063	0.117
OCI total	11,522.83	1	11,522.83	0.132	0.718	0.001	0.002
Depression	490,991.26	1	490,991.26	5.613	0.021*	0.048	0.093
Medication	16,746.94	1	16,746.94	0.191	0.663	0.002	0.003
Disease duration	66,142.75	1	66,142.75	0.756	0.388	0.007	0.014
Scanner	168,298.30	1	168,298.30	5.354	0.024*	0.017	0.089
Error	4,811,035.05	55	87,473.37				
Total	812,213,858.70	66					
Corrected total variation	10,153,310.00	65					

* $= p < 0.05$;
ANCOVA model formulation:
$hippo_{vol} = 2697.20 - 213.42^{*}clust_1 - 306.12^{*}clust_2 - 3.18^{*}age + 275.47^{*}sex + 0.001^{*}ICV + 2.09^{*}OCI_{total} - 204.19^{*}depression + 38.93^{*}medication + 5.14^{*}disease\ duration + 231.78^{*}scanner.$

Table 4
ANCOVA model details for between groups analysis.

	Sum of squares (Typ III)	df	Mean squares	F	Significance	η^2	Partial η^2
Corrected model	5,882,377.33	7	840,339.618	11.003	< 0.001		0.383
Constant term	9,327,886.03	1	9,327,886.03	122.130	< 0.001		0.496
Cluster	1,088,735.90	3	362,911.97	4.752	0.004*	0.071	0.103
Age	6681.42	1	6681.42	0.087	0.768	< 0.001	0.001
Sex	833,600.24	1	833,600.24	10.914	0.001*	0.054	0.081
ICV	1,356,312.68	1	1,356,312.68	17.758	< 0.001*	0.088	0.125
scanner	519,145.23	1	519,145.23	6.797	0.010*	0.034	0.052
Error	9,470,732.19	124	76,376.87				
Total	1,647,001,109.00	132					
Corrected total variation	15,353,109.51	131					

* $= p < 0.05$;
ANCOVA model formulation:
$\text{hippo}_{\text{vol}} = 2534.54 - 69.89^{*}\text{clust}_1 - 167.43^{*}\text{clust}_2 + 124.29^{*}\text{clust}_3 + 0.70^{*}\text{age} + 200.56^{*}\text{sex} + 0.001^{*}\text{ICV} + 159.60^{*}\text{scanner}$.

4. Discussion

To find out more about the clinical relevance of hippocampal volume changes in OCD, in the present study we categorized a large sample of OCD patients into three distinct symptom profiles and compared alterations in hippocampal volume between the resulting groups. We further compared the resulting clusters with healthy participants. With this procedure we aimed at further elucidating the clinical significance of hippocampal volume alterations by better accounting for the clinical heterogeneity of the disorder. The cluster analysis showed that the relatively large patient sample could be subdivided most adequately into three symptom profile groups. Common to all clusters was the moderate to high level of obsessing symptoms. This feature thus does not seem be the major driving factor regarding hippocampus volume differences. Similar, but less pronounced are the dimensions neutralizing and hoarding. Here, the overall symptom strength is low to moderate with slight differences between clusters. The main differences between clusters could be found for the dimensions washing, ordering, and checking. Here cluster 1 revealed by far the highest washing scores while being on par with cluster 3 on ordering and checking symptoms. Cluster 2 revealed intermediate washing symptoms while scoring the highest on ordering as well as checking symptoms. On a side note, cluster 1, characterized by the highest washing symptoms, contained only a single male patient and 16 female patients. This is in line with earlier studies reporting washing symptoms predominantly in female patients (Labad et al., 2008; Mathis et al., 2011; Torresan et al., 2013). As a main finding the present analysis demonstrated that hippocampus volume differed significantly between the three groups with post-hoc tests indicating that cluster 2 had significantly smaller hippocampal volumes than cluster 3. Importantly, this result was corrected for the influence of overall symptom severity (i.e., OCI-R total score) which indicates that the respective symptom profiles account for variation in hippocampal volume independent of overall symptom severity. Hence, present findings clearly demonstrate that the classification into different OCD symptom profiles – an approach which has been recommended already years ago (Mataix-Cols et al., 2005) – significantly accounts for variation in hippocampal volume reduction. Additionally, there was a difference between hippocampal volumes when including a group of healthy subjects, with post-hoc tests indicating significant differences between cluster 2 and healthy controls. Present findings moreover extend recent results from the currently largest meta-analysis on structural alterations in OCD (i.e., the ENIGMA consortium meta-analysis) which revealed significantly smaller hippocampal volumes in adult OCD patients compared to healthy controls (Boedhoe et al., 2017). The meta-analysis showed the effect to be stronger in medicated patients compared to controls but not significantly related to clinical symptoms. However, unlike in the present study, in this meta-analysis symptom spectra or the interrelation between different symptoms was not taken into account but symptoms were assessed independently for each Y-BOCS checklist symptom dimension. Present findings not only corroborate the clinical relevance of hippocampal volume alterations in OCD as reported before (Honda et al., 2017) but strongly suggest that the interrelation of symptom dimensions should be taken into account in this regard. As also shown in Fig. 1A, it seems that a high severity of mainly ordering and checking symptoms (i.e., cluster 2) may be predominantly indicative of a reduction in hippocampus volume. The hippocampus is a highly stress-sensitive structure (Kim et al., 2015) and is often found to be reduced in volume in other stress-related disorders such as depression (MacQueen, 2009) and PTSD (Ahmed-Leitao et al., 2016). Hence, there is reason to assume that the association between a high level of predominantly ordering/checking (cluster 2) and - to a somewhat lesser extent predominantly washing (cluster 1) symptoms - and reduced hippocampal volume may be mediated via stress and stress-related physiological processes going along with these symptom profiles and their associated behavior. In this context it is interesting to note that the association remained significant even after correcting for the comorbidity of depression. Moreover, the association between symptom profile and hippocampal volume also remained significant after correcting for the influence of disease duration. In this case, disease duration did not have a significant effect on hippocampal volume. This finding seems to contradict the above formulated assumption that stress going along with the disorder may play a relevant role in this context. However, findings from meta-analyses on hippocampal volumes in depression produced relatively conflicting results and suggested that disease duration may be a significant influencing factor mainly in elderly patients (Eker and Gonul, 2010) (i.e., hippocampal degenerative processes due to disorder-related stress may become manifest predominantly in elderly patients who had been suffering from depression for various years). Of note, the average disease duration between clusters was not significantly different, i.e., overall effects of disease duration had no significant influence on this type of analysis. This finding does therefore not rule out the possibility of disease duration related effects on hippocampal volumes in general. Apart from the above mentioned meta-analysis (Boedhoe et al., 2017) which showed a significantly decreased hippocampal volume in patients with OCD, a limited amount of previous studies already reported alterations in hippocampus structure and neurochemistry in patients with OCD. For instance, Honda et al. (2017) found a decreased hippocampal volume in OCD patients employing voxel-based analyses and Hong et al. (2007) observed a bilateral hippocampal shape deformity in OCD patients compared to healthy controls when performing a shape analysis of the hippocampus. Regarding hippocampal neurochemistry lower hippocampal ratio of *N*-acetyl-L-aspartate/choline (NAA/CHO) which is considered to indicate loss of neurons and axons has been reported in patients with OCD (Atmaca et al., 2009). Interestingly, follow-up studies found these alterations to partly normalize by effective treatment and clinical improvement (Atmaca et al., 2015). Hence, our finding that patients with a symptom profile characterized by a high level of

predominantly checking/ordering symptoms (cluster 2) showed stronger hippocampal volume differences compared to patients without a high severity in any specific domain as well as an overall lower symptom severity (cluster 3) complements these results. Taken together, present and earlier findings suggest that alterations in hippocampal volume in terms of neuroplasticity or partial reversal of tissue loss may be an indicator of treatment-related clinical improvement whereas hippocampal volume in terms of volumetric loss may represent a state marker of disease severity if assessed dimensionally according to specific symptom spectra or the interrelation between specific symptom dimensions. Longitudinal study designs might further elucidate an interaction between attenuation of strength in symptom profiles due to therapy and associated hippocampus volume changes.

5. Limitations

In opposition to the results of the currently largest meta-analysis (Boedhoe et al., 2017) which found that hippocampal volume reductions were stronger in medicated patients compared to controls we only found a trend significant influence of medication on volumes. These partly conflicting findings may have mainly statistical reasons as it must be assumed that the meta-analysis based on a sample of 1495 adult OCD patients had considerably larger detection power than the present study. The definition of clinically relevant depression was based on two different questionnaires (self-rated and clinician-rated) resulting from the aggregation of two different samples. Therefore, the factor depression should be assessed in further studies using the same questionnaires for the definition of cut-offs.

Funding

This study was supported by German Research Foundation (DFG) grants to KK (DFG KO 3744/2-1 and DFG KO 3744/7-1) and GW (DFG WA 3001/3-1). Additionally, this work was supported by the German Research Foundation (DFG) and the Technical University of Munich (TUM) in the framework of the Open Access Publishing Program. The funding agency had no influence on the design and conduct of the study including collection, management, analysis and interpretation of data, as well as preparation, review and approval of the manuscript.

Declaration of interest

The authors report no biomedical financial interests or potential conflict of interest.

Appendix A. Supplementary data

Supplementary data to this article can be found online at https://doi.org/10.1016/j.nicl.2017.11.006.

References

Ahmed-Leitao, F., Spies, G., van den Heuvel, L., Seedat, S., 2016. Hippocampal and amygdala volumes in adults with posttraumatic stress disorder secondary to childhood abuse or maltreatment: a systematic review. Psychiatry Res. Neuroimaging 256, 33–43.

Atmaca, M., Yildirim, H., Ozdemir, H., Koc, M., Ozler, S., Tezcan, E., 2009. Neurochemistry of the hippocampus in patients with obsessive–compulsive disorder. Psychiatry Clin. Neurosci. 63, 486–490.

Atmaca, M., Yildirim, H., Yilmaz, S., Caglar, N., Mermi, O., Gurok, M.G., Kekilli, Y., Turkcapar, H., 2015. 1HMRS results of hippocampus in the patients with obsessive–compulsive disorder before and after cognitive behavioral therapy. Int. J. Psychiatry Clin. Pract. 19, 285–289.

Beck, A.T., Steer, R.A., Brown, G., 1996. Manual for the Beck Depression Inventory-II. Psychological Corporation, San Antonio, TX.

Boedhoe, P.S., Schmaal, L., Abe, Y., Ameis, S.H., Arnold, P.D., Batistuzzo, M.C., Benedetti, F., Beucke, J.C., Bollettini, I., Bose, A., Brem, S., Calvo, A., Cheng, Y., Cho, K.I., Dallaspezia, S., Denys, D., Fitzgerald, K.D., Fouche, J.P., Gimenez, M., Gruner, P., Hanna, G.L., Hibar, D.P., Hoexter, M.Q., Hu, H., Huyser, C., Ikari, K., Jahanshad, N., Kathmann, N., Kaufmann, C., Koch, K., Kwon, J.S., Lazaro, L., Liu, Y., Lochner, C., Marsh, R., Martinez-Zalacain, I., Mataix-Cols, D., Menchon, J.M., Minuzzi, L., Nakamae, T., Nakao, T., Narayanaswamy, J.C., Piras, F., Piras, F., Pittenger, C., Reddy, Y.C., Sato, J.R., Simpson, H.B., Soreni, N., Soriano-Mas, C., Spalletta, G., Stevens, M.C., Szeszko, P.R., Tolin, D.F., Venkatasubramanian, G., Walitza, S., Wang, Z., van Wingen, G.A., Xu, J., Xu, X., Yun, J.Y., Zhao, Q., Group, E.O.W, Thompson, P.M., Stein, D.J., van den Heuvel, O.A., 2017. Distinct subcortical volume alterations in pediatric and adult OCD: a worldwide meta- and mega-analysis. Am. J. Psychiatry 174, 60–69.

Dale, A.M., Fischl, B., Sereno, M.I., 1999. Cortical surface-based analysis. I. Segmentation and surface reconstruction. NeuroImage 9, 179–194.

De Wit, S.J., Alonso, P., Schweren, L., Mataix-Cols, D., Lochner, C., Menchón, J.M., Stein, D.J., Fouche, J.-P., Soriano-Mas, C., Sato, J.R., 2014. Multicenter voxel-based morphometry mega-analysis of structural brain scans in obsessive-compulsive disorder. Am. J. Psychiatry 171, 340–349.

DGPPN, B., KBV, A., 2015. S3-Leitlinie/Nationale Versorgungsleitlinie Unipolare Depression-Langfassung. DGPPN, ÄZQ, AWMF–Berlin, Düsseldorf.

Eker, C., Gonul, A.S., 2010. Volumetric MRI studies of the hippocampus in major depressive disorder: meanings of inconsistency and directions for future research. World J. Biol. Psychiatry 11, 19–35.

Fan, Q., Palaniyappan, L., Tan, L., Wang, J., Wang, X., Li, C., Zhang, T., Jiang, K., Xiao, Z., Liddle, P., 2013. Surface anatomical profile of the cerebral cortex in obsessive–compulsive disorder: a study of cortical thickness, folding and surface area. Psychol. Med. 43, 1081–1091.

Fischl, B., Sereno, M.I., Dale, A.M., 1999. Cortical surface-based analysis. II: inflation, flattening, and a surface-based coordinate system. NeuroImage 9, 195–207.

Fischl, B., Salat, D.H., Busa, E., Albert, M., Dieterich, M., Haselgrove, C., van der Kouwe, A., Killiany, R., Kennedy, D., Klaveness, S., Montillo, A., Makris, N., Rosen, B., Dale, A.M., 2002. Whole brain segmentation: automated labeling of neuroanatomical structures in the human brain. Neuron 33, 341–355.

Foa, E.B., Huppert, J.D., Leiberg, S., Langner, R., Kichic, R., Hajcak, G., Salkovskis, P.M., 2002. The obsessive-compulsive inventory: development and validation of a short version. Psychol. Assess. 14, 485–496.

Fouche, J.P., du Plessis, S., Hattingh, C., Roos, A., Lochner, C., Soriano-Mas, C., Sato, J.R., Nakamae, T., Nishida, S., Kwon, J.S., Jung, W.H., Mataix-Cols, D., Hoexter, M.Q., Alonso, P., Consortium, O.C.D.B.I., de Wit, S.J., Veltman, D.J., Stein, D.J., van den Heuvel, O.A., 2017. Cortical thickness in obsessive-compulsive disorder: multisite mega-analysis of 780 brain scans from six centres. Br. J. Psychiatry 210, 67–74.

Frodl, T., O'Keane, V., 2013. How does the brain deal with cumulative stress? A review with focus on developmental stress, HPA axis function and hippocampal structure in humans. Neurobiol. Dis. 52, 24–37.

Gonner, S., Leonhart, R., Ecker, W., 2008. The obsessive-compulsive inventory-revised (OCI-R): validation of the German version in a sample of patients with OCD, anxiety disorders, and depressive disorders. J. Anxiety Disord. 22, 734–749.

Goodman, W.K., Price, L.H., Rasmussen, S.A., Mazure, C., Fleischmann, R.L., Hill, C.L., Heninger, G.R., Charney, D.S., 1989. The Yale-Brown obsessive compulsive scale. I. Development, use, and reliability. Arch. Gen. Psychiatry 46, 1006–1011.

Hamilton, M., 1960. A rating scale for depression. J. Neurol. Neurosurg. Psychiatry 23, 56–62.

Hand, I., Büttner-Westphal, H., 1991. Die Yale-Brown Obsessive Compulsive Scale (Y-BOCS): Ein halbstrukturiertes Interview zur Beurteilung des Schweregrades von Denk-und Handlungszwängen. Verhaltenstherapie 1, 223–225.

Hautzinger, M., Keller, F., Kühner, C., 2009. BDI-II. Beck-Depressions-Inventar. Revision., 2. Auflage ed. Pearson Assessment, Frankfurt.

Honda, S., Nakao, T., Mitsuyasu, H., Okada, K., Gotoh, L., Tomita, M., Sanematsu, H., Murayama, K., Ikari, K., Kuwano, M., 2017. A pilot study exploring the association of morphological changes with 5-HTTLPR polymorphism in OCD patients. Ann. General Psychiatry 16, 2.

Hong, S.B., Shin, Y.-W., Kim, S.H., Yoo, S.Y., Lee, J.-M., Kim, I.Y., Kim, S.I., Kwon, J.S., 2007. Hippocampal shape deformity analysis in obsessive–compulsive disorder. Eur. Arch. Psychiatry Clin. Neurosci. 257, 185–190.

Iglesias, J.E., Augustinack, J.C., Nguyen, K., Player, C.M., Player, A., Wright, M., Roy, N., Frosch, M.P., McKee, A.C., Wald, L.L., Fischl, B., Van Leemput, K., Alzheimer's Disease Neuroimaging, I., 2015. A computational atlas of the hippocampal formation using ex vivo, ultra-high resolution MRI: application to adaptive segmentation of in vivo MRI. NeuroImage 115, 117–137.

Kim, E.J., Pellman, B., Kim, J.J., 2015. Stress effects on the hippocampus: a critical review. Learn. Mem. 22, 411–416.

Kuhn, S., Kaufmann, C., Simon, D., Endrass, T., Gallinat, J., Kathmann, N., 2013. Reduced thickness of anterior cingulate cortex in obsessive-compulsive disorder. Cortex 49, 2178–2185.

Labad, J., Menchon, J.M., Alonso, P., Segalas, C., Jimenez, S., Jaurrieta, N., Leckman, J.F., Vallejo, J., 2008. Gender differences in obsessive-compulsive symptom dimensions. Depress. Anxiety 25, 832–838.

MacQueen, G.M., 2009. A meta-analysis examining clinical predictors of hippocampal volume in patients with major depressive disorder. J. Psychiatry Neurosci. 34, 41.

Malykhin, N., Coupland, N., 2015. Hippocampal neuroplasticity in major depressive disorder. Neuroscience 309, 200–213.

Mataix-Cols, D., do Rosario-Campos, M.C., Leckman, J.F., 2005. A multidimensional model of obsessive-compulsive disorder. Am. J. Psychiatry 162, 228–238.

Mathis, M.A., Alvarenga, P., Funaro, G., Torresan, R.C., Moraes, I., Torres, A.R., Zilberman, M.L., Hounie, A.G., 2011. Gender differences in obsessive-compulsive disorder: a literature review. Rev. Bras. Psiquiatr. 33, 390–399.

Nakamae, T., Narumoto, J., Sakai, Y., Nishida, S., Yamada, K., Kubota, M., Miyata, J., Fukui, K., 2012. Reduced cortical thickness in non-medicated patients with obsessive-compulsive disorder. Prog. Neuro-Psychopharmacol. Biol. Psychiatry 37, 90–95.

O'Doherty, D.C., Chitty, K.M., Saddiqui, S., Bennett, M.R., Lagopoulos, J., 2015. A

systematic review and meta-analysis of magnetic resonance imaging measurement of structural volumes in posttraumatic stress disorder. Psychiatry Res. Neuroimaging 232, 1–33.
Piras, F., Piras, F., Chiapponi, C., Girardi, P., Caltagirone, C., Spalletta, G., 2015. Widespread structural brain changes in OCD: a systematic review of voxel-based morphometry studies. Cortex 62, 89–108.
Rus, O., Reess, T., Wagner, G., Zaudig, M., Zimmer, C., Koch, K., 2016. Hypogyrification in obsessive-compulsive disorder. Psychol. Med. 1–9.
Shaw, P., Sharp, W., Sudre, G., Wharton, A., Greenstein, D., Raznahan, A., Evans, A., Chakravarty, M., Lerch, J., Rapoport, J., 2015. Subcortical and cortical morphological anomalies as an endophenotype in obsessive-compulsive disorder. Mol. Psychiatry 20, 224–231.
Shin, Y.W., Yoo, S.Y., Lee, J.K., Ha, T.H., Lee, K.J., Lee, J.M., Kim, I.Y., Kim, S.I., Kwon, J.S., 2007. Cortical thinning in obsessive compulsive disorder. Hum. Brain Mapp. 28, 1128–1135.
Stein, D.J., Fineberg, N.A., Bienvenu, O.J., Denys, D., Lochner, C., Nestadt, G., Leckman, J.F., Rauch, S.L., Phillips, K.A., 2010. Should OCD be classified as an anxiety disorder in DSM-V? Depress. Anxiety 27, 495–506.
Torresan, R.C., Ramos-Cerqueira, A.T., Shavitt, R.G., do Rosario, M.C., de Mathis, M.A., Miguel, E.C., Torres, A.R., 2013. Symptom dimensions, clinical course and comorbidity in men and women with obsessive-compulsive disorder. Psychiatry Res. 209, 186–195.
Venkatasubramanian, G., Zutshi, A., Jindal, S., Srikanth, S.G., Kovoor, J.M., Kumar, J.K., Janardhan Reddy, Y.C., 2012. Comprehensive evaluation of cortical structure abnormalities in drug-naive, adult patients with obsessive-compulsive disorder: a surface-based morphometry study. J. Psychiatr. Res. 46, 1161–1168.
Wobrock, T., Gruber, O., McIntosh, A.M., Kraft, S., Klinghardt, A., Scherk, H., Reith, W., Schneider-Axmann, T., Lawrie, S.M., Falkai, P., 2010. Reduced prefrontal gyrification in obsessive–compulsive disorder. Eur. Arch. Psychiatry Clin. Neurosci. 260, 455–464.

Supplementary Information

Reess TJ, Rus OA, Gürsel DA, Schmitz-Koep B, Wagner G, Berberich G, Koch K. Association between hippocampus volume and symptom profiles in obsessive–compulsive disorder.

Cluster Analysis

In order to determine a sensible number of clusters (k) to be extracted, the cluster analysis was repeated with various k's (2 <= k <= 6). For each k, the sum of squared errors of the euclidian distance between a subject and it's respective cluster centroid was computed using the following formula:

$$SSE = \sum_{i=1}^{K} \sum_{x \in c_i} distance(x, c_i)^2$$

with *K* = the number of different clusters, c_i = the i^{th} cluster centroid, and *x* a vector indicating all subjects belonging to cluster c_i. In order to achieve a sufficiently good differentiability in symptom profiles while reaching a sufficiently large number of subjects within each cluster, k=3 was chosen. For a depiction of the number of subjects per cluster with increasing k see Supplementary Figure 1 A) and for a depiction of the sum of squared errors according to variation in the number of clusters see Supplementary Figure 1 B)

Supplementary Figure 1: K-means clustering details. Number of subjects **(A)** and sum of squared errors **(B)** for various numbers of predefined clusters.

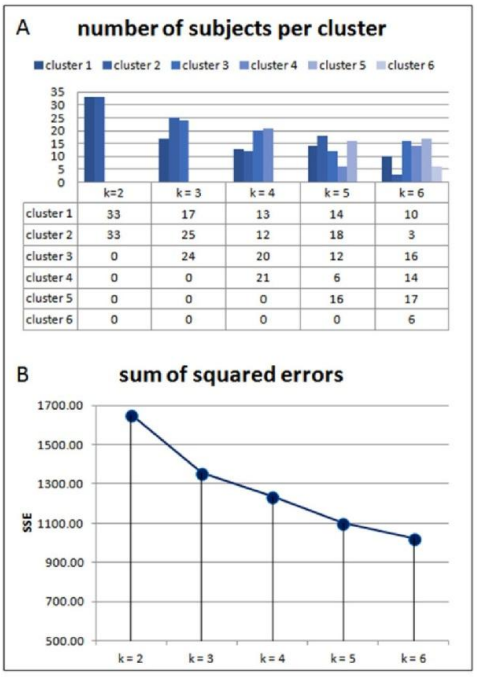

	k=2	k = 3	k = 4	k = 5	k = 6
cluster 1	33	17	13	14	10
cluster 2	33	25	12	18	3
cluster 3	0	24	20	12	16
cluster 4	0	0	21	6	14
cluster 5	0	0	0	16	17
cluster 6	0	0	0	0	6

Supplementary Table I: ANCOVA results for cluster effects on hippocampus subfield volumes within the patient group.

Hippocampus subfield	F-statistic	Significance	η^2	Partial η^2
Hippocampus tail	4.159	0.021*	0.106	0.131
Presubiculum	4.228	0.020*	0.072	0.133
Molecular layer	2.842	0.067	0.051	0.094
CA1	2.741	0.073	0.050	0.091
GC-ML-DG	2.672	0.078	0.045	0.089
CA4	2.512	0.090	0.041	0.084
Subiculum	1.744	0.184	0.035	0.060
Hippocampal fissure	1.362	0.265	0.023	0.047
CA3	1.320	0.276	0.022	0.046
HATA	1.101	0.340	0.016	0.039
Fimbria	0.730	0.486	0.014	0.026
Parasubiculum	0.460	0.634	0.008	0.016

Values reported are results of the main effects of the variable "cluster". * = p<0.05, uncorrected for number of subfields. Volumes for left and right hemisphere were averaged for each subfield. Each model is adjusted for age, sex, total intracranial volume, total OCI-R score, clinically relevant depression, medication, disease duration and scanner. GC-ML-DG: Granule cell – molecular layer – dentate gyrus; HATA: hippocampus-amygdala-transition-area. For further details regarding the subfields see Iglesias et al. (1)

References

1. Iglesias JE, Augustinack JC, Nguyen K, Player CM, Player A, Wright M, et al. (2015): A computational atlas of the hippocampal formation using ex vivo, ultra-high resolution mri: Application to adaptive segmentation of in vivo mri. *Neuroimage*. 115:117-137.

Chapter 5

General Discussion

The current thesis mainly focused on the application of network-based modeling techniques to examine brain networks derived from *in-vivo* neuroimaging data acquired in OCD and healthy controls. Additionally, the potential importance of recognizing symptom profiles and their relationship with structural hippocampus alterations was assessed. The following chapter is organized into four sections: Firstly, the results of each project will be briefly summarized and the implications across projects will be discussed. Secondly, methodological considerations and limitation are addressed. The third section will touch on potential future directions in research. Finally, the fourth section will conclude the thesis.

5.1 Main Findings and Implications across Projects

In order to advance our understanding of neurobiological alterations in OCD from a network perspective, two studies were conducted that focused on the examination of structural networks derived from T1-weighted as well as DW imaging: 1) the first project used deterministic fiber tracking to reconstruct macroanatomical networks based on white matter fiber connectivity and aimed at the quantification of alterations of these networks in comparisons with healthy subjects (Reess et al., 2016); 2) the second project aimed at advancing our understanding of neurodevelopmental aspects in OCD comparing the covariance patterns of local gyrification indices, a marker that is assumed to be sensitive to neurodevelopment, between groups (Reess et al., 2018b). A third study was conducted to explore whether specifically taking into consideration the interrelation between various symptoms, i.e. symptom profiles, might be of use to disentangle why in some studies, a brain-behavior correlation is missing. To this end, patients were clustered on the basis of their entire range of systems and cluster status was related to hippocampus volumes (Reess et al., 2018a).

5.1.1 Project 1: Beyond fronto-striato-thalamo-cortical circuitry

As presented above, neurobiological theories of OCD pathophysiology have been constantly evolving and are regularly revised to incorporate new findings (see section 1.2.2). However, the currently favored model as described in Milad and Rauch (2012) does not specifically take into consideration various regions assumed to be of importance for OCD. Furthermore, the majority of studies focus either on functional alterations or structural alterations that are mainly based on classical approaches to study brain morphology (see section 1.3.1). Thus, using an innovative, data-driven, whole-brain network analysis approach, Reess et al. (2016) set out to assess whether analyses performed at the network level would provide further evidence in favor or against the assumption that regions outside of CSTC circuitry are of importance in OCD. Given that anxiety/distress, are cardinal features of OCD, the involvement of areas implicated in emotion processing seemed very likely.

The analyses yielded several important findings: firstly, using the NBS as a framework, it was shown that OCD patients displayed a network of connections that was consistently marked by a decreased structural connectivity in terms of number of streamlines (NOS). Multiple nodes within this network are commonly associated with OCD pathophysiology and have been implicated in the CSTC model. Closer assessment of the topology of impaired connections revealed a striking resemblance with regions adjacent to a major fiber bundle connecting the orbital and temporal gyrus, namely the uncinate fasciculus (UF). The UF has been described as being a be part of the limbic system (Von Der Heide et al., 2013). The second key finding relates to the embedding of amygdala in the network topology. It was found that left amygdala's global connectivity strength was decreased in addition to an increase in shortest path length. Together these measures indicate that overall the left amygdala appears to be less well connected to neighbors and displays diminished efficiency of connections. Furthermore, a reduced clustering coefficient indicates that the topological neighbors of amygdala are less well connected amongst each other. This diminished connectivity among amygdala's neighbors may point towards an altered role of amygdala in mediating information flow between these neighboring nodes. Information flow that is likely to be rather direct between adjacent nodes in healthy subjects may thus be more prone to be mediated by amygdala, therefore increasing its potential control over information flow. Thirdly, clustering coefficients for left and right temporal pole were also found to be impaired, indicating a potentially similar effect as reported for amygdala. It was shown that the magnitude of functional activation in

amygdala as well as anterior temporal pole during symptom provocation is associated with subsequent treatment response to CBT (Olatunji et al., 2014). The findings of the current study suggest to further address the importance of the UF for the disorder. Several tract-based spatial statistics (TBSS) as well as VBM studies previously reported an involvement of the uncinate in OCD (Benedetti et al., 2013; Jayarajan et al., 2012). Furthermore alterations in the uncinate were found to be associated with processing deficits in the emotional domain in OCD (Piras et al., 2013). Importantly, these findings were derived from voxel-based methods (see Section 1.3.1.2) and are restricted to focal findings. NBS results, on the other hand, indicate that directly applying fiber tracking algorithms to recover the uncinate fasciculus may prove useful in further elucidating UF's role for the pathophysiology. Interestingly, the alterations found on a network level in OCD do not correlate with various clinical measures such as overall symptom severity or subscales. However, various edges comprising the NBS cluster revealed a trend significant ($p<0.1$) correlation with different clinical measures such as washing and obsessing scores as well as total Y-BOCS. These results may be useful for replication studies allowing to drastically decrease the number of comparisons using region of interest approaches and thus increasing power. Taken together, the findings provide further evidence for the need to extend the classical CSTC circuit model to incorporate temporo-limbic regions and connections between these. Additionally, amygdala appears to play a prominent role in the pathophysiology of OCD.

5.1.2 Project 2: Neurodevelopmental aspects of OCD

First evidence points toward neurodevelopmental aspects to play an important role in OCD (Huyser et al., 2009) and Rosenberg and Keshavan (1998) proposed that neurodevelopmental dysplasia may be of importance, especially in case of pediatric OCD. Gyrification has been proposed as a potential marker for neurodevelopment and it was previously shown that alterations in gyrification occurs in diseases with a neurodevelopmental component such as autism spectrum disorder (Ecker et al., 2016) and schizophrenia (Palaniyappan & Liddle, 2012; Palaniyappan et al., 2016). Evidence for alterations of gyrification in OCD is relatively scarce and somewhat heterogeneous while studies were again based on univariate analysis strategies (Fan et al., 2013; Rus et al., 2017; Shim et al., 2009; Venkatasubramanian et al., 2012; Wobrock et al., 2010). Interestingly, using a network approach employing gyrification-based structural covariance patterns, Palaniyappan et al. (2015) showed that in schizophrenia, the coordinated

development of gyrification appears to be impaired. Additionally, various studies indicated that structural covariance analyses are useful to assess synchronized developmental changes (Alexander-Bloch et al., 2013; Khundrakpam et al., 2013; Zielinski et al., 2010) and network approaches to studying gyrification patterns appear to be well suited to further disentangle factors that may be contributing to pathophysiological mechanisms. More specifically, measures of segregation and integration can be employed to characterize whether alterations are potentially more related to modular or global aspects.

The analyses yielded several important findings: NBS analyses revealed one network with consistently smaller structural covariance in OCD patients as compared with healthy controls. This network was rather large comprising 31 nodes and 34 edges that were distributed throughout both hemispheres. The global network topology was found to be in the small-world regime in OCD patients and did not significantly differ between healthy controls and patients. However, the normalized average characteristic path length revealed a trend significant difference ($p=0.0510$) with higher path length in OCD patients. Assessment of local measures revealed a significant decrease in local clustering for left middle frontal sulcus in patients. Finally, several frontal nodes revealed significant positive correlations between lGI values and age of onset indicating that larger lGIs were associated with later age of onset. Control analyses were performed to assess group x age interaction effects as well as exploratory subgroup analyses to assess the stability of results when taking into consideration the effects of medication, comorbidity, and early vs. late onset. The decreased structural covariance revealed by the NBS analyses followed a rather interesting pattern. The nodes and edges involved were mainly concentrated in ventral brain regions, thus marking an imbalance in the pattern. The developmental trajectory of gyrification typically follows a specific pattern and proceeds from dorsal parieto-occipital areas to first superior frontal and temporal regions and finally ends in inferior frontal and temporal regions (Takahashi et al., 2012). Comparing these patterns with the pattern of altered gyrification in OCD leads to the proposition, that the decoupling in gyrification covariance may potentially be time-locked to later stages of development. Furthermore, a similar pattern of alterations in gray matter has been observed in preterm birth (Ball et al., 2012). Interestingly, a recently published population-based study reported preterm birth to be a risk factor for OCD (Brander et al., 2016). The absence of correlation between symptom severity and nodal lGI values may indicate that lGI is best interpreted as a trait marker instead of state marker, especially in light of the fact that gyrification is rather stable over time as well as the lack of group x age interaction effects. Of note, the trend

significant difference in normalized average characteristic path length may potentially indicate a decrease in global integration capabilities in patients. However, this may also be an effect that more strongly affects a subset of nodes, for example the set of nodes found to be involved in the NBS network. The decrease in local clustering found in patients for the middle frontal sulcus may be associated with impaired planning abilities in OCD. van den Heuvel et al. (2005) report a decreased activity in left DLPFC (part of which is the middle frontal sulcus) and striatal responsiveness while patients performed a Tower of London Task. Finally, the positive correlation between age of onset and gyrification likely indicated that structural alterations in gyrification covariance patterns are best understood as trait instead of state markers, especially in the absence of group x age interaction effects.

5.1.3 Project 3: The importance of considering symptom profiles

Recent evidence obtained from the largest meta-analysis performed on structural brain alterations in OCD to date, indicated volume reductions to be present in pallidum as well as hippocampus (Boedhoe, Schmaal, Abe, Alonso, et al., 2017). While the results regarding the pallidum are in line with current accounts of pathophysiology, the hippocampus is not typically associated with OCD pathophysiology and its role for the disease has rarely been examined. Results from the above mentioned meta-analysis did not report a relationship between hippocampus volumes and symptoms in OCD, however, the approach taken correlated individual symptoms with hippocampus volumes, disregarding potential relationships between symptoms. Since the large majority of patients typically displays a multitude of symptoms simultaneously (see section 1.1.2), a potential relationship between the symptom profile, i.e. interrelation between symptoms, and hippocampus volumes may exist.

In order to assess whether specific symptom profiles, i.e. taking into consideration the interrelation between various symptoms instead of isolated symptoms, are differentially related to hippocampus volumes in OCD, a k-means cluster analysis was performed to form groups of subjects according to their symptom profiles. Subsequently, hippocampus volumes were compared between each cluster membership group. Hippocampus volumes were indeed found to be differentially affected among different cluster membership groups. Of note, the analysis was adjusted for a multitude of confounds including age, sex, total intracranial volume, total symptom severity score, clinically relevant depression,

medication, disease duration, as well as scanner. Additionally, a comparison including healthy subjects was performed. Here, it was shown that patients of one specific cluster also had significantly different hippocampus volumes when compared to healthy controls. It could thus be demonstrated, that taking symptom profiles into consideration may be useful when exploring structure-symptom relationships.

5.1.4 Implications across projects

From a methodological perspective, the application of network based analysis strategies appears to be useful in several ways: firstly, these approaches allow to advance our understanding of underlying pathophysiological alterations and potential mechanisms by adding a perspective that complements traditional univariate analyses strategies. Secondly, the methods are readily adoptable to accommodate a wide range of different types of data as was demonstrated in this manuscript. Regarding the clinical perspective, the results clearly support the view that current accounts of OCD pathophysiology should incorporate various regions not commonly found in disease models. Additionally, application of network based analysis strategies allowed to directly generate new hypotheses (for more information as well as suggestions see section 5.3). The overall network topology was found to be in the small-world regime when using different definitions of connectivity, further confirming findings from other studies (Kim et al., 2013; Palaniyappan et al., 2016; Palaniyappan et al., 2015; Zhong et al., 2014). Thus, it appears that fundamental organizational principles are largely intact in OCD. Of note, the trend significant finding of impaired normalized average characteristic path length described in Project 2 needs further assessment as it indicates potentially altered large scale organization at least in networks based on gyrification covariance patterns.

5.2 Limitations & Methodological Considerations

As with any study, several limitations should be considered when interpreting the findings presented in this manuscript. This section will firstly address issues that are common to all three studies and are mainly resulting from the heterogeneity of the disorder regarding symptoms, comorbidities as well as the impact of medication. Secondly, there are limitations that are specific to the methods of network based analyses. This is especially true in light of the fact that in general, the field of network science is comparatively new, and the applications to brain imaging even more so. Therefore, while the strengths are manifold, so are potential limitations.

5.2.1 Issues regarding sample heterogeneity

With a prevalence of about 2.3% OCD is certainly not considered to be a specifically rare psychiatric disorder. Nevertheless, trying to disentangle structural and functional alterations underlying specific symptoms turns out to be a rather difficult endeavor given the large heterogeneity of symptoms. As described above (see section 1.1.2), the majority of patients presents with a mix of different symptoms and pure types are rarely described. This fact leads to a dilemma: one can either choose to acquire immensely large amounts of data in order to be able to stratify the sample into patient groups. This approach comes at the price of high financial burdens and takes extended periods of time needed for data acquisition. On the other hand, one might aim at a more selective composition of smaller samples comprising patients with a very distinct profile, for example treatment-naïve patients with mainly checking symptoms and generalized anxiety disorder as the only comorbidity. Even though results of such an approach may be of value, they clearly raise questions regarding the generalizability. The fact that the presence of multiple comorbidities appears to be the rule rather than the exception further complicates the subject matter. Though one of the main purposes of Project 3 was to disentangle the influence of symptom profiles and therefore directly addressing the issue imposed by heterogeneous symptoms, this apparently important factor was not implemented in the other two studies. This is largely due to the substantial number of subjects needed to conduct such analyses as well as the fact that it is so far unclear how stable the results, regarding clustering of patients according to symptom profiles, are. Increasing the number of parameters that enter the cluster analysis, i.e. number of different symptom items, may lead to potentially more complex profile patterns. Therefore repeating the cluster analysis

with a different sample of subjects may well lead to different clusters and therefore different associations with structural parameters. Taken together, more research is needed to further disentangle the importance of symptom profiles in OCD. Several studies conducted using primate animal models of depression report evidence for interaction effects of disease and SSRI treatment on brain structures (Shively et al., 2017; Willard et al., 2015). Given that SSRIs are the first line pharmacological treatment option in OCD, it appears sensible to take this factor into account. To address this issue, the analyses conducted in all projects of this thesis aimed at adjusting for medication effects. Nevertheless, the broad spectrum of different medications encountered in the samples was simply binarized to indicate either presence or absence of medication. While this approach was chosen for practical purposes, future studies that more thoroughly examine potential effects, e.g. differential effects between SSRIs and for example selective serotonin-norepinephrine reuptake inhibitors (SSNRIs), are highly desirable. Additionally, it is conceivable that dose-effect relationships may exist. While first efforts to provide dose equivalents for antidepressants are undertaken (Hayasaka et al., 2015), the issue is further complicated by the fact that in OCD also other medications are used (see section 1.1.4). Taken together, in all three projects outlined above, efforts were made to account for various influencing factors by adjusting statistical analyses, for example taking into consideration effects of comorbidity and medication. Subject to replication, the results of Project 3 raise various questions about best practices on how to incorporate effects of symptom profiles for future studies and discussions regarding different approaches are highly welcome.

5.2.2 Issues regarding network-based approaches

A common practice for the derivation of macroscale MRI-based brain nodes is the application of an atlas-based parcellation scheme to T1-weighted data. Importantly, all atlases are dealing with the same system, however different approaches during atlas construction may be used, e.g. various registration techniques or differences regarding higher or lower target resolution. As mentioned above (see section 1.3.2.2), different atlases can also be based on various different properties such as cytoarchitectonic features, anatomical landmarks, functional properties, or other features (de Reus & van den Heuvel, 2013). While it was shown, that global topological features such as sparsity or small-worldness are conserved across applications of various different atlases (Bassett et

al., 2011), changes in parcellation scheme resolution were shown to potentially affect global as well as local graph measures (van Wijk, Stam, & Daffertshofer, 2010), therefore limiting the possibility to directly compare networks that were constructed based on different atlases (de Reus & van den Heuvel, 2013). Another caveat relates to differences in atlas boundaries, or more precisely on the question whether it is sensible to assume clear cut borders between regions to be functionally important. It has previously been shown that the density of connections within a connectivity matrix influences the computation of graph measures (Fornito et al., 2016). In Project 1, edges were defined based on the number of streamlines, naturally resulting in a rather sparse matrix since not every pair of nodes will be connected. Nevertheless, the results were computed over a range of density thresholds to explore potential difference (Supplementary Table 7, Reess et al. (2016)). In case of Project 2, the use of gyrification based structural covariance provided a dense matrix, since for every possible pair of nodes one correlation was computed. Here, only those edges with a significant r-value after FDR-correction were used for the analysis. A further issue concerns the difficulties associated with the definition and interpretation of edges. This is especially true for using tractography based methods to define edges. Various algorithms used for tractography perform somewhat differently while still tending to reconstruct a high rate of false positive connections (Maier-Hein et al., 2017), and present with their own inherent limitations (Shi & Toga, 2017). To the best of the author's knowledge, virtually every connectome-based study conducted *in-vivo* in humans so far was based on undirected graphs, i.e. the directionality of connectivity between nodes has been neglected. Given the fact that neurons, as the structural and functional units of the brain, form connections that are clearly directional in nature, what can macroanatomical structural network analyses offer? With the currently available technology the issue of directionality does not appear to be solved any time soon, however, using undirected graphs in the analyses may still lead to interesting hypothesis and narrow down where to search and what to search for on a more detailed level. Taken together, so far no gold standard has been established regarding the tracking of macroanatomical white matter fiber bundles. Nevertheless, improvements in scanner hardware and sequences will likely provide increased reproducibility and allow for more accurate reconstructions in the future. As mentioned above (see section 1.3.2.2), structural covariance approaches provide measures that can only be computed on a group basis, therefore rendering the opportunity to assist diagnosis on an individual subject basis impossible. Nevertheless, studies employing the framework of structural covariance may be utilized to generate new hypotheses as was done suggested in Project 2.

Finally, there are various issues and pitfalls related to the statistical analysis as well as thresholding of graphs. One major difficulty arises from the sheer number of statistical tests typically associated with graph theoretical studies. Since many measures are computed on a per node basis, the number of tests to be performed increases exponentially with the number of nodes defined in the network. Since in depth descriptions of these issues is beyond the scope of this manuscript, the interested reader is referred to Fornito, Zalesky, and Breakspear (2013), as well as Fornito, Bullmore, and Zalesky (2017).

5.3 Future directions

The results presented in this thesis hopefully stimulate future research to further address the importance and clarify the role of brain morphological alterations in OCD. This section is divided into three parts. The first part highlights how the results may inspire potential follow-up experiments that are directly related to the projects described in the thesis. The second part describes future directions that are emerging at a more global scale regarding structural brain research in OCD. Finally, the third part briefly addresses emerging ideas on transdiagnostic approaches to the study of psychiatric disorders.

5.3.1 Potential for follow-up studies in light of current findings

Project 1 provides a framework to formulate a concrete research hypothesis derived from the results of the NBS analysis, which implicate an involvement of uncinate for the pathophysiology of OCD. More specifically, the results indicate that there might be a decreased micro-structural connectivity between fronto-temporal regions. To test this hypothesis, one might directly employ fiber tracking algorithms. As previous studies found focal alterations in FA-values in UF, one might also combine the results from fiber tracking, i.e. NOS and FA values to derive different metrics. Importantly, there are different approaches to conduct such experiments. The fiber tracking might be chosen to reconstruct the UF as defined within an atlas, or one might start tracking based on target and seed regions. With the latter approach, there are more parameters potentially increasing the sensitivity at the cost of the need to more rigorously correct more multiple comparisons. In summary, various methods to assess the importance of UF are available and should be employed to clarify its role for OCD pathophysiology.

Project 2 provides evidence that gyrification may be a sensitive marker for neurodevelopment. In conjunction with findings from preterm born subjects as well as the notion that preterm birth increases the risk to subsequently develop OCD, it is proposed to aim at including information about preterm birth when studying OCD. This should especially hold true for studies examining structural alterations, given the finding that structural alterations in preterm born adults correlate with functional connectivity networks (Bauml et al., 2015). Measures to quantify severity of preterm birth such as gestational week and birth weight may be modeled using regression analysis with parameters derived from structural brain scans to further address potential “dose-effect”

relationships. Additionally, it is conceivable that various symptoms may be differentially linked to these parameters. Therefore, correlating for example gestational week with symptoms may shed light on symptom specific mechanisms. Of note, the assessment of such information, i.e. gestation week or birth weight, may be difficult given that many patients may neither be aware of it nor have the chance to try to acquire it especially in case of older patients. However, with increased demands regarding medical documentation standards and digitization, the potential to recover medical records containing this information is higher, especially in case of younger patients.

Project 3 may spark future research on the role of hippocampus alterations in mediating various symptoms in OCD. In general the approach of clustering subjects according to an entire symptom profile can readily be translated to other brain structures of the whole brain. Logically, one might aim at probing whether cluster membership is not only associated with differences in hippocampus volumes but whether it may be associated to other brain regions that are commonly found to show structural alterations such as BG, thalamus, OFC, putamen, pallidum, etc. Indeed finding those associations would speak in favor of a dimensional model of OCD that should comprise not only individual dimensions but instead be based on the entire symptom profile, i.e. inter-relation between various symptoms. Furthermore, the approach of clustering according to symptom profiles may be put in relation to above mentioned proxies for preterm birth such as gestational age.

5.3.2. The Promise of Large-scale Imaging Initiatives

In recent years, extraordinary efforts have been made to aggregate data from various labs world-wide, streamline the analysis process and use meta-analytic approaches to disentangle structural as well as functional alterations in psychiatric disorders and also clarify the relationship with genetics (Thompson et al., 2014). These kinds of initiatives allow unmatched statistical power to also indentify subtle effects and have already provided new insights not only for OCD (Boedhoe, Schmaal, Abe, Alonso, et al., 2017) but also a multitude of other psychiatric disorders (see http://enigma.ini.usc.edu/). For example, Project 3 presented in this thesis was directly inspired by results from Boedhoe, Schmaal, Abe, Alonso, et al. (2017). Applying network based approaches to these data appears to be especially promising. However, one drawback that is still unresolved lies in the fact that these initiatives currently use data that was acquired in different labs, often using different acquisition parameters. The future might see not only harmonized analysis

pipelines but maybe even harmonized imaging protocols as well as standardization of other parameters regarding diagnostics or use of questionnaires.

5.3.3 Transdiagnostic Approaches to Psychiatric Disorders

A recent development, in part also driven by findings from network-based studies, is an emphasis of transdiagnostic aspects of psychiatric disorders. Today, there are substantial efforts made to investigate how dimensional approaches to psychiatric illness might be useful in gaining a deeper understanding of disease mechanisms. Buckholtz and Meyer-Lindenberg (2012) argue, that psychopathology goes along with disruptions in interregional relationships of networks and that influences on the network level mediate psychopathological susceptibility over various domains instead of nosologically discrete disorder entities. Similarly, Crossley et al. (2014) provide evidence from two strands of experiments: 1) based on structural connectivity networks derived from DTI in healthy participant, they isolated hub regions defined as nodes with extraordinarily high topological centrality to the network. Subsequently, disrupting these hub regions with computational attacks revealed a disproportionally strong impact on brain network efficiency; 2) using GM lesion maps from 26 different brain disorders, the authors could show, that the occurrence of lesions shared among disorders was higher in hub regions, indicating that hub regions are overall more likely to be implicated in brain disorders. By means of meta-analysis, (McTeague et al., 2017) provide further evidence that networks typically associated with flexibility of cognition are vulnerable to psychopathology over a rather broad spectrum. Furthermore, alterations in brain activation were characterized by transdiagnostic patterns.

5.5 Conclusion

The current thesis provides further evidence supporting the notion that current accounts of pathophysiological models of OCD should be extended to incorporate regions not classically associated with CSTC circuitry. Furthermore it illustrates the usefulness of network-based approaches in order to generate research hypotheses by shifting the perspective from a focal to a more global network perspective. Additionally, it was shown that neurodevelopmental aspects appear to be important for OCD pathophysiology and future studies, especially when examining structural measures, are encouraged to exploit information on circumstances regarding birth, i.e. gestational age or birth weight. Furthermore, the interesting finding of associations between symptom profiles and volumetric properties of hippocampus call for further research. Taken together, the findings presented in this thesis will hopefully stimulate innovative research to better understand the mechanisms and causes behind the disorder.

REFERENCES

Abramovitch, A., Abramowitz, J. S., & Mittelman, A. (2013). The neuropsychology of adult obsessive-compulsive disorder: a meta-analysis. *Clin Psychol Rev, 33*(8), 1163-1171. doi: 10.1016/j.cpr.2013.09.004

Abramovitch, A., Dar, R., Mittelman, A., & Wilhelm, S. (2015). Comorbidity Between Attention Deficit/Hyperactivity Disorder and Obsessive-Compulsive Disorder Across the Lifespan: A Systematic and Critical Review. *Harv Rev Psychiatry, 23*(4), 245-262. doi: 10.1097/HRP.0000000000000050

Abramowitz, J. S. (2006). The psychological treatment of obsessive-compulsive disorder. *Can J Psychiatry, 51*(7), 407-416. doi: 10.1177/070674370605100702

Abramowitz, J. S., Taylor, S., & McKay, D. (2009). Obsessive-compulsive disorder. *The Lancet, 374*(9688), 491-499. doi: 10.1016/s0140-6736(09)60240-3

Alexander-Bloch, A., Raznahan, A., Bullmore, E., & Giedd, J. (2013). The convergence of maturational change and structural covariance in human cortical networks. *J Neurosci, 33*(7), 2889-2899. doi: 10.1523/JNEUROSCI.3554-12.2013

Alexander, G. E., DeLong, M. R., & Strick, P. L. (1986). Parallel organization of functionally segregated circuits linking basal ganglia and cortex. *Annu Rev Neurosci, 9*, 357-381. doi: 10.1146/annurev.ne.09.030186.002041

Alvarenga, P. G., do Rosario, M. C., Batistuzzo, M. C., Diniz, J. B., Shavitt, R. G., Duran, F. L., . . . Hoexter, M. Q. (2012). Obsessive-compulsive symptom dimensions correlate to specific gray matter volumes in treatment-naive patients. *J Psychiatr Res, 46*(12), 1635-1642. doi: 10.1016/j.jpsychires.2012.09.002

American Psychiatric Association. (2013). *Diagnostic and statistical manual of mental disorders : DSM-5* (5th ed.). Washington, D.C.: American Psychiatric Association.

Anholt, G. E., Aderka, I. M., van Balkom, A. J., Smit, J. H., Schruers, K., van der Wee, N. J., . . . van Oppen, P. (2014). Age of onset in obsessive-compulsive disorder: admixture analysis with a large sample. *Psychol Med, 44*(1), 185-194. doi: 10.1017/S0033291713000470

Annesley, P. T. (1969). Nardil response in a chronic obsessive compulsive. *Br J Psychiatry, 115*(523), 748.

Aouizerate, B., Guehl, D., Cuny, E., Rougier, A., Bioulac, B., Tignol, J., & Burbaud, P. (2004). Pathophysiology of obsessive-compulsive disorder: a necessary link between

phenomenology, neuropsychology, imagery and physiology. *Prog Neurobiol, 72*(3), 195-221. doi: 10.1016/j.pneurobio.2004.02.004

Armstrong, E., Schleicher, A., Omran, H., Curtis, M., & Zilles, K. (1995). The ontogeny of human gyrification. *Cereb Cortex, 5*(1), 56-63.

Ashburner, J., & Friston, K. J. (2000). Voxel-based morphometry--the methods. *Neuroimage, 11*(6 Pt 1), 805-821. doi: 10.1006/nimg.2000.0582

Aylward, E. H., Harris, G. J., Hoehn-Saric, R., Barta, P. E., Machlin, S. R., & Pearlson, G. D. (1996). Normal caudate nucleus in obsessive-compulsive disorder assessed by quantitative neuroimaging. *Arch Gen Psychiatry, 53*(7), 577-584.

Ball, G., Boardman, J. P., Rueckert, D., Aljabar, P., Arichi, T., Merchant, N., . . . Counsell, S. J. (2012). The effect of preterm birth on thalamic and cortical development. *Cereb Cortex, 22*(5), 1016-1024. doi: 10.1093/cercor/bhr176

Bassett, D. S., Brown, J. A., Deshpande, V., Carlson, J. M., & Grafton, S. T. (2011). Conserved and variable architecture of human white matter connectivity. *Neuroimage, 54*(2), 1262-1279. doi: 10.1016/j.neuroimage.2010.09.006

Bassett, D. S., & Bullmore, E. (2006). Small-world brain networks. *Neuroscientist, 12*(6), 512-523. doi: 10.1177/1073858406293182

Bauml, J. G., Daamen, M., Meng, C., Neitzel, J., Scheef, L., Jaekel, J., . . . Sorg, C. (2015). Correspondence Between Aberrant Intrinsic Network Connectivity and Gray-Matter Volume in the Ventral Brain of Preterm Born Adults. *Cereb Cortex, 25*(11), 4135-4145. doi: 10.1093/cercor/bhu133

Baxter, L. R., Jr., Phelps, M. E., Mazziotta, J. C., Guze, B. H., Schwartz, J. M., & Selin, C. E. (1987). Local cerebral glucose metabolic rates in obsessive-compulsive disorder. A comparison with rates in unipolar depression and in normal controls. *Arch Gen Psychiatry, 44*(3), 211-218.

Baxter, L. R., Jr., Saxena, S., Brody, A. L., Ackermann, R. F., Colgan, M., Schwartz, J. M., . . . Phelps, M. E. (1996). Brain Mediation of Obsessive-Compulsive Disorder Symptoms: Evidence From Functional Brain Imaging Studies in the Human and Nonhuman Primate. *Semin Clin Neuropsychiatry, 1*(1), 32-47. doi: 10.1053/SCNP00100032

Baxter, L. R., Jr., Schwartz, J. M., Bergman, K. S., Szuba, M. P., Guze, B. H., Mazziotta, J. C., . . . et al. (1992). Caudate glucose metabolic rate changes with both drug and behavior therapy for obsessive-compulsive disorder. *Arch Gen Psychiatry, 49*(9), 681-689.

Baxter, L. R., Jr., Schwartz, J. M., Mazziotta, J. C., Phelps, M. E., Pahl, J. J., Guze, B. H., & Fairbanks, L. (1988). Cerebral glucose metabolic rates in nondepressed patients with obsessive-compulsive disorder. *Am J Psychiatry, 145*(12), 1560-1563. doi: 10.1176/ajp.145.12.1560

Behar, D., Rapoport, J. L., Berg, C. J., Denckla, M. B., Mann, L., Cox, C., . . . Wolfman, M. G. (1984). Computerized tomography and neuropsychological test measures in adolescents with obsessive-compulsive disorder. *Am J Psychiatry, 141*(3), 363-369. doi: 10.1176/ajp.141.3.363

Benedetti, F., Giacosa, C., Radaelli, D., Poletti, S., Pozzi, E., Dallaspezia, S., . . . Smeraldi, E. (2013). Widespread changes of white matter microstructure in obsessive-compulsive disorder: effect of drug status. *Eur Neuropsychopharmacol, 23*(7), 581-593. doi: 10.1016/j.euroneuro.2012.07.002

Benkelfat, C., Nordahl, T. E., Semple, W. E., King, A. C., Murphy, D. L., & Cohen, R. M. (1990). Local cerebral glucose metabolic rates in obsessive-compulsive disorder. Patients treated with clomipramine. *Arch Gen Psychiatry, 47*(9), 840-848.

Boccaletti, S., Latora, V., Moreno, Y., Chavez, M., & Hwang, D. (2006). Complex networks: Structure and dynamics. *Physics Reports, 424*(4-5), 175-308. doi: 10.1016/j.physrep.2005.10.009

Boedhoe, P. S., Schmaal, L., Abe, Y., Alonso, P., Ameis, S. H., Anticevic, A., . . . ENIGMA OCD Working Group. (2017). Cortical Abnormalities Associated With Pediatric and Adult Obsessive-Compulsive Disorder: Findings From the ENIGMA Obsessive-Compulsive Disorder Working Group. *Am J Psychiatry, epub ahead of print*. doi: 10.1176/appi.ajp.2017.17050485

Boedhoe, P. S., Schmaal, L., Abe, Y., Ameis, S. H., Arnold, P. D., Batistuzzo, M. C., . . . van den Heuvel, O. A. (2017). Distinct Subcortical Volume Alterations in Pediatric and Adult OCD: A Worldwide Meta- and Mega-Analysis. *Am J Psychiatry, 174*(1), 60-69. doi: 10.1176/appi.ajp.2016.16020201

Brakoulias, V., Starcevic, V., Belloch, A., Brown, C., Ferrao, Y. A., Fontenelle, L. F., . . . Viswasam, K. (2017). Comorbidity, age of onset and suicidality in obsessive-compulsive disorder (OCD): An international collaboration. *Compr Psychiatry, 76*, 79-86. doi: 10.1016/j.comppsych.2017.04.002

Brander, G., Rydell, M., Kuja-Halkola, R., Fernandez de la Cruz, L., Lichtenstein, P., Serlachius, E., . . . Mataix-Cols, D. (2016). Association of Perinatal Risk Factors With Obsessive-Compulsive Disorder: A Population-Based Birth Cohort, Sibling Control

Study. *JAMA Psychiatry, 73*(11), 1135-1144. doi: 10.1001/jamapsychiatry.2016.2095

Brunelin, J., Mondino, M., Bation, R., Palm, U., Saoud, M., & Poulet, E. (2018). Transcranial Direct Current Stimulation for Obsessive-Compulsive Disorder: A Systematic Review. *Brain Sci, 8*(2). doi: 10.3390/brainsci8020037

Buckholtz, J. W., & Meyer-Lindenberg, A. (2012). Psychopathology and the human connectome: toward a transdiagnostic model of risk for mental illness. *Neuron, 74*(6), 990-1004. doi: 10.1016/j.neuron.2012.06.002

Bullmore, E., & Sporns, O. (2009). Complex brain networks: graph theoretical analysis of structural and functional systems. *Nat Rev Neurosci, 10*(3), 186-198. doi: 10.1038/nrn2575

Bush, G., Vogt, B. A., Holmes, J., Dale, A. M., Greve, D., Jenike, M. A., & Rosen, B. R. (2002). Dorsal anterior cingulate cortex: a role in reward-based decision making. *Proc Natl Acad Sci U S A, 99*(1), 523-528. doi: 10.1073/pnas.012470999

Carmona, S., Bassas, N., Rovira, M., Gispert, J. D., Soliva, J. C., Prado, M., . . . Vilarroya, O. (2007). Pediatric OCD structural brain deficits in conflict monitoring circuits: a voxel-based morphometry study. *Neurosci Lett, 421*(3), 218-223. doi: 10.1016/j.neulet.2007.05.047

Childers, M. K., Rupright, J., Jones, P. S., & Merveille, O. (1998). Assessment of neuroendocrine dysfunction following traumatic brain injury. *Brain Inj, 12*(6), 517-523.

Christensen, R. (2011). *Plane answers to complex questions : the theory of linear models* (4th ed.). New York: Springer.

Clarkson, M. J., Cardoso, M. J., Ridgway, G. R., Modat, M., Leung, K. K., Rohrer, J. D., . . . Ourselin, S. (2011). A comparison of voxel and surface based cortical thickness estimation methods. *Neuroimage, 57*(3), 856-865. doi: 10.1016/j.neuroimage.2011.05.053

Crossley, N. A., Mechelli, A., Scott, J., Carletti, F., Fox, P. T., McGuire, P., & Bullmore, E. T. (2014). The hubs of the human connectome are generally implicated in the anatomy of brain disorders. *Brain, 137*, 2382-2395. doi: 10.1093/brain/awu132

D'Alcante, C. C., Diniz, J. B., Fossaluza, V., Batistuzzo, M. C., Lopes, A. C., Shavitt, R. G., . . . Hoexter, M. Q. (2012). Neuropsychological predictors of response to randomized treatment in obsessive-compulsive disorder. *Prog Neuropsychopharmacol Biol Psychiatry, 39*(2), 310-317. doi: 10.1016/j.pnpbp.2012.07.002

Dale, A. M., Fischl, B., & Sereno, M. I. (1999). Cortical surface-based analysis. I. Segmentation and surface reconstruction. *Neuroimage, 9*(2), 179-194. doi: 10.1006/nimg.1998.0395

Davis, J., Maes, M., Andreazza, A., McGrath, J. J., Tye, S. J., & Berk, M. (2015). Towards a classification of biomarkers of neuropsychiatric disease: from encompass to compass. *Mol Psychiatry, 20*(2), 152-153. doi: 10.1038/mp.2014.139

de Reus, M. A., & van den Heuvel, M. P. (2013). The parcellation-based connectome: limitations and extensions. *Neuroimage, 80*, 397-404. doi: 10.1016/j.neuroimage.2013.03.053

Deco, G., Tononi, G., Boly, M., & Kringelbach, M. L. (2015). Rethinking segregation and integration: contributions of whole-brain modelling. *Nat Rev Neurosci, 16*(7), 430-439. doi: 10.1038/nrn3963

Del Casale, A., Kotzalidis, G. D., Rapinesi, C., Serata, D., Ambrosi, E., Simonetti, A., . . . Girardi, P. (2011). Functional neuroimaging in obsessive-compulsive disorder. *Neuropsychobiology, 64*(2), 61-85. doi: 10.1159/000325223

Eaton, W. W., Martins, S. S., Nestadt, G., Bienvenu, O. J., Clarke, D., & Alexandre, P. (2008). The burden of mental disorders. *Epidemiol Rev, 30*, 1-14. doi: 10.1093/epirev/mxn011

Ecker, C., Andrews, D., Dell'Acqua, F., Daly, E., Murphy, C., Catani, M., . . . Murphy, D. G. (2016). Relationship Between Cortical Gyrification, White Matter Connectivity, and Autism Spectrum Disorder. *Cereb Cortex, 26*(7), 3297-3309. doi: 10.1093/cercor/bhw098

Eddy, K. T., Dutra, L., Bradley, R., & Westen, D. (2004). A multidimensional meta-analysis of psychotherapy and pharmacotherapy for obsessive-compulsive disorder. *Clin Psychol Rev, 24*(8), 1011-1030. doi: 10.1016/j.cpr.2004.08.004

Eisen, J. L., Sibrava, N. J., Boisseau, C. L., Mancebo, M. C., Stout, R. L., Pinto, A., & Rasmussen, S. A. (2013). Five-year course of obsessive-compulsive disorder: predictors of remission and relapse. *J Clin Psychiatry, 74*(3), 233-239. doi: 10.4088/JCP.12m07657

Fan, Q., Palaniyappan, L., Tan, L., Wang, J., Wang, X., Li, C., . . . Liddle, P. F. (2013). Surface anatomical profile of the cerebral cortex in obsessive-compulsive disorder: a study of cortical thickness, folding and surface area. *Psychol Med, 43*(5), 1081-1091. doi: 10.1017/S0033291712001845

Fernandez de la Cruz, L., Rydell, M., Runeson, B., D'Onofrio, B. M., Brander, G., Ruck, C., . . . Mataix-Cols, D. (2017). Suicide in obsessive-compulsive disorder: a population-

based study of 36 788 Swedish patients. *Mol Psychiatry, 22*(11), 1626-1632. doi: 10.1038/mp.2016.115

Fischl, B., & Dale, A. M. (2000). Measuring the thickness of the human cerebral cortex from magnetic resonance images. *Proc Natl Acad Sci U S A, 97*(20), 11050-11055. doi: 10.1073/pnas.200033797

Fischl, B., Sereno, M. I., & Dale, A. M. (1999). Cortical surface-based analysis. II: Inflation, flattening, and a surface-based coordinate system. *Neuroimage, 9*(2), 195-207. doi: 10.1006/nimg.1998.0396

Fontenelle, L. F., Harrison, B. J., Yucel, M., Pujol, J., Fujiwara, H., & Pantelis, C. (2009). Is there evidence of brain white-matter abnormalities in obsessive-compulsive disorder?: a narrative review. *Top Magn Reson Imaging, 20*(5), 291-298. doi: 10.1097/RMR.0b013e3181e8f22c

Fontenelle, L. F., Oostermeijer, S., Harrison, B. J., Pantelis, C., & Yucel, M. (2011). Obsessive-compulsive disorder, impulse control disorders and drug addiction: common features and potential treatments. *Drugs, 71*(7), 827-840. doi: 10.2165/11591790-000000000-00000

Fornito, A., & Bullmore, E. T. (2015). Connectomics: a new paradigm for understanding brain disease. *Eur Neuropsychopharmacol, 25*(5), 733-748. doi: 10.1016/j.euroneuro.2014.02.011

Fornito, A., Bullmore, E. T., & Zalesky, A. (2017). Opportunities and Challenges for Psychiatry in the Connectomic Era. *Biol Psychiatry Cogn Neurosci Neuroimaging, 2*(1), 9-19. doi: 10.1016/j.bpsc.2016.08.003

Fornito, A., Zalesky, A., & Breakspear, M. (2013). Graph analysis of the human connectome: promise, progress, and pitfalls. *Neuroimage, 80*, 426-444. doi: 10.1016/j.neuroimage.2013.04.087

Fornito, A., Zalesky, A., & Breakspear, M. (2015). The connectomics of brain disorders. *Nat Rev Neurosci, 16*(3), 159-172. doi: 10.1038/nrn3901

Fornito, A., Zalesky, A., & Bullmore, E. T. (2016). *Fundamentals of Brain Network Analysis*. San Diego, CA: Elsevier.

Garber, H. J., Ananth, J. V., Chiu, L. C., Griswold, V. J., & Oldendorf, W. H. (1989). Nuclear magnetic resonance study of obsessive-compulsive disorder. *Am J Psychiatry, 146*(8), 1001-1005. doi: 10.1176/ajp.146.8.1001

Gehring, W. J., Himle, J., & Nisenson, L. G. (2000). Action-monitoring dysfunction in obsessive-compulsive disorder. *Psychol Sci, 11*(1), 1-6. doi: 10.1111/1467-9280.00206

Gilbert, A. R., Mataix-Cols, D., Almeida, J. R., Lawrence, N., Nutche, J., Diwadkar, V., . . . Phillips, M. L. (2008). Brain structure and symptom dimension relationships in obsessive-compulsive disorder: a voxel-based morphometry study. *J Affect Disord, 109*(1-2), 117-126. doi: 10.1016/j.jad.2007.12.223

Glasser, M. F., Coalson, T. S., Robinson, E. C., Hacker, C. D., Harwell, J., Yacoub, E., . . . Van Essen, D. C. (2016). A multi-modal parcellation of human cerebral cortex. *Nature, 536*(7615), 171-178. doi: 10.1038/nature18933

Grant, J. E., Mancebo, M. C., Pinto, A., Williams, K. A., Eisen, J. L., & Rasmussen, S. A. (2007). Late-onset obsessive compulsive disorder: clinical characteristics and psychiatric comorbidity. *Psychiatry Res, 152*(1), 21-27. doi: 10.1016/j.psychres.2006.09.015

Griffa, A., Baumann, P. S., Thiran, J. P., & Hagmann, P. (2013). Structural connectomics in brain diseases. *Neuroimage, 80*, 515-526. doi: 10.1016/j.neuroimage.2013.04.056

Guye, M., Bettus, G., Bartolomei, F., & Cozzone, P. J. (2010). Graph theoretical analysis of structural and functional connectivity MRI in normal and pathological brain networks. *MAGMA, 23*(5-6), 409-421. doi: 10.1007/s10334-010-0205-z

Ha, T. H., Kang, D. H., Park, J. S., Jang, J. H., Jung, W. H., Choi, J. S., . . . Kwon, J. S. (2009). White matter alterations in male patients with obsessive-compulsive disorder. *Neuroreport, 20*(7), 735-739. doi: 10.1097/WNR.0b013e32832ad3da

Hagmann, P. (2005). *From Diffusion MRI to Brain Connectomics.* (Doctoral Thesis), École Polytechnique Fédérale de Lausanne.

Hasler, G., LaSalle-Ricci, V. H., Ronquillo, J. G., Crawley, S. A., Cochran, L. W., Kazuba, D., . . . Murphy, D. L. (2005). Obsessive-compulsive disorder symptom dimensions show specific relationships to psychiatric comorbidity. *Psychiatry Res, 135*(2), 121-132. doi: 10.1016/j.psychres.2005.03.003

Hayasaka, Y., Purgato, M., Magni, L. R., Ogawa, Y., Takeshima, N., Cipriani, A., . . . Furukawa, T. A. (2015). Dose equivalents of antidepressants: Evidence-based recommendations from randomized controlled trials. *J Affect Disord, 180*, 179-184. doi: 10.1016/j.jad.2015.03.021

Hirschtritt, M. E., Bloch, M. H., & Mathews, C. A. (2017). Obsessive-Compulsive Disorder: Advances in Diagnosis and Treatment. *JAMA, 317*(13), 1358-1367. doi: 10.1001/jama.2017.2200

Hofer, P. D., Wahl, K., Meyer, A. H., Miche, M., Beesdo-Baum, K., Wong, S. F., . . . Lieb, R. (2018). Obsessive-compulsive disorder and the risk of subsequent mental

disorders: A community study of adolescents and young adults. *Depress Anxiety, 35*(4), 339-345. doi: 10.1002/da.22733

Hu, X., Du, M., Chen, L., Li, L., Zhou, M., Zhang, L., . . . Gong, Q. (2017). Meta-analytic investigations of common and distinct grey matter alterations in youths and adults with obsessive-compulsive disorder. *Neurosci Biobehav Rev, 78*, 91-103. doi: 10.1016/j.neubiorev.2017.04.012

Huey, E. D., Zahn, R., Krueger, F., Moll, J., Kapogiannis, D., Wassermann, E. M., & Grafman, J. (2008). A psychological and neuroanatomical model of obsessive-compulsive disorder. *J Neuropsychiatry Clin Neurosci, 20*(4), 390-408. doi: 10.1176/jnp.2008.20.4.390

Hulshoff Pol, H., & Bullmore, E. (2013). Neural networks in psychiatry. *Eur Neuropsychopharmacol, 23*(1), 1-6. doi: 10.1016/j.euroneuro.2012.12.004

Huyser, C., Veltman, D. J., de Haan, E., & Boer, F. (2009). Paediatric obsessive-compulsive disorder, a neurodevelopmental disorder? Evidence from neuroimaging. *Neurosci Biobehav Rev, 33*(6), 818-830. doi: 10.1016/j.neubiorev.2009.01.003

Insel, T. R. (1988). Obsessive-compulsive disorder: a neuroethological perspective. *Psychopharmacol Bull, 24*(3), 365-369.

Insel, T. R., Donnelly, E. F., Lalakea, M. L., Alterman, I. S., & Murphy, D. L. (1983). Neurological and neuropsychological studies of patients with obsessive-compulsive disorder. *Biol Psychiatry, 18*(7), 741-751.

Jayarajan, R. N., Venkatasubramanian, G., Viswanath, B., Janardhan Reddy, Y. C., Srinath, S., Vasudev, M. K., & Chandrashekar, C. R. (2012). White matter abnormalities in children and adolescents with obsessive-compulsive disorder: a diffusion tensor imaging study. *Depress Anxiety, 29*(9), 780-788. doi: 10.1002/da.21890

Kanwisher, N. (2010). Functional specificity in the human brain: a window into the functional architecture of the mind. *Proc Natl Acad Sci U S A, 107*(25), 11163-11170. doi: 10.1073/pnas.1005062107

Kellner, C. H., Jolley, R. R., Holgate, R. C., Austin, L., Lydiard, R. B., Laraia, M., & Ballenger, J. C. (1991). Brain MRI in obsessive-compulsive disorder. *Psychiatry Res, 36*(1), 45-49.

Khundrakpam, B. S., Reid, A., Brauer, J., Carbonell, F., Lewis, J., Ameis, S., . . . Brain Development Cooperative, Group. (2013). Developmental changes in organization of structural brain networks. *Cereb Cortex, 23*(9), 2072-2085. doi: 10.1093/cercor/bhs187

Kim, S. G., Jung, W. H., Kim, S. N., Jang, J. H., & Kwon, J. S. (2013). Disparity between dorsal and ventral networks in patients with obsessive-compulsive disorder: evidence

revealed by graph theoretical analysis based on cortical thickness from MRI. *Front Hum Neurosci, 7*, 302. doi: 10.3389/fnhum.2013.00302

Koch, K., Reess, T. J., Rus, O. G., Zimmer, C., & Zaudig, M. (2014). Diffusion tensor imaging (DTI) studies in patients with obsessive-compulsive disorder (OCD): a review. *J Psychiatr Res, 54*, 26-35. doi: 10.1016/j.jpsychires.2014.03.006

Kwon, J. S., Jang, J. H., Choi, J. S., & Kang, D. H. (2009). Neuroimaging in obsessive-compulsive disorder. *Expert Rev Neurother, 9*(2), 255-269. doi: 10.1586/14737175.9.2.255

Lazar, M. (2010). Mapping brain anatomical connectivity using white matter tractography. *NMR Biomed, 23*(7), 821-835. doi: 10.1002/nbm.1579

Leckman, J. F., Grice, D. E., Boardman, J., Zhang, H., Vitale, A., Bondi, C., . . . Pauls, D. L. (1997). Symptoms of obsessive-compulsive disorder. *Am J Psychiatry, 154*(7), 911-917. doi: 10.1176/ajp.154.7.911

Lerch, J. P., van der Kouwe, A. J., Raznahan, A., Paus, T., Johansen-Berg, H., Miller, K. L., . . . Sotiropoulos, S. N. (2017). Studying neuroanatomy using MRI. *Nat Neurosci, 20*(3), 314-326. doi: 10.1038/nn.4501

Lerch, J. P., Worsley, K., Shaw, W. P., Greenstein, D. K., Lenroot, R. K., Giedd, J., & Evans, A. C. (2006). Mapping anatomical correlations across cerebral cortex (MACACC) using cortical thickness from MRI. *Neuroimage, 31*(3), 993-1003. doi: 10.1016/j.neuroimage.2006.01.042

Linnman, C., Rougemont-Bucking, A., Beucke, J. C., Zeffiro, T. A., & Milad, M. R. (2011). Unconditioned responses and functional fear networks in human classical conditioning. *Behav Brain Res, 221*(1), 237-245. doi: 10.1016/j.bbr.2011.02.045

Lochner, C., Fouche, J. P., du Plessis, S., Spottiswoode, B., Seedat, S., Fineberg, N., . . . Stein, D. J. (2012). Evidence for fractional anisotropy and mean diffusivity white matter abnormalities in the internal capsule and cingulum in patients with obsessive-compulsive disorder. *J Psychiatry Neurosci, 37*(3), 193-199. doi: 10.1503/jpn.110059

Luxenberg, J. S., Swedo, S. E., Flament, M. F., Friedland, R. P., Rapoport, J., & Rapoport, S. I. (1988). Neuroanatomical abnormalities in obsessive-compulsive disorder detected with quantitative X-ray computed tomography. *Am J Psychiatry, 145*(9), 1089-1093. doi: 10.1176/ajp.145.9.1089

Macy, A. S., Theo, J. N., Kaufmann, S. C., Ghazzaoui, R. B., Pawlowski, P. A., Fakhry, H. I., . . . IsHak, W. W. (2013). Quality of life in obsessive compulsive disorder. *CNS Spectr, 18*(1), 21-33. doi: 10.1017/S1092852912000697

Maier-Hein, K. H., Neher, P. F., Houde, J. C., Cote, M. A., Garyfallidis, E., Zhong, J., . . . Descoteaux, M. (2017). The challenge of mapping the human connectome based on diffusion tractography. *Nat Commun, 8*(1), 1349. doi: 10.1038/s41467-017-01285-x

Marsden, C. D. (1982). The mysterious motor function of the basal ganglia: the Robert Wartenberg Lecture. *Neurology, 32*(5), 514-539.

Mataix-Cols, D., Rauch, S. L., Manzo, P. A., Jenike, M. A., & Baer, L. (1999). Use of factor-analyzed symptom dimensions to predict outcome with serotonin reuptake inhibitors and placebo in the treatment of obsessive-compulsive disorder. *Am J Psychiatry, 156*(9), 1409-1416. doi: 10.1176/ajp.156.9.1409

Mataix-Cols, D., Rosario-Campos, M. C., & Leckman, J. F. (2005). A multidimensional model of obsessive-compulsive disorder. *Am J Psychiatry, 162*(2), 228-238. doi: 10.1176/appi.ajp.162.2.228

Matsumoto, R., Ito, H., Takahashi, H., Ando, T., Fujimura, Y., Nakayama, K., . . . Suhara, T. (2010). Reduced gray matter volume of dorsal cingulate cortex in patients with obsessive-compulsive disorder: a voxel-based morphometric study. *Psychiatry Clin Neurosci, 64*(5), 541-547. doi: 10.1111/j.1440-1819.2010.02125.x

McTeague, L. M., Huemer, J., Carreon, D. M., Jiang, Y., Eickhoff, S. B., & Etkin, A. (2017). Identification of Common Neural Circuit Disruptions in Cognitive Control Across Psychiatric Disorders. *Am J Psychiatry, 174*(7), 676-685. doi: 10.1176/appi.ajp.2017.16040400

Menzies, L., Chamberlain, S. R., Laird, A. R., Thelen, S. M., Sahakian, B. J., & Bullmore, E. T. (2008). Integrating evidence from neuroimaging and neuropsychological studies of obsessive-compulsive disorder: the orbitofronto-striatal model revisited. *Neurosci Biobehav Rev, 32*(3), 525-549. doi: 10.1016/j.neubiorev.2007.09.005

Milad, M. R., Quirk, G. J., Pitman, R. K., Orr, S. P., Fischl, B., & Rauch, S. L. (2007). A role for the human dorsal anterior cingulate cortex in fear expression. *Biol Psychiatry, 62*(10), 1191-1194. doi: 10.1016/j.biopsych.2007.04.032

Milad, M. R., & Rauch, S. L. (2012). Obsessive-compulsive disorder: beyond segregated cortico-striatal pathways. *Trends Cogn Sci, 16*(1), 43-51. doi: 10.1016/j.tics.2011.11.003

Mindus, P., & Nyman, H. (1991). Normalization of personality characteristics in patients with incapacitating anxiety disorders after capsulotomy. *Acta Psychiatr Scand, 83*(4), 283-291.

Modell, J. G., Mountz, J. M., Curtis, G. C., & Greden, J. F. (1989). Neurophysiologic dysfunction in basal ganglia/limbic striatal and thalamocortical circuits as a pathogenetic mechanism of obsessive-compulsive disorder. *J Neuropsychiatry Clin Neurosci, 1*(1), 27-36. doi: 10.1176/jnp.1.1.27

Mori, S., & Zhang, J. (2006). Principles of diffusion tensor imaging and its applications to basic neuroscience research. *Neuron, 51*(5), 527-539. doi: 10.1016/j.neuron.2006.08.012

Nakamae, T., Narumoto, J., Sakai, Y., Nishida, S., Yamada, K., Nishimura, T., & Fukui, K. (2011). Diffusion tensor imaging and tract-based spatial statistics in obsessive-compulsive disorder. *J Psychiatr Res, 45*(5), 687-690. doi: 10.1016/j.jpsychires.2010.09.016

Newman, M. E. J. (2010). *Networks : An introduction*. Oxford, New York: Oxford University Press.

Nordahl, T. E., Benkelfat, C., Semple, W. E., Gross, M., King, A. C., & Cohen, R. M. (1989). Cerebral glucose metabolic rates in obsessive compulsive disorder. *Neuropsychopharmacology, 2*(1), 23-28.

Northoff, G. (2014). Localization *versus* holism and intrinsic *versus* extrinsic views of the brain: a neurophilosophical approach. *Minerva Psichiatr, 55*, 1-15.

O'Neill, J., & Feusner, J. D. (2015). Cognitive-behavioral therapy for obsessive-compulsive disorder: access to treatment, prediction of long-term outcome with neuroimaging. *Psychol Res Behav Manag, 8*, 211-223. doi: 10.2147/PRBM.S75106

Okada, K., Nakao, T., Sanematsu, H., Murayama, K., Honda, S., Tomita, M., . . . Kanba, S. (2015). Biological heterogeneity of obsessive-compulsive disorder: A voxel-based morphometric study based on dimensional assessment. *Psychiatry Clin Neurosci, 69*(7), 411-421. doi: 10.1111/pcn.12269

Olatunji, B. O., Ferreira-Garcia, R., Caseras, X., Fullana, M. A., Wooderson, S., Speckens, A., . . . Mataix-Cols, D. (2014). Predicting response to cognitive behavioral therapy in contamination-based obsessive-compulsive disorder from functional magnetic resonance imaging. *Psychol Med, 44*(10), 2125-2137. doi: 10.1017/S0033291713002766

Ost, L. G., Havnen, A., Hansen, B., & Kvale, G. (2015). Cognitive behavioral treatments of obsessive-compulsive disorder. A systematic review and meta-analysis of studies published 1993-2014. *Clin Psychol Rev, 40*, 156-169. doi: 10.1016/j.cpr.2015.06.003

Palaniyappan, L., & Liddle, P. F. (2012). Aberrant cortical gyrification in schizophrenia: a surface-based morphometry study. *J Psychiatry Neurosci, 37*(6), 399-406. doi: 10.1503/jpn.110119

Palaniyappan, L., Marques, T. R., Taylor, H., Mondelli, V., Reinders, Aats, Bonaccorso, S., . . . Dazzan, P. (2016). Globally Efficient Brain Organization and Treatment Response in Psychosis: A Connectomic Study of Gyrification. *Schizophr Bull, 42*(6), 1446-1456. doi: 10.1093/schbul/sbw069

Palaniyappan, L., Park, B., Balain, V., Dangi, R., & Liddle, P. (2015). Abnormalities in structural covariance of cortical gyrification in schizophrenia. *Brain Struct Funct, 220*(4), 2059-2071. doi: 10.1007/s00429-014-0772-2

Pallanti, S., Grassi, G., Sarrecchia, E. D., Cantisani, A., & Pellegrini, M. (2011). Obsessive-compulsive disorder comorbidity: clinical assessment and therapeutic implications. *Front Psychiatry, 2*, 70. doi: 10.3389/fpsyt.2011.00070

Park, S. E., & Jeong, G. W. (2015). Cerebral white matter volume changes in patients with obsessive-compulsive disorder: Voxel-based morphometry. *Psychiatry Clin Neurosci, 69*(11), 717-723. doi: 10.1111/pcn.12317

Pauls, D. L., Abramovitch, A., Rauch, S. L., & Geller, D. A. (2014). Obsessive-compulsive disorder: an integrative genetic and neurobiological perspective. *Nat Rev Neurosci, 15*(6), 410-424. doi: 10.1038/nrn3746

Perani, D., Colombo, C., Bressi, S., Bonfanti, A., Grassi, F., Scarone, S., . . . Fazio, F. (1995). [18F]FDG PET study in obsessive-compulsive disorder. A clinical/metabolic correlation study after treatment. *Br J Psychiatry, 166*(2), 244-250.

Piras, F., Piras, F., Caltagirone, C., & Spalletta, G. (2013). Brain circuitries of obsessive compulsive disorder: a systematic review and meta-analysis of diffusion tensor imaging studies. *Neurosci Biobehav Rev, 37*(10), 2856-2877. doi: 10.1016/j.neubiorev.2013.10.008

Piras, F., Piras, F., Chiapponi, C., Girardi, P., Caltagirone, C., & Spalletta, G. (2015). Widespread structural brain changes in OCD: a systematic review of voxel-based morphometry studies. *Cortex, 62*, 89-108. doi: 10.1016/j.cortex.2013.01.016

Radua, J., & Mataix-Cols, D. (2009). Voxel-wise meta-analysis of grey matter changes in obsessive-compulsive disorder. *Br J Psychiatry, 195*(5), 393-402. doi: 10.1192/bjp.bp.108.055046

Rapoport, J. L., & Wise, S. P. (1988). Obsessive-compulsive disorder: evidence for basal ganglia dysfunction. *Psychopharmacol Bull, 24*(3), 380-384.

Rasmussen, S. A., & Eisen, J. L. (1992). The epidemiology and clinical features of obsessive compulsive disorder. *Psychiatr Clin North Am, 15*(4), 743-758.

Rasmussen, S. A., & Tsuang, M. T. (1986). Epidemiologic and clinical findings of significance to the design of neuropharmacologic studies of obsessive-compulsive disorder. *Psychopharmacol Bull, 22*(3), 723-729.

Reess, T. J., Rus, O. G., Gursel, D. A., Schmitz-Koep, B., Wagner, G., Berberich, G., & Koch, K. (2018a). Association between hippocampus volume and symptom profiles in obsessive-compulsive disorder. *Neuroimage Clin, 17*, 474-480. doi: 10.1016/j.nicl.2017.11.006

Reess, T. J., Rus, O. G., Gursel, D. A., Schmitz-Koep, B., Wagner, G., Berberich, G., & Koch, K. (2018b). Network-based decoupling of local gyrification in obsessive-compulsive disorder. *Hum Brain Mapp*. doi: 10.1002/hbm.24071

Reess, T. J., Rus, O. G., Schmidt, R., de Reus, M. A., Zaudig, M., Wagner, G., . . . Koch, K. (2016). Connectomics-based structural network alterations in obsessive-compulsive disorder. *Transl Psychiatry, 6*(9), e882. doi: 10.1038/tp.2016.163

Robinson, D., Wu, H., Munne, R. A., Ashtari, M., Alvir, J. M., Lerner, G., . . . Bogerts, B. (1995). Reduced caudate nucleus volume in obsessive-compulsive disorder. *Arch Gen Psychiatry, 52*(5), 393-398.

Rosario-Campos, M. C., Miguel, E. C., Quatrano, S., Chacon, P., Ferrao, Y., Findley, D., . . . Leckman, J. F. (2006). The Dimensional Yale-Brown Obsessive-Compulsive Scale (DY-BOCS): an instrument for assessing obsessive-compulsive symptom dimensions. *Mol Psychiatry, 11*(5), 495-504. doi: 10.1038/sj.mp.4001798

Rosenberg, D. R., & Keshavan, M. S. (1998). A.E. Bennett Research Award. Toward a neurodevelopmental model of of obsessive--compulsive disorder. *Biol Psychiatry, 43*(9), 623-640.

Rotge, J. Y., Guehl, D., Dilharreguy, B., Tignol, J., Bioulac, B., Allard, M., . . . Aouizerate, B. (2009). Meta-analysis of brain volume changes in obsessive-compulsive disorder. *Biol Psychiatry, 65*(1), 75-83. doi: 10.1016/j.biopsych.2008.06.019

Rubinov, M., & Bullmore, E. (2013). Fledgling pathoconnectomics of psychiatric disorders. *Trends Cogn Sci, 17*(12), 641-647. doi: 10.1016/j.tics.2013.10.007

Rubinov, M., & Sporns, O. (2010). Complex network measures of brain connectivity: uses and interpretations. *Neuroimage, 52*(3), 1059-1069. doi: 10.1016/j.neuroimage.2009.10.003

Rus, O. G., Reess, T. J., Wagner, G., Zaudig, M., Zimmer, C., & Koch, K. (2017). Hypogyrification in obsessive-compulsive disorder. *Psychol Med, 47*(6), 1053-1061. doi: 10.1017/S0033291716003202

Ruscio, A. M., Stein, D. J., Chiu, W. T., & Kessler, R. C. (2010). The epidemiology of obsessive-compulsive disorder in the National Comorbidity Survey Replication. *Mol Psychiatry, 15*(1), 53-63. doi: 10.1038/mp.2008.94

Rydon-Grange, M., & Coetzer, R. (2015). What do we know about obsessive-compulsive disorder following traumatic brain injury? *CNS Spectr, 20*(5), 463-465. doi: 10.1017/S109285291500053X

Sawle, G. V., Hymas, N. F., Lees, A. J., & Frackowiak, R. S. (1991). Obsessional slowness. Functional studies with positron emission tomography. *Brain, 114 (Pt 5)*, 2191-2202.

Saxena, S., Bota, R. G., & Brody, A. L. (2001). Brain-behavior relationships in obsessive-compulsive disorder. *Semin Clin Neuropsychiatry, 6*(2), 82-101.

Saxena, S., Brody, A. L., Maidment, K. M., Dunkin, J. J., Colgan, M., Alborzian, S., . . . Baxter, L. R., Jr. (1999). Localized orbitofrontal and subcortical metabolic changes and predictors of response to paroxetine treatment in obsessive-compulsive disorder. *Neuropsychopharmacology, 21*(6), 683-693. doi: 10.1016/S0893-133X(99)00082-2

Saxena, S., Brody, A. L., Schwartz, J. M., & Baxter, L. R. (1998). Neuroimaging and frontal-subcortical circuitry in obsessive-compulsive disorder. *Br J Psychiatry Suppl*(35), 26-37.

Saxena, S., & Rauch, S. L. (2000). Functional neuroimaging and the neuroanatomy of obsessive-compulsive disorder. *Psychiatr Clin North Am, 23*(3), 563-586.

Scarone, S., Colombo, C., Livian, S., Abbruzzese, M., Ronchi, P., Locatelli, M., . . . Smeraldi, E. (1992). Increased right caudate nucleus size in obsessive-compulsive disorder: detection with magnetic resonance imaging. *Psychiatry Res, 45*(2), 115-121.

Schaer, M., Cuadra, M. B., Tamarit, L., Lazeyras, F., Eliez, S., & Thiran, J. P. (2008). A surface-based approach to quantify local cortical gyrification. *IEEE Trans Med Imaging, 27*(2), 161-170. doi: 10.1109/TMI.2007.903576

Schlosser, R. G., Wagner, G., Schachtzabel, C., Peikert, G., Koch, K., Reichenbach, J. R., & Sauer, H. (2010). Fronto-cingulate effective connectivity in obsessive compulsive disorder: a study with fMRI and dynamic causal modeling. *Hum Brain Mapp, 31*(12), 1834-1850. doi: 10.1002/hbm.20980

Schwartz, J. M., Stoessel, P. W., Baxter, L. R., Jr., Martin, K. M., & Phelps, M. E. (1996). Systematic changes in cerebral glucose metabolic rate after successful behavior

modification treatment of obsessive-compulsive disorder. *Arch Gen Psychiatry, 53*(2), 109-113.

Seeley, W. W., Crawford, R. K., Zhou, J., Miller, B. L., & Greicius, M. D. (2009). Neurodegenerative diseases target large-scale human brain networks. *Neuron, 62*(1), 42-52. doi: 10.1016/j.neuron.2009.03.024

Shavitt, R. G., de Mathis, M. A., Oki, F., Ferrao, Y. A., Fontenelle, L. F., Torres, A. R., . . . Simpson, H. B. (2014). Phenomenology of OCD: lessons from a large multicenter study and implications for ICD-11. *J Psychiatr Res, 57*, 141-148. doi: 10.1016/j.jpsychires.2014.06.010

Shi, Y., & Toga, A. W. (2017). Connectome imaging for mapping human brain pathways. *Mol Psychiatry, 22*(9), 1230-1240. doi: 10.1038/mp.2017.92

Shim, G., Jung, W. H., Choi, J. S., Jung, M. H., Jang, J. H., Park, J. Y., . . . Kwon, J. S. (2009). Reduced cortical folding of the anterior cingulate cortex in obsessive-compulsive disorder. *J Psychiatry Neurosci, 34*(6), 443-449.

Shively, C. A., Silverstein-Metzler, M., Justice, J., & Willard, S. L. (2017). The impact of treatment with selective serotonin reuptake inhibitors on primate cardiovascular disease, behavior, and neuroanatomy. *Neurosci Biobehav Rev, 74*(Pt B), 433-443. doi: 10.1016/j.neubiorev.2016.08.037

Sinopoli, V. M., Burton, C. L., Kronenberg, S., & Arnold, P. D. (2017). A review of the role of serotonin system genes in obsessive-compulsive disorder. *Neurosci Biobehav Rev, 80*, 372-381. doi: 10.1016/j.neubiorev.2017.05.029

Skoog, G., & Skoog, I. (1999). A 40-year follow-up of patients with obsessive-compulsive disorder [see commetns]. *Arch Gen Psychiatry, 56*(2), 121-127.

Soares, J. M., Marques, P., Alves, V., & Sousa, N. (2013). A hitchhiker's guide to diffusion tensor imaging. *Front Neurosci, 7*, 31. doi: 10.3389/fnins.2013.00031

Sporns, O. (2012). *Discovering the Human Connectome*. Cambridge, Mass.: MIT Press.

Sporns, O. (2013a). The human connectome: origins and challenges. *Neuroimage, 80*, 53-61. doi: 10.1016/j.neuroimage.2013.03.023

Sporns, O. (2013b). Network attributes for segregation and integration in the human brain. *Curr Opin Neurobiol, 23*(2), 162-171. doi: 10.1016/j.conb.2012.11.015

Sporns, O., Tononi, G., & Kotter, R. (2005). The human connectome: A structural description of the human brain. *PLoS Comput Biol, 1*(4), e42. doi: 10.1371/journal.pcbi.0010042

Stein, D. J., Hollander, E., Chan, S., DeCaria, C. M., Hilal, S., Liebowitz, M. R., & Klein, D. F. (1993). Computed tomography and neurological soft signs in obsessive-compulsive disorder. *Psychiatry Res, 50*(3), 143-150.

Stengler-Wenzke, K., Kroll, M., Riedel-Heller, S., Matschinger, H., & Angermeyer, M. C. (2007). Quality of life in obsessive-compulsive disorder: the different impact of obsessions and compulsions. *Psychopathology, 40*(5), 282-289. doi: 10.1159/000104744

Swanson, L. W., & Bota, M. (2010). Foundational model of structural connectivity in the nervous system with a schema for wiring diagrams, connectome, and basic plan architecture. *Proc Natl Acad Sci U S A, 107*(48), 20610-20617. doi: 10.1073/pnas.1015128107

Swedo, S. E., Schapiro, M. B., Grady, C. L., Cheslow, D. L., Leonard, H. L., Kumar, A., . . . Rapoport, J. L. (1989). Cerebral glucose metabolism in childhood-onset obsessive-compulsive disorder. *Arch Gen Psychiatry, 46*(6), 518-523.

Takahashi, E., Folkerth, R. D., Galaburda, A. M., & Grant, P. E. (2012). Emerging cerebral connectivity in the human fetal brain: an MR tractography study. *Cereb Cortex, 22*(2), 455-464. doi: 10.1093/cercor/bhr126

Tang, W., Huang, X., Li, B., Jiang, X., Li, F., Xu, J., . . . Gong, Q. (2015). Structural brain abnormalities correlate with clinical features in patients with drug-naive OCD: A DARTEL-enhanced voxel-based morphometry study. *Behav Brain Res, 294*, 72-80. doi: 10.1016/j.bbr.2015.07.061

Taylor, S. (2011). Etiology of obsessions and compulsions: a meta-analysis and narrative review of twin studies. *Clin Psychol Rev, 31*(8), 1361-1372. doi: 10.1016/j.cpr.2011.09.008

Taylor, S. (2013). Molecular genetics of obsessive-compulsive disorder: a comprehensive meta-analysis of genetic association studies. *Mol Psychiatry, 18*(7), 799-805. doi: 10.1038/mp.2012.76

Thompson, P. M., Stein, J. L., Medland, S. E., Hibar, D. P., Vasquez, A. A., Renteria, M. E., . . . Alzheimer's Disease Neuroimaging Initiative, Epigen Consortium Imagen Consortium Saguenay Youth Study Group. (2014). The ENIGMA Consortium: large-scale collaborative analyses of neuroimaging and genetic data. *Brain Imaging Behav, 8*(2), 153-182. doi: 10.1007/s11682-013-9269-5

Thorsen, A. L., Hagland, P., Radua, J., Mataix-Cols, D., Kvale, G., Hansen, B., & van den Heuvel, O. A. (2018). Emotional Processing in Obsessive-Compulsive Disorder: A

Systematic Review and Meta-analysis of 25 Functional Neuroimaging Studies. *Biol Psychiatry Cogn Neurosci Neuroimaging*. doi: 10.1016/j.bpsc.2018.01.009

Tononi, G., Sporns, O., & Edelman, G. M. (1994). A measure for brain complexity: relating functional segregation and integration in the nervous system. *Proc Natl Acad Sci U S A, 91*(11), 5033-5037.

van den Heuvel, M. P., & Sporns, O. (2013). Network hubs in the human brain. *Trends Cogn Sci, 17*(12), 683-696. doi: 10.1016/j.tics.2013.09.012

van den Heuvel, O. A., Remijnse, P. L., Mataix-Cols, D., Vrenken, H., Groenewegen, H. J., Uylings, H. B., . . . Veltman, D. J. (2009). The major symptom dimensions of obsessive-compulsive disorder are mediated by partially distinct neural systems. *Brain, 132*, 853-868. doi: 10.1093/brain/awn267

van den Heuvel, O. A., van Wingen, G., Soriano-Mas, C., Alonso, P., Chamberlain, S. R., Nakamae, T., . . . Veltman, D. J. (2016). Brain circuitry of compulsivity. *Eur Neuropsychopharmacol, 26*(5), 810-827. doi: 10.1016/j.euroneuro.2015.12.005

van den Heuvel, O. A., Veltman, D. J., Groenewegen, H. J., Cath, D. C., van Balkom, A. J., van Hartskamp, J., . . . van Dyck, R. (2005). Frontal-striatal dysfunction during planning in obsessive-compulsive disorder. *Arch Gen Psychiatry, 62*(3), 301-309. doi: 10.1001/archpsyc.62.3.301

van Veen, V., & Carter, C. S. (2002). The anterior cingulate as a conflict monitor: fMRI and ERP studies. *Physiol Behav, 77*, 477-482.

van Wijk, B. C., Stam, C. J., & Daffertshofer, A. (2010). Comparing brain networks of different size and connectivity density using graph theory. *PLoS One, 5*(10), e13701. doi: 10.1371/journal.pone.0013701

Veale, D., & Roberts, A. (2014). Obsessive-compulsive disorder. *BMJ, 348*, g2183. doi: 10.1136/bmj.g2183

Venkatasubramanian, G., Zutshi, A., Jindal, S., Srikanth, S. G., Kovoor, J. M., Kumar, J. K., & Janardhan Reddy, Y. C. (2012). Comprehensive evaluation of cortical structure abnormalities in drug-naive, adult patients with obsessive-compulsive disorder: a surface-based morphometry study. *J Psychiatr Res, 46*(9), 1161-1168. doi: 10.1016/j.jpsychires.2012.06.003

Von Der Heide, R. J., Skipper, L. M., Klobusicky, E., & Olson, I. R. (2013). Dissecting the uncinate fasciculus: disorders, controversies and a hypothesis. *Brain, 136*(Pt 6), 1692-1707. doi: 10.1093/brain/awt094

Watts, D. J., & Strogatz, S. H. (1998). Collective dynamics of 'small-world' networks. *Nature, 393*(6684), 440-442. doi: 10.1038/30918

Wen, W., He, Y., & Sachdev, P. (2011). Structural brain networks and neuropsychiatric disorders. *Curr Opin Psychiatry, 24*(3), 219-225. doi: 10.1097/YCO.0b013e32834591f8

Whitwell, J. L. (2009). Voxel-based morphometry: an automated technique for assessing structural changes in the brain. *J Neurosci, 29*(31), 9661-9664. doi: 10.1523/JNEUROSCI.2160-09.2009

Willard, S. L., Uberseder, B., Clark, A., Daunais, J. B., Johnston, W. D., Neely, D., . . . Shively, C. A. (2015). Long term sertraline effects on neural structures in depressed and nondepressed adult female nonhuman primates. *Neuropharmacology, 99*, 369-378. doi: 10.1016/j.neuropharm.2015.06.011

Williams, M. T., Mugno, B., Franklin, M., & Faber, S. (2013). Symptom dimensions in obsessive-compulsive disorder: phenomenology and treatment outcomes with exposure and ritual prevention. *Psychopathology, 46*(6), 365-376. doi: 10.1159/000348582

Winslow, J. T., & Insel, T. R. (1990). Neurobiology of obsessive compulsive disorder: a possible role for serotonin. *J Clin Psychiatry, 51 Suppl*, 27-31.

Wobrock, T., Gruber, O., McIntosh, A. M., Kraft, S., Klinghardt, A., Scherk, H., . . . Moorhead, T. W. (2010). Reduced prefrontal gyrification in obsessive-compulsive disorder. *Eur Arch Psychiatry Clin Neurosci, 260*(6), 455-464. doi: 10.1007/s00406-009-0096-z

Zalesky, A., Fornito, A., Seal, M. L., Cocchi, L., Westin, C. F., Bullmore, E. T., . . . Pantelis, C. (2011). Disrupted axonal fiber connectivity in schizophrenia. *Biol Psychiatry, 69*(1), 80-89. doi: 10.1016/j.biopsych.2010.08.022

Zarei, M., Mataix-Cols, D., Heyman, I., Hough, M., Doherty, J., Burge, L., . . . James, A. (2011). Changes in gray matter volume and white matter microstructure in adolescents with obsessive-compulsive disorder. *Biol Psychiatry, 70*(11), 1083-1090. doi: 10.1016/j.biopsych.2011.06.032

Zhong, Z., Zhao, T., Luo, J., Guo, Z., Guo, M., Li, P., . . . Li, Z. (2014). Abnormal topological organization in white matter structural networks revealed by diffusion tensor tractography in unmedicated patients with obsessive-compulsive disorder. *Prog Neuropsychopharmacol Biol Psychiatry, 51*, 39-50. doi: 10.1016/j.pnpbp.2014.01.005

Zielinski, B. A., Gennatas, E. D., Zhou, J., & Seeley, W. W. (2010). Network-level structural covariance in the developing brain. *Proc Natl Acad Sci U S A, 107*(42), 18191-18196. doi: 10.1073/pnas.1003109107

ACKNOWLEDGEMENTS

Firstly, I would like to thank my main supervisor PD Dr. Kathrin Koch not only for being **very** patient whenever I came up with new ideas or the need to “run one more analysis”, but also for the constant motivation and encouragement, especially considering the sometimes cumbersome peculiarities of the scientific process. Without her I would have probably quit along the way. Furthermore I would like to thank Georgiana Rus who I have had the pleasure to work with over several years of my PhD studies. I think it is fair to say that as a team we both grew together tremendously and I will always look back with a smile. A big “Thank you” also goes out to the many people working either in the Department of Neuroradiology or at the TUM-NIC. I believe the atmosphere among all students and PIs alike has truly been special and was highly appreciated. Furthermore I would like to thank Dr. Afra Wohlschläger and Dr. Virginia Flanagin for valuable feedback and additional supervision during my PhD as well as everyone at the GSN. I’m thankful for being a part of this great program. I would like to thank Prof. Martijn van den Heuvel and everyone at the Dutch Connectome Lab at the UMC Utrecht where I had the pleasure to stay for several months to conduct research. I thoroughly enjoyed the company as well as the academic input.

I would also like to thank my family who has always encouraged and supported me no matter what. After many turns along the way it now feels like everything is finally coming together. Thank you for always believing in me! Finally, I would like to express my gratitude to Lisa who has been there basically from the start of the thesis and has constantly supported me with her down to earth attitude, especially in times of doubt. I deeply appreciate her affection, as well as her energy and enthusiasm even for the smallest things. Thank you!

LIST OF PUBLICATIONS

Network-based decoupling of local gyrification in obsessive-compulsive disorder: a graph theoretical study.

Reess TJ, Rus OG, Gürsel DA, Schmitz-Koep B, Wagner G, Berberich G, Koch K (2018).

Human Brain Mapping, *epub ahead of print*, DOI: 10.1002/hbm.24071

Association between hippocampus volume and symptom profiles in obsessive-compulsive disorder.

Reess TJ, Rus OG, Gürsel DA, Schmitz-Koep B, Wagner G, Berberich G, Koch K (2018).

Neuroimage: Clinical, 17, 474-480, DOI: 10.1016/j.nicl.2017.11.006

Cortical Abnormalities Associated With Pediatric and Adult Obsessive-Compulsive Disorder: Findings From the ENIGMA Obsessive-Compulsive Disorder Working Group.

Boedhoe PSW, Schmaal L, Abe Y, Alonso P, Ameis SH, Anticevic A, Arnold PD, Batistuzzo MC, Benedetti F, Beucke JC, Bollettini I, Bose A, Brem S, Calvo A, Calvo R, Cheng Y, Cho KIK, Ciullo V, Dallaspezia S, Denys D, Feusner JD, Fitzgerald KD, Fouche JP, Fridgeirsson EA, Gruner P, Hanna GL, Hibar DP, Hoexter MQ, Hu H, Huyser C, Jahanshad N, James A, Kathmann N, Kaufmann C, Koch K, Kwon JS, Lazaro L, Lochner C, Marsh R, Martínez-Zalacaín I, Mataix-Cols D, Menchón JM, Minuzzi L, Morer A, Nakamae T, Nakao T, Narayanaswamy JC, Nishida S, Nurmi E, O'Neill J, Piacentini J, Piras F, Piras F, Reddy YCJ, **Reess TJ**, Sakai Y, Sato JR, Simpson HB, Soreni N, Soriano-Mas C, Spalletta G, Stevens MC, Szeszko PR, Tolin DF, van Wingen GA, Venkatasubramanian G, Walitza S, Wang Z, Yun JY; ENIGMA-OCD Working Group, Thompson PM, Stein DJ, van den Heuvel OA; ENIGMA OCD Working Group (2017). *American Journal of Psychiatry*, *epub ahead of print*, DOI: 10.1176/appi.ajp.2017.17050485

Structural alterations in patients with obsessive-compulsive disorder: A surface based analysis of cortical volume, surface area and thickness.

Rus OG, **Reess TJ**, Zimmer C, Zaudig M, Wagner G, Koch K (2017).

Journal of Psychiatry and Neuroscience, 42(6), 395-403, DOI: 10.1503/jpn.170030

Functional and structural connectivity of the amygdala in obsessive-compulsive disorder.

Rus OG, **Reess TJ**, Wagner G, Zimmer C, Zaudig M, Koch K. (2017).

Neuroimage: Clinical, 13, 246-255, DOI: 10.1016/j.nicl.2016.12.007

Hypogyrifaction in Obsessive-Compulsive Disorder.

Rus OG, **Reess TJ**, Zimmer C, Zaudig M, Koch K (2017).

Psychological Medicine, 47, 1053-1061, DOI: 10.1017/S0033291716003202

Connectomics-based structural network alterations in obsessive-compulsive disorder.

Reess TJ, Rus OG, Schmidt R, de Reus MA, Zaudig M, Wagner G, Zimmer C, van den Heuvel M P, Koch K (2016).

Translational Psychiatry, *6 (9)*, e882. DOI: 10.1038/tp.2016.163

Extensive learning is associated with gray matter changes in the right Hippocampus.

Koch K, **Reess TJ**, Rus OG, Zimmer C (2016).

Neuroimage, 125, 627-632, DOI: 10.1016/j.neuroimage.2015.10.056

Diffusion tensor imaging (DTI) studies in patients with obsessive-compulsive disorder (OCD): A review.

Koch K, **Reess TJ**, Rus OG, Zimmer C, Zaudig M (2014).

Journal of Psychiatric Research, 54, 26-35, DOI: 10.1016/j.jpsychires.2014.03.006

Functional connectivity and gray matter volume of the striatum in schizophrenia.

Koch K, Rus OG, **Reeß TJ**, Schachtzabel C, Wagner G, Schultz CC, Sorg C, Schlösser RGM (2014).

British Journal of Psychiatry, 205, 204-213, DOI: 10.1192/bjp.bp.113.138099

Personality traits in patients with restless legs syndrome.

Steinig J, **Reess T**, Klösch G, Sauter C, Zeitlhofer J, Happe S (2013).

Somnologie, 17, 281-283, DOI: 10.1007/s11818-013-0623-z

Perception of sleep: Subjective vs. objective sleep parameters in patients with insomnia, hyper-somnia, parasomnia, and sleep-related movement disorders.

Reess T, Steinig J, Lanz M, Dempewolf S, Bunten S, Happe S (2010).

Somnologie, 14, 253-259, DOI: 10.1007/s11818-010-0491-8

CURRICULUM VITAE

EDUCATION

2013 – 2018 *PhD in Systemic Neurosciences*
Ludwig-Maximilians-Universität München, Germany

2005 – 2011 *Diploma Psychology*
Universität Bremen, Germany

RESEARCH EXPERIENCE

2012 – 2018 *Research Associate*
Department of Neuroradiology, Klinikum rechts der Isar
Technische Universität München, Germany

EIDESSTATTLICHE VERSICHERUNG / AFFIDAVIT

Hiermit versichere ich an Eides statt, dass ich die vorliegende Dissertation „Connectomics-Based Network Analyses and Structure-Symptom Relationships in Obsessive-Compulsive Disorder“ sebstständig angefertigt habe, mich außer der angegebenen keiner weiteren Hilfsmittel bedient und alle Erkenntnisse, die aus dem Schrifttum ganz oder annähernd übernommen sind, als solche kenntlich gemacht und nach ihrer Herkunft unter Bezeichnung der Fundstelle einzeln nachgewiesen habe.

I hereby confirm that the dissertation „Connectomics-Based Network Analyses and Structure-Symptom Relationships in Obsessive-Compulsive Disorder“ is the result of my own work and that I have only used sources or materials listed and specified in the dissertation.

Munich, 26 April 2018 Tim Jonas Reess

DECLARATION OF AUTHOR CONTRIBUTIONS

Project 1

Authors: *Tim Jonas Reess, Oana Georgiana Rus, Ruben Schmidt, Marcel A. de Reus, Michael Zaudig, Gerd Wagner, Claus Zimmer, Martijn P. van den Heuvel, Kathrin Koch*

The author of this thesis is the first author of the manuscript. **T.J.R.**, K.K., O.G.R., with the help of M.Z., C.Z., and G.W. conceived the experiment. **T.J.R.** and O.G.R. recruited participants and conducted data acquisition. **T.J.R.**, R.S., M.A.D.R, M.P.v.d.H performed analyses and contributed analytic tools. **T.J.R.** wrote the manuscript in consultation with O.G.R., R.S., M.A.d.R., M.Z., G.W., C.Z., M.P.v.d.H., K.K. All authors discussed the results and revised the final manuscript.

Project 2

Authors: *Tim Jonas Reess, Oana Georgiana Rus, Deniz A. Gürsel, Benita Schmitz-Koep, Gerd Wagner, Götz Berberich, Kathrin Koch*

The author of this thesis is the first author of the manuscript. **T.J.R.** and K.K. with the help of G.W. and G.B. conceived the experiment. **T.J.R.**, O.G.R., B.S.K., and D.A.G recruited participants and conducted the data acquisition. G.W. contributed data. **T.J.R.** performed analyses. **T.J.R.** wrote the manuscript in consultation with O.G.R., G.W., and K.K. All authors discussed the results and revised the final manuscript.

Project 3

Authors: *Tim Jonas Reess, Oana Georgiana Rus, Deniz A. Gürsel, Benita Schmitz-Koep, Gerd Wagner, Götz Berberich, Kathrin Koch*

The author of this thesis is the first author of the manuscript. **T.J.R.**, K.K., and O.G.R. together with G.W. and G.B. conceived the experiment. **T.J.R.**, O.G.R., D.A.G., and B.S.K. recruited participants and acquired data. G.W. contributed data and analytic tools. T.J.R. performed analyses. **T.J.R.** and K.K. wrote the manuscript in consultation with O.G.R., D.A.G., G.B., and G.W. All authors discussed the results and revised the final manuscript.

Munich, 26 April 2018

Tim Jonas Reess

Kathrin Koch (1st supervisor)